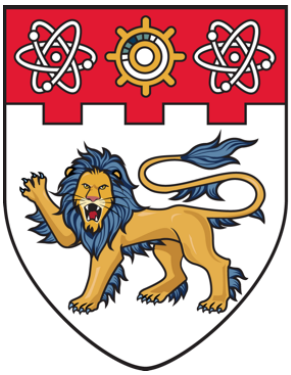

NANYANG TECHNOLOGICAL UNIVERSITY
SINGAPORE

DECOLORIZATION OF AZO DYES WITH *KLEBSIELLA PNEUMONIAE* UNDER HIGH SALINE CONDITIONS

TEJASRI GOPI

Interdisciplinary Graduate School

Nanyang Environment and Water Research Institute @ NTU

2021

DECOLORIZATION OF AZO DYES WITH *KLEBSIELLA PNEUMONIAE* UNDER HIGH SALINE CONDITIONS

TEJASRI GOPI

INTERDISCIPLINARY GRADUATE SCHOOL

A thesis submitted to the Nanyang Technological University in partial fulfillment of the requirement for the degree of Doctor of Philosophy

2021

Statement of Originality

I hereby certify that the work embodied in this thesis is the result of original research, is free of plagiarized materials, and has not been submitted for a higher degree to any other University or Institution.

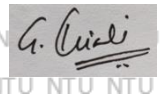

20/09/2021

. . . . . .
Date

. . . . . .
Gopi Tejasri

Supervisor Declaration Statement

I have reviewed the content and presentation style of this thesis and declare itis free of plagiarism and of sufficient grammatical clarity to be examined. To the best of my knowledge, the research and writing are those of the candidate except as acknowledged in the Author Attribution Statement. I confirm that the investigations were conducted in accord with the ethics policies andintegrity standards of Nanyang Technological University and that the research data are presented honestly and without prejudice.

28 Sep 2021

. . . . . .
Date

. . . . . .
Prof William Chen Wei Ning

Authorship Attribution Statement

This thesis **does not** contain any materials from papers published in peer-reviewed journals or from papers accepted at conferences in which I am listed as an author.

The contributions of the co-authors are as follows:

- Prof Ng Wun Jern provided the initial project direction.
- I prepared the manuscript drafts. The manuscript was reviewed by Prof Ng WunJern.
- I co-designed the study with Prof Ng Wun Jern and Dr Chaozhi Pan. I performedall the wet laboratory work at Advanced Environmental Biotechnology Centre (AEBC) and Nanyang Environmental and Water Research Institute (NEWRI). I also analyzed the data.
- Activated sludge collection, isolation of microbes, sample preparation, experiments and sample analysis on various high end analytical instruments wasdone by me.
- Dr Chaozhi Pan helped with the method creation for the liquid chromatographyand mass spectrometry analyses. The sample preparation, analysis and data interpretation were done by me.
- Prof Ng Wun Jern provided guidance in the interpretation of the analytical data.
- Prof William Chen and Prof Liu Yu have provided valuable comments throughout the project on the research direction and interpretation of the gathered data.

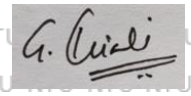

20/09/2021

. . . . . .

Date

. . . . . .

Gopi Tejasri

Acknowledgments

I would like to express my heartfelt gratitude to my supervisor, Prof Ng Wun Jern, for the invaluable encouragement, careful technical guidance, and extraordinary patience throughout my candidature period. Without his support and supervision, this work would not have been possible. I am indebted forever for the kindness and care he had for me when I was going through my hardships.

I would like to thank my co-supervisor, Prof William Chen, and my mentor, Prof Liu Yu, for their valuable suggestions and continuously improving my thesis. I would like to thank Dr. Babu Narayanaswamy for being more than a mentor, especially during the final year of my candidature. I would also extend my thanks for trusting my abilities and allowing me to finish my Graduate Assistantship Program duty under his supervision. I would like to thank Prof Lisak Grzegorz for allowing me to work on his project to clock my Research assistantship duty. I learned a lot during my time as an RA.

Special thanks to Dr. Harish Venkata Krishnan, who taught me microbiological techniques during my first year. Special thanks to Dr. Dave Poh and Dr. Pan Chaozhi for helping me clarify my technical doubts in my research work and providing invaluable feedback on my data and manuscripts.

I would like to express my thanks to all the lab technicians, staff, colleagues, and friends at AEBC, NEWRI. I would like to acknowledge Interdisciplinary Graduate School, Nanyang Technological University (NTU) and NEWRI Singapore, for the financial support throughout this project and the opportunity to conduct this research. I would like to especially thank Ms. Elvy Riani Wanjaya, Dr. Lv Yunbo, Dr. Han Yuan for training me on various high-end analytical instruments that are key for this study. Thanks to Ms. Hera for always being kind and helpful from day one and making my life as easy and smooth as possible at AEBC, NEWRI, SG.

I would like to send my heartfelt love to my mother, who has always encouraged me to pursue my higher education. I would like to mention Dr. Shankar Acharya, Dr. Akshay Kumar, Dr. Lai Hui Ying, Dr. Tharushi, Dr. Dharma Sree, Ms. Dhivya and Dr. Varun Maruvenchery for being my emotional support and my cheerleaders throughout my student life at NTU. Furthermore, thanks to Mr. Saksham for helping me with my technical doubts. I would like to convey my thanks to all my dear friends who have helped me during crises and helped me become a better person with their invaluable friendship.

Summary

Textile industries generate colored wastewater after the dyeing process. The color is still visible even at low concentrations such as ~10 ppm. Due to the ease of operation, economic feasibility, and chemical stability, azo dyes dominate more than 70 % of the world's dye market. They reportedly are toxic in the aquatic environment and may impact soil fertility if disposed of on land. Human health issues like allergic dermatitis, cancer, Heinz body formation, cyanosis, jaundice, quadriplegia, and tissue necrosis are reportedly associated with the acute contact with the dyes and their biochemical intermediates.

Though Physico-chemical treatment methods such as adsorption or advanced oxidation processes (AOPs) are efficient in eliminating these dyes from the dye laden water, they involve high chemical and energy costs limiting them to expand at large scale. Besides that, they require downstream treatment of the waste sludge produced. Many researchers consider biological treatment of dyes because of the cost-effectiveness and eco-friendly nature. But dyes are large and heavy, structurally complex molecules and hence are not readily degradable. In the typical aerobic wastewater treatment systems, they either got trapped in the sludge or exited untreated requiring downstream processing. Though anaerobic conditions are the most suited for the azo dye transformation, it results in the formation of aromatic amines (AAs) and sulfonated aromatic amines (SAAs) that are more toxic and persistent compared to the parent dye molecules.

To overcome this problem, bioremediation of dyes in anaerobic/anoxic - aerobic/micro-aerobic systems are extensively researched throughout the last decade. Very few have reported the aerobic azo dye degradation, but mostly using *Pseudomonas* sp., which is an opportunistic pathogen. Besides that, high dosages of salts such as chlorides and sulfates that are another consequence of dyeing is often ignored by most studies. To address this problem, this thesis work focuses on isolating a halotolerant facultative anaerobe that decolorizes and degrades industrially important sulfonated azo dyes in oxygen abundant conditions under the influence of sulfates and chlorides. Further, it involves tracking the fate of the by-products generated during decolorization.

This study is divided into three parts. Firstly, isolation and identification of a non-pathogenic microbe that decolorizes a variety of textile dyes. For this study, Activated Sludge (AS) collected from a local treatment plant was subjected to a shock load dosage of Acid yellow 17 (a pyridine based anionic dye) to screen and knockdown the most conventional microbial species including *Pseudomonas*. A facultative anaerobe, *Klebsiella*, was isolated and studied for its decolorization potential. Three anionic azo dyes, namely Acid blue 113 (AB113), Direct red 81 (DR81), and Reactive orange 16 (RO16) are chosen based on the category they fell under, their structural complexity, and industrial importance. The second part of this study is to evaluate the decolorization potential of *Klebsiella pneumoniae* in aerobic conditions. Findings revealed that the acid dye favored aerobic conditions while the direct and reactive dyes favored microaerobic conditions. Hence, for the third part of the study, which is the tracking of the degradation by-products, was carried out based on the results from the previous study as the operating conditions.

A 3 h, 6 h and 12 h latent periods are observed for AB113, DR81 and RO16 respectively, during which less than 10 % of the dyes were adsorbed onto the biomass. Azo bridge reduction or the preferential utilization of the glucose in the culture could be the reason for the latent period after which a substantial decolorization was observed. AB113, DR81 and RO16 were not detected in the liquid culture after 24 h, 24 h and 60 h, respectively. Unlike previous reports, RO16, a mono azo dye, required 2.5 times longer period to decolorize as compared to the diazo dyes - DR81 and AB113. This emphasizes that the decolorization kinetics is primarily influenced by the molecular geometry of the dye, branching of the functional groups and the steric hindrance caused by them besides the number of azo bonds and nature of the functional groups – sulfonated, carboxylated or methylated.

A considerable color change was noticed during the end-log and stationary phase of the biomass; it is obvious that the bacterial activity is responsible for the color removal. Also, it is hypothesized that the dye removal occurred via extracellular, or membrane bound activity since the dyes cannot penetrate through the cell membrane. Besides this, various unknown and known metabolites such as SAAs and AAs, long chained aliphatic

compounds, naphthalene, and benzene-based by-products were detected during the aerobic decolorization of AB113. supporting the disintegration of the dye. While the microaerobic degradation of RO16 and DR81 resulted in the accumulation of aromatic amines and other byproducts that are not completely degraded. The qualitative untargeted metabolite analysis could only confirm a few of the by-products. Based on this evidence, a degradation pathway was delineated for all the three dyes. Though all the dyes were broken-down into relatively smaller molecules, low-molecular-weight aliphatic molecules were not formed suggesting the partial accumulation of degradation by-products and incomplete mineralization. The TOC/TN removal efficacy supports the same. The phytotoxicity assay on *Vigan Radiata* seeds suggested that the presence of salts could be also one of the reasons for the poor seed germination and seedling growth. Hence, the treated samples may not be completely innocuous and might further need desalination or dilution.

Table of Contents

Contents

Table Captions

Figure Captions

Symbols and abbreviations

POPs	Persistent Organic Pollutants
ACN	Acetonitrile
WWTP	Wastewater treatment plant
DUP	Domestic stream of Ulu Pandan water treatment plant
DJRP	Domestic stream of Jurong water reclamation plant
IJRP	Industrial stream of Jurong water reclamation plant
LCMS	Liquid chromatography mass spectrometry
UV-Vis	Ultraviolet -Visible
ATR-FTIR spectroscopy	Attenuated Total Reflectance - Fourier Transform Infrared
ATR	Attenuated Total Reflectance
OD_{600}	Optical density at 600nm
AB113	Acid blue 113
DR81	Direct red 81
RO16	Reactive orange 16
AS	Activated sludge
TWW	Textile wastewater
AAs	Aromatic amines
SAAs	Sulfonated aromatic amines
m/z	Mass to charge ratio
η	efficiency
λ_{max}	peak wavelength
λ	wavelength
Å	Armstrong
℃	degree Celsius
µg	microgram
µL	microliter
mg	milligram
g	gram
m	meter

L	liter
HPLC	High Performance Liquid chromatography
min	minute
NA	not applicable
pH	potential of Hydrogen (-log [H^+])
rpm	revolutions per minute
rcf	relative centrifugal force or g-force
VSS	Volatile Suspended Solids
mL	milliliter
h	hour
CE	Collision energy
cm	centimeter
e.g.	for example
et al.	and others
DNA	Deoxyribonucleic acid
RNA	Ribonucleic acid
TOC	Total Organic Carbon
TN	Total Nitrogen
DI	De-Ionized
F/M	Food to Microorganism ratio
DO	Dissolved Oxygen
LC/Q-TOF/MS	Liquid Chromatography Quadrupole Time of Flight Mass Spectrometry
LC-MS/MS	Liquid Chromatography tandem Mass Spectrometry
AOP	Advanced Oxidation Process
COD	Chemical Oxygen Demand
AC	Activated Carbon
PBS	Potassium phosphate Buffer Solution
SPE	Solid Phase Extraction
mM	millimolar
mm	millimeter

V	Voltage
PI	Product Ion
EIC	Extracted Ion Chromatogram
TIC	Total Ion Chromatogram
psi	pounds per square inch
N	Normality
mg/L	milligram per liter
AY17	Acid Yellow 17
EPS	Extracellular Polymeric Substances
ACF	Activated Carbon Fiber
UV	Ultraviolet
ppm	parts per million
MBR	Membrane Bioreactor
L/min	liter per minute
w/w	weight to weight percentage
BLAST	Basic Local Alignment and Sequencing Tool
NCBI	National Centre for Biotechnology Information
NJ	Neighbor joining method
TDS	Total Dissolved Solids
EC	Electrical Conductivity
RT	Retention time
PROKKA	Rapid Prokaryotic Genome Annotation
KAAS	KEGG Automatic Annotation Server)
KEGG	Kyoto Encyclopedia of Genes and Genomes

Chapter 1 INTRODUCTION

1.1 Background

Following the literature review, it is understood that dyes are widely used to make colorful products in various industries generating colored wastewater [1], [2]. Amongst these industries, the textile dyeing industry is the largest colored wastewater producer in terms of effluent composition and volume. Textile dyes usually have complex chemical structures so that the dyed products are resistant to fading on exposure to light, sweat, water, and chemicals such as soaps and surfactants [3]–[5]. On the other hand, the property of resistance to fading possesses challenges in colored wastewater treatment. Currently, only 45 % – 47 % of the 10,000 commercially synthetic dyes are biodegradable [6]–[8]. According to a survey conducted by the Ecological and Toxicological Association of the Dyestuffs Manufacturing Industry (ETAD) on dyes, cationic and diazo direct dyes were found to be comparatively of significant toxicity [3]. There has been some discrepancy in the amount of textile wastewater (TWW) produced. While several reports [3], [9]–[11] state that around 700,000 tons of dyes were produced annually, others [12]–[14] had provided values ranging from 10,000 to 280,000 tons. Consequently, there has been even less certainty on the number of dye wastes released into the environment.

In addition to the color, TWW is loaded with large amounts of salts amongst other dyeing aids and heavy metals [15]–[20]. Salts play a significant role in batch dyeing process as a catalyst that drives the dye into the textile and exhausts the dye molecules promoting more greater fixation and less wastage. [21]. Similar to the amount of dyes released, there is an uncertainty in the amount of salts released in a TWW and largely range between 15 % - 20 % [15], [22], [23], 4 % - 10 % [24], 1 % - 10 % [25].

The increasing use of dyes can cause great deal of environmental pollution and damage unless spent dyes are appropriately managed [3], [6], [14]. Most conventional Physico-chemical and biological techniques could process the textile dyeing effluents in aspects such as suspended solids, temperature, pH, organic and inorganic contaminants at an acceptable cost. However, the color is a challenging parameter to meet the discharge standards [14], [26]. The intense visual impact and persistence pose deleterious effects on receiving water bodies is presented in *Figure 1.1* [27], [28].

When textile dyeing wastewaters are released into water bodies, they cause eutrophication and generate potentially toxic by-products through various chemical reactions [29]. Diseases like dermatitis, skin allergy, cancer, mammalian cell mutation, rapid heart rate, Heinz bodies, cyanosis, jaundice, quadriplegia, and tissue necrosis are associated with the acute physical contact with TWW [1], [27], [30]. Azo dyes constitute more than 50 % of all dyes listed in the Color Index (CI) [31] and are integral components of numerous industrial dyes. Due to the ease of preparation, low cost, stable chemistry, and versatility, they account for about 70 % of the world dye market [8], [31], [32]. Commercial azo dyes show resistance to photo-degradation and persistence in the aquatic environment, often taking weeks before substantial degradation occurs [33]. Post the dyeing process, 10 – 15 % of the azo dye would remain unbound to the fiber and is discharged as wastewater [18], [34]–[37]. They are highly visible, causing adverse aesthetic effects at concentrations as low as 10 – 15 mg/L. Moreover, they hinder photosynthesis in aquatic plants by absorbing and reflecting sunlight. Therefore, over 99 % of color removal is required. Despite the natural remediation potential of aquatic ecosystems, biological and physicochemical degradation of these compounds may produce toxic intermediate metabolites [1], [26], [28], [32], [38], [39].

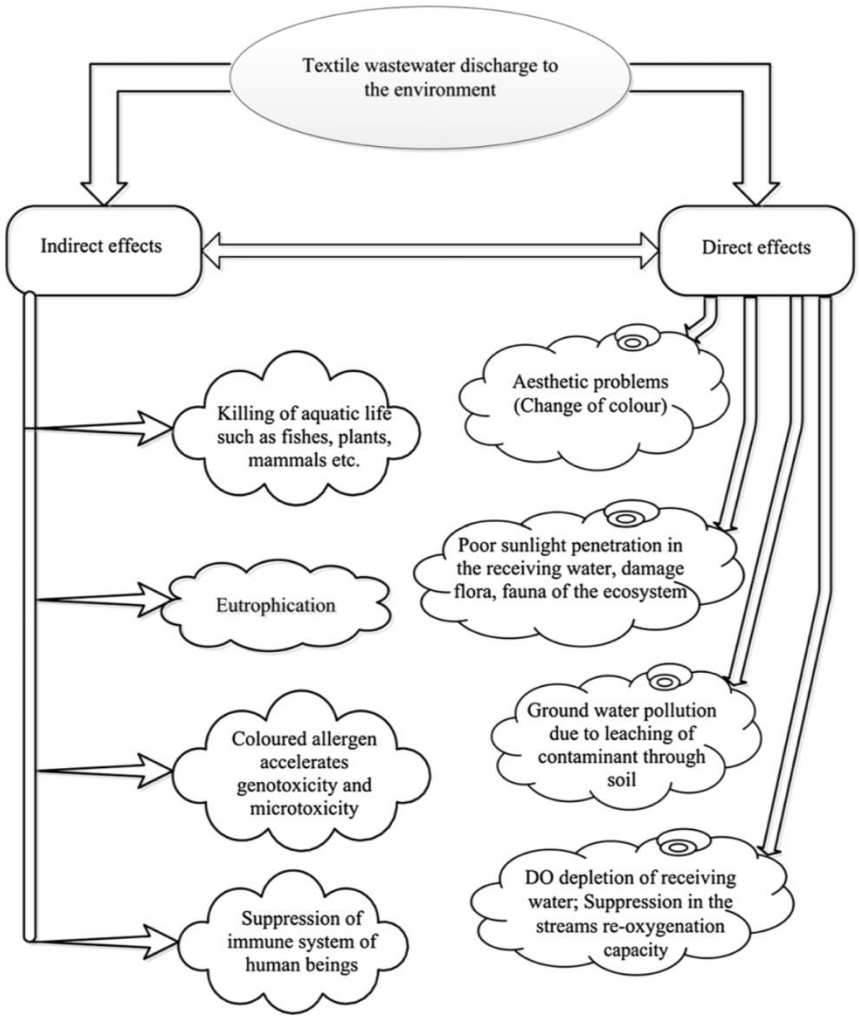

Figure 1. 1 Effect of textile wastewater on man and various segments of the environment (adopted from [40])

1.2 Dissertation Overview

This thesis consists of five chapters with the contents as given below:

Chapter 1 gives a brief introduction and background information about the impact of textile wastewater and the environmental significance of dye removal.

Chapter 2 presents a comprehensive review of the literature on various azo dye treatment techniques – physical, chemical, and biological and their evolution overtime.

Chapter 3 elaborates various materials and methods used for the experiments in this study.

Chapter 4 discusses the isolate sequestered from activated sludge collected from a local wastewater treatment plant, and the evaluation of its decolorization potential on the azo dyes - Acid blue 113, Direct red 81 and Reactive orange 16, in aerobic and microaerobic conditions. It further elaborates on the dye removal mechanisms and their degradation pathways and the toxicity studies of the decolorized effluents.

Chapter 5 summarizes the key findings of this study and suggests recommendations for future works.

Chapter 2 LITERATURE REVIEW

2.1 Textile dyes and their classification

Textile dyes are grouped into acidic/anionic, basic/cationic, disperse/non-ionic and mono azo, poly azo, anthraquinone, and metal complex dyes based on their ionic properties and chemical structure, respectively [41]. Anionic dyes could be further categorized into direct and reactive dyes [42], [43].

Anionic dyes are water-soluble with relatively smaller molecular weight and contain sulfonic acid groups attached to the organic part. They have an affinity for natural fibers, but typical levels of fixation on the fibers leave 10 % – 50 % of the applied dyes in the spent dye bath [1], [18], [34], [36]. At the same time, cationic dyes are soluble in alcohol and methylated spirits but insoluble in water [44]. They have an affinity for jute, acrylic, and wool fibers [45] and form ionic bonds with the acid groups on the fiber [42]. Non-ionic dyes are soluble in organic solvents and sparsely soluble in water [46]–[48]. They have an affinity for synthetic fibers [45].

On the other hand, azo dyes constitute more than 50 % of all dyes listed in the Color Index (CI) [31] and are integral components of numerous industrial dyes. Due to the ease of preparation, low cost, stable chemistry, and versatility, they account for about 70 % of the world dye market [8], [31], [32].

The chromophore units, characterized by nitrogen-nitrogen double bonds (-N=N-), are responsible for the azo dyes' color [48]. Commercial azo dyes are resistant to photo-degradation and their persistence in the aquatic environment, often take long periods before a substantial degradation occurs [33], [49], [50]. After the dyeing process, 10 % – 15 % of the azo dye would remain unbound to the fiber and is discharged as wastewater [18], [34]–[37]. Azo dyes are highly visible, causing adverse aesthetic effects at concentrations as low as 10 – 15 mg/L. Moreover, they hinder photosynthesis in aquatic plants by absorbing and reflecting sunlight. Therefore, over 99 % of color removal is required. Despite the natural remediation potential of aquatic ecosystems, biological and physicochemical degradation of these compounds may produce toxic intermediate metabolites [1], [26], [28], [32], [38], [39]. Hence, treatment techniques that degrade the original

dye compound and convert their respective intermediates to the innocuous metabolic endpoints are necessary.

2.2 Challenges to conventional WWTPs

Since dye compounds have high molecular weight, they typically are not readily biodegradable in conventional wastewater treatment plants [51]. The colored compounds and their by-products, such as aromatic amines (AAs), have been found trapped or adsorbed onto the bio-sludge or exited unaltered from the biotreatment process their stability under aerobic conditions. Though physical/chemical methods such as adsorption or advanced oxidation processes (AOPs) can be efficient, they have also been commercially non-viable due to high chemical and energy expenses [51]–[55].

Though anaerobic processes have lower energy demands and lower operation costs and degrade a range of pollutants with chloro, nitro ,and azo groups that are more amenable to degradation under anaerobic conditions, they need longer hydraulic retention times [56]. A consequence of the latter would be larger reactors to accommodate the slower anaerobic reaction rates [55]. Further, secondary pollutants following the anaerobic treatment, such as AAs require downstream treatment [57]. Combined treatment techniques were found necessary to overcome the shortcomings of the individual techniques [58].

Synthetic dyes have been reported to exhibit impact on various biological activities, resulting in various by-products potentially harmful to the environment and man. This has triggered research on the fate of azo dyes in treatment systems [14].

2.3 Physico-chemical treatment technologies for azo dye removal

Physico-chemical techniques are quick and compact [59]. However, due to the associated high capital costs and operational costs and their high treatment specificity, they are not ubiquitous in the industry [6], [60]. The non-destructive methods transfer dyes from the dissolved phase into the solids phase [6] demanding post-treatment and the management of the dyes in a solid phase. Membrane separations, ion exchange, and adsorption are the only reported non-destructive techniques for dye recovery with varying difficulty levels [61]. In contrast, chemical reactions

occur in the destructive techniques, releasing precursors and other degradation products, which require further treatment for complete mineralization [6], [59], [60].

Various physical and chemical techniques and their combinations have been traditionally used to treat dye wastewater [62]. Some physicochemical treatment methods employed for the treatment of dye wastewater with varying degrees of success include Ozonation [26], [63], Coagulation – flocculation [27], [28], [64], Photocatalytic oxidation [65], [66], Membrane filtration [67]–[69] and Adsorption [70]–[72]. The most effective treatment methods for dye removal to date include AOPs or combined oxidation processes [28], [60], [62], [73]–[76]. Various destructive and non-destructive physicochemical treatment methods and their advantages and disadvantages are further summed up in *Table 2.1*.

2.3.1 Advent and evolution of combined dye degradation treatment techniques

Coupling of destructive techniques with a non-destructive technique is a common practice to complement the disadvantages of the individual techniques. This section deals with the evolution of various individual treatment techniques into combined ones.

With more than 95 % dye recovery, membrane technology was considered the most promising dye removal technique with technical and economic feasibility [69], [77]. It offered dye recovery and reusable water making it a sustainable technique and might even achieve “zero liquid discharge” by cutting off the water drainage that eliminates all the problems associated with the environment besides benefiting the industry [69], [78]. However, the pH dependency of the flux and its variability for various dyes [78] prompted the researchers to shift their focus on membrane modification and search for novel membrane materials to cater to various dyes and elevated salt concentrations occurring along with them, to overcome membrane fouling and to enhance the flux all at the same time [67], [68], [78].

Adsorption using Activated Carbon (AC) is a well-established, swift, and compact technique for dye removal from wastewaters [79]. Since commercial AC is very expensive to expand the technique at a large scale, the quest for low cost, non-conventional materials for the preparation of adsorbents began at the end of the 20th century [72]. Some researchers prepared biochar from a

variety of agricultural refuses such as rice husk [79], de-oiled soya [80], coir pith [81], sawdust [72] and have reported their adsorption capacity for direct and acid dyes and basic dyes at acidic and basic conditions respectively. The materials that adsorb disperse and vat dyes are not widely known [46], [61], [82]. Most adsorbents function ideally at high adsorbent dosages, low dye concentrations and low pH [37], [79]. Nanoscale Zero Valent Iron (nZVI) supported on biochar enhanced the adsorption of the dye onto the surface of the biochar, while ZVI has aided in the transport of electrons to reduce and decolorize the dyes [37]. Similarly, ozonation experimented with both biochar and AC cutdown the treatment time to less than an hour [63]. However, a compulsory acidification step prior to the treatment, is of great concern which adds up to the treatment costs.

High molecular weight coagulants such as aluminum and ferric salts often adsorb cationic, anionic or non-ionic dyes and are suitable over a wide-ranging pH [83]. But. it is well-known that the cost of conventional coagulants and sludge handling and disposal are the main reasons why coagulation/flocculation is considered a non-viable option for wastewater treatment. To cutdown the treatment costs, waterworks sludge was experimented as a feasible and economical alternative for coagulants [27]. Despite the process optimization with a variety of that might result in an appreciable increase in the color removal with a consequent decrease in the chemical dosage, there still arises secondary treatment issues [28]. Electrocoagulation/floatation which offers competitive advantages over the classic coagulation techniques has drawn the interests of most researchers [84]. Activated Carbon Fiber (ACF) as an electrode material exhibited superior results in terms of dye removal as it could adsorb and catalyze almost all dye types such as direct, acidic, basic, vat, and reactive dyes [85]. However, the pH-dependency [27], consumption of space and power by the electrodes and the production of secondary sludge [86] still remains a problem.

Fenton and Fenton – like processes are non – selective color removal techniques with a narrow acidic working pH range [74], [76], [87]. Papic et al. [76] made efforts to improve decolorization, mineralization and broaden the working range of pH by coupling Fenton process with Zeolite. The by-products were adsorbed onto the solid particles instead of getting oxidized. Also, addition of zeolite did not alter the color removal remarkably. Lan et al. [87] integrated Fenton's catalyst with ACF and photoirradiation only to report 43 % mineralization which is reasonably unacceptable.

Ozonation and photo mineralization have gained popularity in the 20th century as clean and green techniques since they oxidatively degrade the dyes without the generation of any carcinogenic agents or toxicants [66], [96]-[97]. However, UV production required higher energy input [74] and ozonation was ineffective for disperse dyes [90]. Hence, photodegradation was integrated with ozonation to achieve higher mineralization rates [76]. Likewise, ozonation conjoined with hydrogen peroxide offers advantages like low radical generation costs, color and odor removal besides working efficiently at neutral pH [76]. However, at higher dosages, peroxide released O_2H radicals that had a scavenging effect on OH radical [74].

Photocatalytic oxidation with UV/H_2O_2/TiO_2 showed a superior COD and color removal at a workable alkaline pH making it suitable for real TWW treatment [88]. But TiO_2 is stable, photoactive, insoluble, and nontoxic nature metal oxide catalyst requiring higher transition energy [88]. Efforts to dope TiO_2 with several transition metals were made to lessen the transition energy while simultaneously enhancing the mineralization proved unsuccessful [91].

Further research should be pursued to improve the overall decolorization and organic load removal efficacy in the presence of surfactants, salts, and other natural suspended impurities in the TWW that impede the reaction rates.

Table 2. 1 Compilation of all the advantages and disadvantages of various destructive and non-destructive techniques

Technique		Method description	Advantages	Disadvantages	References
Non-destructive techniques	Adsorption	- Dye removal on to solid support	- Low capital expenditure - Small footprint - Simple design and easy operation - Not affected by toxicity - Superior removal of organic waste constituents	- Regeneration and replacement of sorbents is expensive - The small particle size of the adsorbent makes it difficult to separate solid and liquid - Requires efficient solid-liquid separation technique - Performance is altered by equilibrium	[40], [62], [68], [75], [77], [92]–[95]
	Membrane filtration	- Physical separation - Ultrafiltration, nanofiltration, and reverse osmosis	- Cost-effective, energy-efficient, and environmentally friendly approach - Dye and Salt recovery from the dye bath - High-quality	- Concentrated retentate requires further treatment - Pre-treatment requirement - Severe membrane scaling, fouling, and	[40], [67]–[69], [75], [77], [94], [96]

			effluent - No sludge production - Reuse of water - Moderate to low space requirements	blocking - Adsorption of dye on the membrane surface - Stability of membrane material - Prone to Concentration Polarization effect	
	Coagulation – flocculation	- Formation of large flocs for separation	- Greater color removal - Economically feasible	- Generate toxic sludge and are not suitable for large-scale applications - More energy consumption and chemicals usage	[40], [68]
Destructive techniques	Chemical oxidation	- Oxidation with a strong oxidizing agent (e.g., ClO_2)	- High efficiency	- Strongly influenced by the type of oxidant - More energy consumption and chemicals used	[14], [105]-[106]

				- Toxic sludge production in case of incomplete destruction	
	Ozonation	- Oxidation using ozone gas.	- The volume of the wastewater remains unchanged. - Single-step removal of color and organic matter - Low space requirement - Easy installation on site - Residual ozone decomposes into oxygen. - High efficiency	- Incomplete mineralization even at high dosage - High operational cost - Requires additional steps to enhance the overall decolorization efficiency.	[26], [40], [73], [98]
	AOPs	- Oxidation using H_2O_2/UV, O_3 /, UV, and H_2O_2 /O_3 / UV	- Rapid, non-selective oxidation of organic matters - Sludge free process - Complete or partial mineralization of organic	- Energy and cost-intensive	[73]–[76]

			carbon		
	Fenton process	- Oxidation using H_2O_2-Fe(II)	- Very suitable for the treatment of colored waters - High efficiency - Low cost	- Long retention time required for higher mineralization efficiency	[40], [60]
	Photocatalytic degradation	- Photo-Oxidation using TiO2 or ZnO and UV or Solar radiation	- Strong oxidizing power, non-toxic - Long-term photostability - Inexpensive catalyst	- Formation of toxic by-products - Separation of catalyst is time-consuming	[29], [40], [99]

2.4 Biological treatment techniques – and the dye removal mechanisms

Biological treatment methods are both non-destructive and destructive in nature occurring due to membrane bound adsorption and biochemical reactions by microorganisms, respectively. Microorganisms like bacteria, fungi, and algae [100]–[103] are capable of degrading azo dyes and their effectiveness depends on the survival, adaptability, and activity of the selected microorganism [104]. Bacteria efficiently degrade the most recalcitrant azo dyes, [57], [105] , unlike a Fungi and Algae with moderate decolorization rates [106]. The mechanisms involved in the cleavage of the azo dyes and their advantages and disadvantages of using different types of microbes in azo dye degradation are compiled in *Table 2.2.*

2.4.1 Advances in non-destructive biological treatment techniques

Bioaccumulation and biosorption are the two biological mechanisms in the dye removal process. Bioaccumulation is the active uptake of toxicants by living cells transported into the cell, accumulated intracellularly, across the cell membrane, and through the cell metabolic cycle. Conversely, biosorption is the passive uptake of toxicants by either live or dead microorganisms or their derivatives and is considered the primary color removal mechanism [41], [107]. The pollutant molecules diffuse to the cell surface and bind to the sites that show a chemical affinity. This step is followed by the irreversible binding of additional chemicals/pollutants which often occurs at a slower rate [41], [108], [109].

Since the 1980s microbial materials have been identified as the efficient, economical, eco-friendly and innovative options for the adsorption of pollutants from aqueous solutions containing heavy metals [110]–[112], textile dyes [43], [53], [108], [113]–[116] and hence possess great potential for application in several other fields. They are naturally occurring, abundant sources for removing pollutants and a possible alternative for expensive adsorbents like AC. Their performance is even proved to be equivalent to that of Poly Vinyl Alcohol (PVA) and sodium alginate on immobilization [108]–[111].

Won et al. [53] reported that the microbial cells' binding sites were found to be active even after 8 rounds of regeneration. Loss of cell viability or presence of suitable binding sites leads to bio-

sorption of the dyes. Cells with positively charged protein molecules often serve as good bio-sorbents for dyes with sulphonate, hydroxyl and vinyl sulfone functional groups which are anionic while those with methyl, methoxy, amine and other positively charged groups have less affinity [10], [48], [53], [102], [106].

The microbial pellets can be separated from the aqueous solution entirely by filtration, makings them a potential bio sorbent. However, their low density, low mechanical strength and low rigidity make it challenging to separate the biomass in practice. Immobilization of the biomass onto a solid matrix has overcome this problem besides retaining the native properties and improving the operation and regeneration characteristics [43], [110]. Despite all the advantages stated, bio sorption is still not ubiquitous at larger scales due to exorbitant chemicals like ethanol, methanol, and organic surfactants, further increasing the treatment costs besides transferring back the biologically adsorbed dyes to aqueous solution [53].

In the field of textile dyes, despite having emerged only a decade ago, Extracellular Polymeric Substances (EPS) is an excellent and cheap sorbent [117], [118]. The negatively charged EPS electrostatically interact with positively charged organic contaminants like basic/ cationic dyes [119]. The lipid and phosphate groups provide binding sites for Reactive dyes. The amine, carboxyl, phosphate and lipid interact with direct dyes [120]. Although the specificity of binding sites is dependent on the dye structure, there is still some ambiguity in the mechanism responsible for the migration of dye from liquid to EPS – biosorption [117], [118], [120] or chemisorption [121]. Also, the effectiveness of EPS as an effective sorbent for anionic, non-ionic, vat, and disperse dyes stands unanswered.

2.4.2 Destructive biological treatment techniques

Microbial degradation of azo dyes is a two-step process involving the breaking down of the chromophore groups leading to decolorization, followed by an aerobic or anaerobic break down of the corresponding sulphonated aromatic amines (SAAs) and AAs for the complete mineralization of the dye molecules [75], [122]–[124].

Reductive cleavage of azo bond is illustrated in the reactions below:

$2e^- + 2H^+ + (R–N=N–R_1) \rightarrow (R–NH–NH–R_1)$ (1)

$2e^- + 2H^+ + (R–NH–NH–R_1) \rightarrow (R–NH_2) + (R_1–NH_2)$ (2)

where, R and R_1 are benzene rings with various functional groups [125]

The symmetric reductive cleavage of the azo bonds (–N=N–) may involve different mechanisms such as enzymes, low molecular weight redox mediators which occurs either intracellularly or extracellularly [75], [126]. Direct enzymatic reduction of the azo bond occurs in the presence of the azo reductase enzymes [5], [133]-[134] that require electron donors like NADH, NADPH and $FADH_2$. Redox mediated reduction occurs in low molecular weight compounds, which could either be the by-products of substrates consumed by bacteria or externally added compounds [128]. These mechanisms are illustrated in *Figure 2.1*.

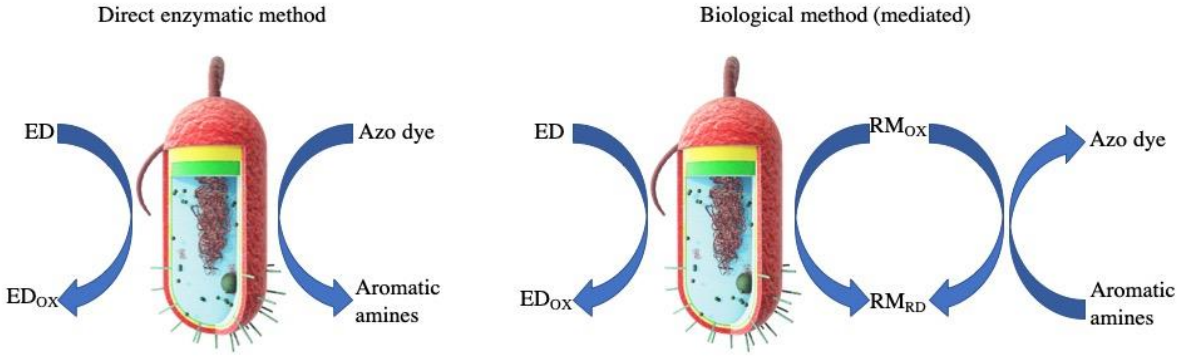

Figure 2. 1 Various azo dye reduction mechanisms (ED = Electron Donor, RM = Redox Mediator, OX= oxidizing, RD= Reducing, AD= Azo Dye, AAs= Aromatic Amines) (re-created based on [138])

Many researchers [5], [57], [129]–[134] have reported that azo reductase is the enzyme which plays an active and predominant role in the azo bond reduction. Azo reductase catalyzes the reductive cleavage of azo groups in the dye molecules via a "Bi–Bi Ping–Pong" mechanism which results in the colorless metabolites homologous to the aromatic amines, [122], [135]. These aromatic amines are resistant to anaerobic biological treatment due to toxicity effects on the microorganisms [57], [136] and are readily mineralized in aerobic or oxidative environments [56]. Therefore, complete degradation of azo dye and its intermediate products is feasible only through

the combination of anaerobic followed by aerobic conditions [135].

In contrast, a few researchers [76], [128], [137], [138] reported that the azo bond is stable in aerobic conditions due to the preferential oxidation of reduced redox mediator by oxygen, excluding a few exceptionally simple structured azo dyes like Acid Orange 7 [139]. However, Senan and Abraham [140] and Kodam et al. [141] reported aerobic degradation of more structurally complex molecules such as Reactive Red 141, Direct Yellow 86, Acid Red 260 with diazo bonds and sulfonic groups, contradicting the reports mentioned above. Taking a step ahead, Li et al. [119] investigated the aerobic degradation of a diazo dye, Congo Red, in the absence of a co-substrate. Azo reduction is reported to be accelerated in the presence of a hydroxyl group in the 2nd position of the naphthol ring while the second polar and charged groups in the vicinity of the azo group hinder the reaction [126]. *Figure 2.2* aptly depicts the abovementioned contradicting dye degradation mechanisms. *Table 2.3* lists various pure and mixed bacterial cultures that have degraded multiple dyes previously. *Figure 2.3* shows the azo dye decolorization investigated in different oxygenated conditions by various authors and particularly highlights the extensive research carried out on aerobic azo dye degradation by *Pseudomonas*.

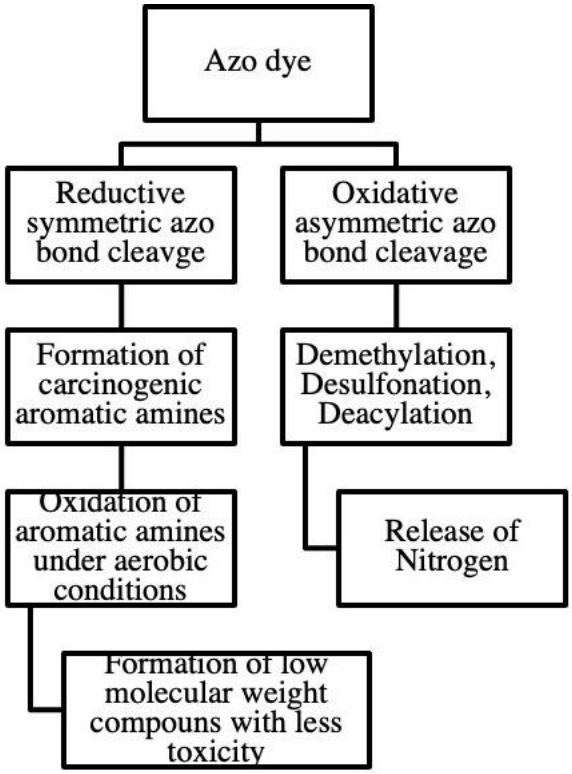

Figure 2. 2 Metabolic pathways of dye degradation [46], [47], [143]-[144], [146], [148]

Table 2. 2 Compilation of the pros and cons of all the existing biological treatment techniques

Type of micro-organisms	Method description	Pros	Cons	Possible improvements	References
Bacteria	- Two-step processes: bio decolorization and mineralization - Reduction of azo bond under anaerobic/ anoxic/ aerobic conditions - Oxidation of aromatic amines formed after reductive cleavage	- High activity, extensive distribution, and strong adaptability of the bacteria	- Aromatic amines can inhibit the activity of bacteria - Sensitive to saline conditions	- Salt-tolerant microbes or microbes that thrive in saline conditions can be exploited for their dye removal competence	[62], [69], [77], [94], [105]
Algae	- The degradation pathway is the same as the reduction	- Hydroxyl or amino groups are fully decolorized	- Poor decolorization of Methyl, methoxy, nitro, or	- Algae that have faster growth rate	[100]–[102]

	mechanism of bacteria	- Versatile ability to degrade various dyes - Ability to survive in saline conditions	Sulfo derivatives - Poor degradation of sulfated dyes - Aromatic amines are mostly not metabolized - toxic end products - low biomass specific activities	in the presence of dyes and media can be a practical solution	
Fungi	- Enzymatic degradation by extracellular and intracellular enzymes	- Non-specific enzymes degrade many aromatic compounds - Biomass served as sorbent before biodegradation - High tolerance and uptake capacities - Strong adaptability and efficiency in the removal of aromatic compounds - Degrades complex organics with	- Biodegradation requires simple carbon and nitrogen sources	- Suitable C, N sources can be utilized to support the growth of the fungi	[13], [41], [107], [142]

		extracellular ligninolytic enzymes through catalysis - High efficiency due to large surface area - Easy solid-liquid separation			

Table 2. 3 Degradation of various dyes by both mixed and pure bacterial strains

Genus	Active enzymes			Dye	η (%)	Contact time (h)	Reference
	Unmentioned	Extracellular	Intracellular				
Staphylococcus	Azo reductase	Not applicable (NA)	NA	Acid blue 113	92 – 35	70	[130]
Enterococcus	NA	NA	Azo reductase and NADH-DCIP reductase, laccase, and lignin	Direct Red 81	100	1.5	[131]
					85.74	54	
					> 80	< 10	

			peroxidase				
Bacillus	NA	Phenol oxidase[a] and NADH–DCIP reductase	Phenol oxidase[b], azo reductase and MG reductase	Reactive Orange 16	88	1	[129]
	NA	NA	Azo reductase	Polar red B	94.2	< 24	[24]
Brevibacterium	NA	Tyrosinase	NA	Reactive Yellow 107, Reactive Red 198, Reactive Black 5, and Direct Blue 71	94	168 ± 3	[143]
Pseudomonas	NA	NA	Laccase	Direct Blue 6, Green HE4B, and	100	12 – 16	[144]

				Red HE7B			
	Azo reductase	NA	-NA	Acid Yellow 17	100		[5]
	NADPH-DCIP reductase and aminopyrine N-demethylase, malachite green reductase (activity observed only after 48 h) *	Lignin peroxidase[a]	Laccase, Tyrosinase, Lignin peroxidase[b]	Direct Blue 6	88.95	72	[145]
					100 – 92	72	
					80 – 40	72	
					100	60	
					100	72	
					15	72	
	Laccase	NA	NA	B15; B19; B31; B36; B54; B69; B86; R34; R90; R91; Y15; Y79; Y87 and	> 80 (*P. oleovorans* only)	48	[146]

				Methyl orange			
	Azo reductase	NA	NA	Orange 2			[126]
	NA	NA	NA	Reactive black 5	98.5	48	[17]
	NA	NA	Azo reductase	Reactive red 22	> 95	120	[127]
Exiguobacterium	Laccase and azo reductase	Lignin peroxidase	NA	Navy blue HE2R	up to 91.2	48	[132]
Paenibacillus	NA	NA	Azo reductase	Reactive Red 195	> 95	-	[133]
Stentrophomonas	Unknown	NA	NA	SITEX Black, an industrial effluent rich in black sulfur dye	82	24	[147]

Marinobacter	Unknown	NA	NA	Direct Blue 1	100	6	[18]
Providencia	NA	Lignin peroxidase	Lignin Peroxidase, Laccase, Tyrosinase, Azo reductase, and DCIP Reductase	Acid Black 210	100	1.5	[134]
Nocardiopsis	NA	NA	NA	Reactive orange 16	95	< 24	[54]
Micrococcus	Lignin peroxidase, Laccase, Azo reductase, Riboflavin reductase, and NADH–DCIP reductase	NA	NA	Reactive Green 19A	100	42	[148]

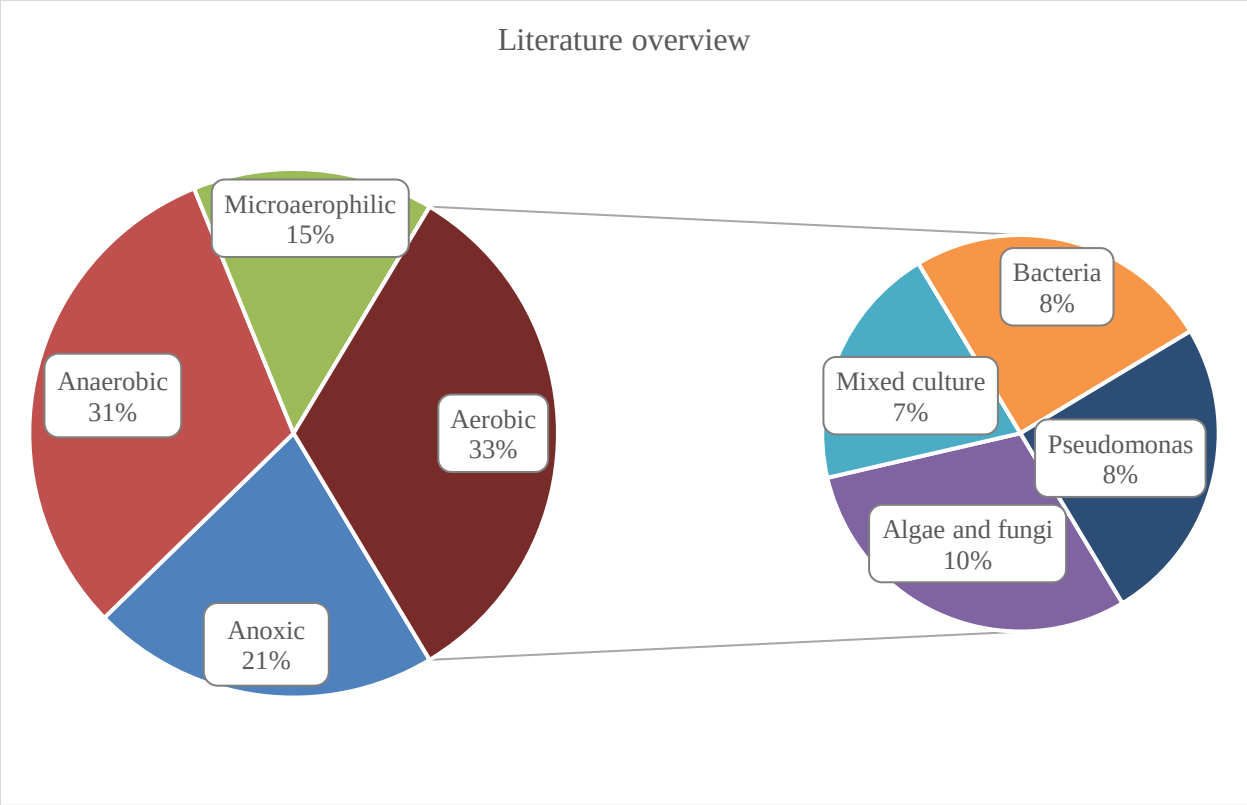

Figure 2. 3 Literature overview on biodegradation of azo dyes (created based on the literature survey on [4], [5], [7], [8], [25], [26], [28], [29], [31], [41], [44]–[47], [71], [72], [106], [109], [111]–[116], [128]–[130], [132]–[134], [136]–[141], [143], [144], [147]-[148], [150], [152]–[169])

2.5 Research gaps

In summary, the existing individual and combined Physico-chemical treatment techniques may not effectively remove all types of dyes at neutral or alkaline pH without compromising the process efficacy. Membrane technologies are often suitable for reactive and disperse dye removal. Adsorption works best for basic dyes at alkaline conditions. Coagulation/ flocculation is suitable for acid dyes removal. AOPs are non-selective techniques, suitable for a variety of dyes such as - direct, acidic, basic, reactive and vat dyes. But they are cost and energy intensive and sometimes produce toxic end-products requiring further treatment. Though time consuming, microbiological techniques attain a higher degree of dye removal and degradation resulting in innocuous end-products. It is also a sustainable, eco-friendly, cost-competitive, and non-substrate specific approach. Most importantly, there is no secondary sludge disposal problem arising. Hence, this

thesis focuses on microbial degradation of dyes. Based on the literature study and the observations made from the *Figure 2.3* the following research gaps were identified:

- Since azo bond is stable in aerobic conditions due to the preferential oxidation of reduced redox mediator by oxygen [139], only anaerobic azo reduction is well documented and very little information is available on the aerobic dye degradation [130].
- *Pseudomonas sp.*, an opportunistic pathogen [162], is the extensively researched in the aerobic degradation of dyes [5], [17], [38], [126], [127], [144]–[146]. Hence, there is a need to identify less pathogenic microbe(s) that can aerobically degrade dyes more effectively.
- Salinity, another consequence of the TWW, significantly impedes the bacterial activity especially in aerobic conditions [76], [128], [137], [140]. Lack of sufficient information on the biological dye removal under the influence of salts remain a bottleneck to interpret the decolorization kinetics and understand the mechanisms involved.

Based on these research gaps, a research problem was identified for the present study and the aims and objectives were formulated.

2.6 Research objectives and scope

In the light of the aforenamed views, the overall aim of this study is to holistically remove the azo dyes using a halotolerant, non-pathogenic bacterium under the influence of salts and to track the degradation by-products. Following are the specific objectives of this study:

- To isolate and identify a halotolerant, non-pathogenic microbe
  - Study various bacterial sources locally available and choose the most efficient source
  - Use the efficient bacterial source to isolate a robust microbe upon shock-loading the culture with 1000 mg/L of dye as a sole carbon source
  - Identify the bacteria
- To evaluate the dye removal potential of the isolate
  - Test the isolate in oxygen-rich and deficient conditions to identify the optimal incubation conditions for the different azo dyes investigated in this study
  - Evaluate the dye decolorization efficiency of the isolate under the influence of chlorides and sulfates

- Study the effect of dye and high salt dosage induced stress on the growth of the isolate
- Evaluate the degree of decolorization and degradation

- To track the fate of the azo dyes post degradation
  - Establish a degradation mechanism
  - Track the fate of the dyes upon degradation and identify the compounds
  - Discuss the environmental significance and the toxicity of the by-products identified

2.7 Research significance

All the three research objectives were achieved in this study which led to several novel outcomes:

1. Isolated and identified a halotolerant facultative anaerobe - *Klebsiella pneumoniae* strain dye1, which can withstand the adverse environmental stress due to dye toxicity and high saline concentrations.
2. In contrast to various previous studies, *Klebsiella* aerobically decolorized and degraded Acid blue 113 under the influence of high salt dosages.
3. Successfully decolorized sulfonated reactive and direct azo dyes in microaerobic conditions
4. Contradicting earlier studies, *Klebsiella* decolorized diazo dyes faster than mono azo dye. This signifies the role of steric hinderance due to functional groups and the structural linearity of the dye besides the number of azo bonds or the molecular weight of the dyes
5. Proposed dye degradation pathways for three industrially important azo dyes with metabolites that were not previously reported nor available on the mass spectral libraries.

Chapter 3 MATERIALS AND METHODS

3.1 Chemicals and media

All the chemicals used in the experiment are of analytical grade. AB113 (purity 50 %), DR81 (purity 50 %), RO16 (purity ≥ 70 %) were obtained from Sigma Aldrich, Singapore. The dimensions of the dyes were computed on Avogadro software version 12.0. M9 minimal medium [163] spiked with 1700 ppm of chlorides and 560 ppm of sulfates for all the dye decolorization experiments as mentioned elsewhere [164]. The autoclaved medium was then supplemented with 100 ± 10 mg/L of sterile-filtered dyes.

3.2 Isolation of the microbes

Besides possessing the capability of degrading SAAs [25], [130], [135], [156], [157] and high sorption capacity [106], biomass from industrial and domestic sewage treatment plants can withstand the extreme dye toxicity [3]. Similar to the study by [92], Activated sludge (AS) was collected from Jurong water reclamation plant, Singapore, that treats wastes from petrochemical, electroplating, pharmaceuticals and food industries. To induce stress, 1700 mg/L of chlorides and 560 mg/L of sulphates were used [164] besides shock loading with 1000 mg/L of Acid yellow 17, as a sole carbon source was supplemented to thickened AS, maintained at VSS 6.122 ± 0.178 g/L in the conical flask. As a result, all the incompetent strains are knocked down. After 48 h of incubation, 1 mL of culture was serially diluted and plated on the agar plate containing M9 minimal media and 1000 mg/L of AY17. Four distinct microbial colonies were identified and isolated from a petri plate with dilution factor 100 (shown in *Figure 3.1*). Subsequently, to obtain pure strains, all the four colonies were passed through three rounds of subcultures. Replicates of pure cultures were stored at – 80 °C as stock in 50 % glycerol.

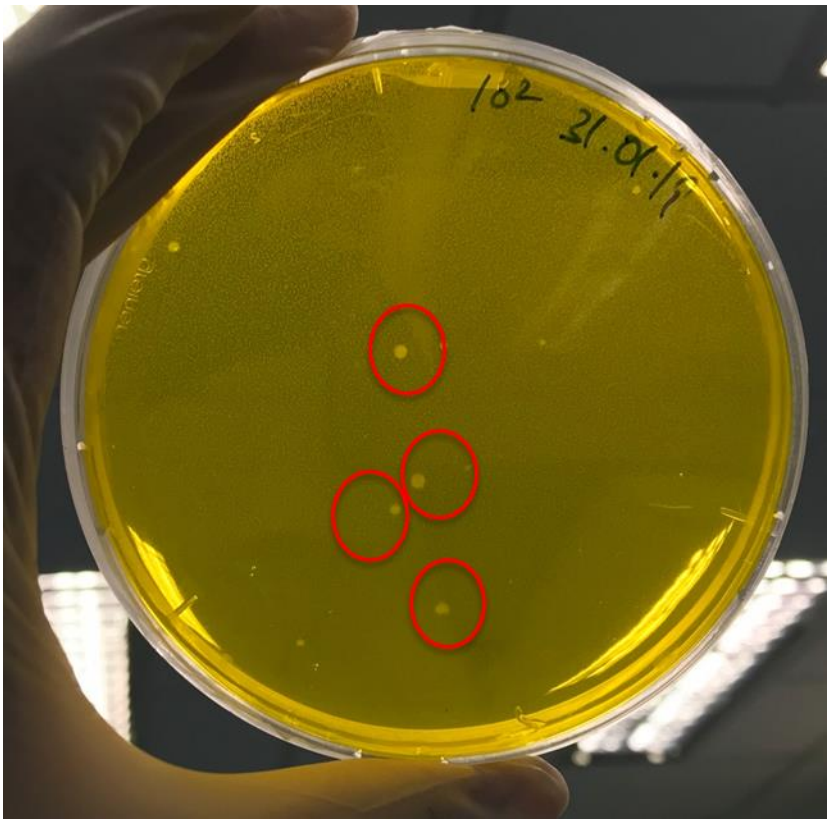

Figure 3. 1 Identification of 4 distinct colonies (circled in red) on a petri dish with inoculum diluted to 100 times

3.2.1 DNA extraction

48 h cultures grown in M9 minimal media are centrifuged at 7000 rcf for 5 min to separate the pellets. The pellets are washed with 0.1 M Potassium phosphate buffer solution (PBS) twice to remove any impurities and resuspended in the 0.1 M PBS to a final volume of 1 mL. Genomic DNA of the isolate was extracted using Fast DNA spin kit for soil (MP Bio, Singapore) following the standard extraction protocol as described in the manual. The final DNA elution volume was 100 µL. The extracted DNA was stored at - 20 ℃ until further use.

3.2.2 Bacterial growth curves

Stock cultures were grown in M9 minimal media at 37°C in a temperature controlled shaking incubator. The 24 h cultures from the same were used as the seed cultures for the bacterial growth curve study. The cell cultures were maintained in M9 minimal media and transferred to 96 well plate with the initial cell concentrations adjusted to 0.01%. [165], [166] and the same was repeated with the media spiked with salts as mentioned in *section 3.1*. The Optical density was measured

by an automated program on microplate reader with the incubation temperature set to 37°C (Tecan microplate reader, Singapore). From *Figures 3.2 & 3.3*, it is evident that the *AZD3_KP_dye1* is the most active organism of all the four even in the high saline stress conditions and therefore was chosen for the dye degradation experiments in this study.

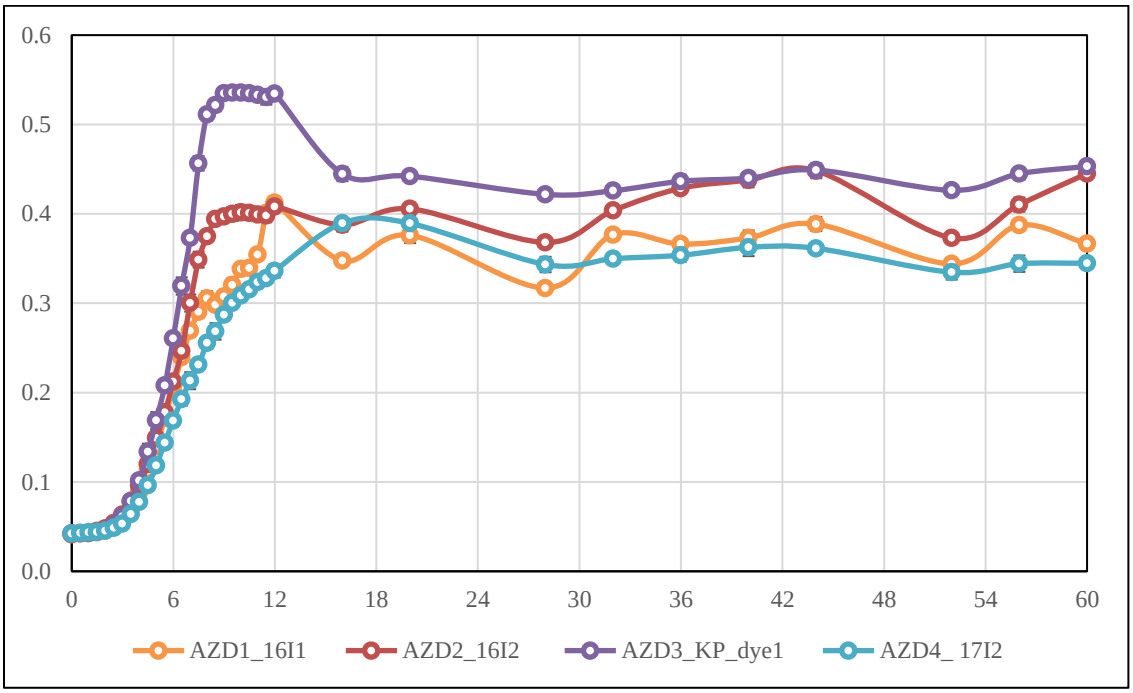

Figure 3. 2 Bacterial growth curves of the four isolates in M9 minimal media

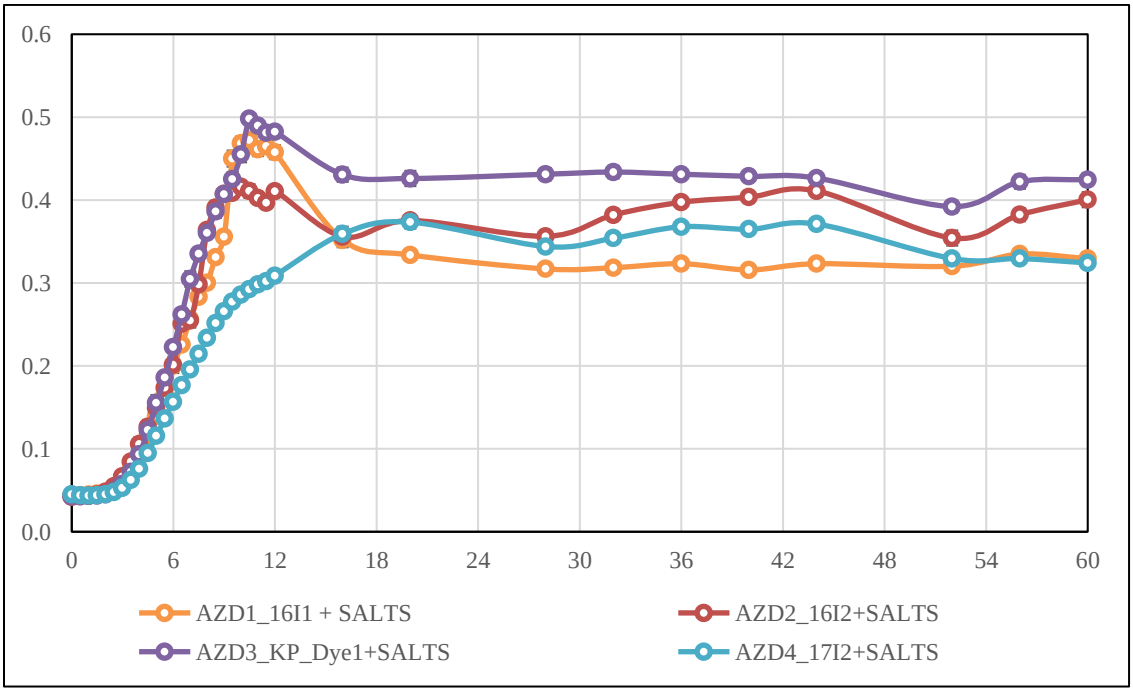

Figure 3. 3 Bacterial growth curves of the four isolates in M9 minimal media spiked with salts

3.2.3 Identification of the microbes

Genomic DNA of all the four isolates were sequenced by Sanger sequencing. The trimmed forward and reverse sequences of 16S rRNA were assembled on a web based tool, CAP3 [167]. The alignment search was carried out on web-based Basic Local Alignment Search Tool (BLAST) on National Centre for Biotechnology Information (NCBI) (https://www.ncbi.nlm.nih.gov/). Twelve identical species were chosen for the phylogenetic reconstruction. Neighbor-joining (NJ) algorithm, was used with Kimura 2 parameter model and bootstrap values calculated from 500 replicate runs, keeping the other default settings in the [168], [169] MEGAX software version 10.1.8-1 [170]. The results for minimum evolution and maximum likelihood algorithms were found to be similar. *Figure 3.4* shows the phylogenetic relationship between the four isolates and other closely related microorganisms retrieved from GenBank 16S database. In the phylogenetic tree, the number at nodes represent the percentage of the replicate trees in which the associated taxa clustered together in the bootstrap test based on data for 500 replications and numbers in parenthesis represent GenBank accession numbers. It is evident that the isolates belong to *Klebsiella* and *Enterobacter* genera.

The sequence of the most active and halotolerant strain AZD3_KP_dye1 is named as *Klebsiella Pneumoniae_dye1*. It is submitted to GenBank (https://www.ncbi.nlm.nih.gov/genbank/) and can be accessed with accession ID: MW13240. It is 99.72 % identical to *K. pneumoniae* DSM 30104 (accession no: NR_117683.1).

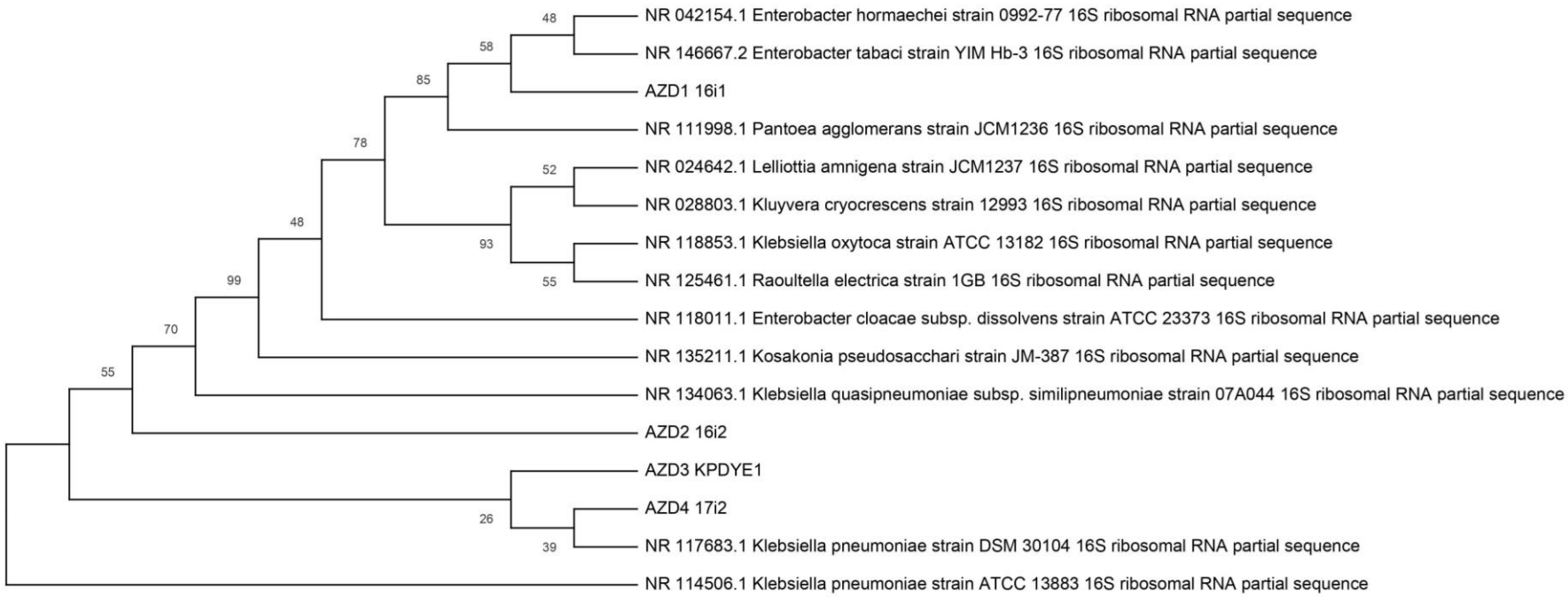

Figure 3. 4 Bootstrap consensus tree with GenBank Accession numbers in the parenthesis

3.2.4 Metabolic pathway annotation

The whole genome of the most active isolate *KP_dye1* was sequenced, assembled, and further annotated on PROKKA (Rapid Prokaryotic Genome Annotation) for the whole genome. The output of PROKKA was used for functional annotation of the pathways on KAAS (KEGG Automatic Annotation Server) to understand the cellular processes such as metabolic pathways, cell cycle etc. KEGG stands for Kyoto Encyclopedia of Genes and Genomes and can be accessed at KEGG: Kyoto Encyclopedia of Genes and Genomes. Bi-directional Best Hit (BBH) method was chosen to assign the orthologs on KAAS (KAAS - KEGG Automatic Annotation Server (genome.jp))**.** The results contained the automatically generated pathways, KEGG Orthology (KO) and the enrichment numbers as given in *Table 3.1*. The isolate has metabolic pathways that could possibly degrade toxic aromatic compounds such as azo dyes in this study highlighted in the pie chart in *Figure 3.5*. To investigate the same, the decolorization assays were performed as given in *Section 3.3.*

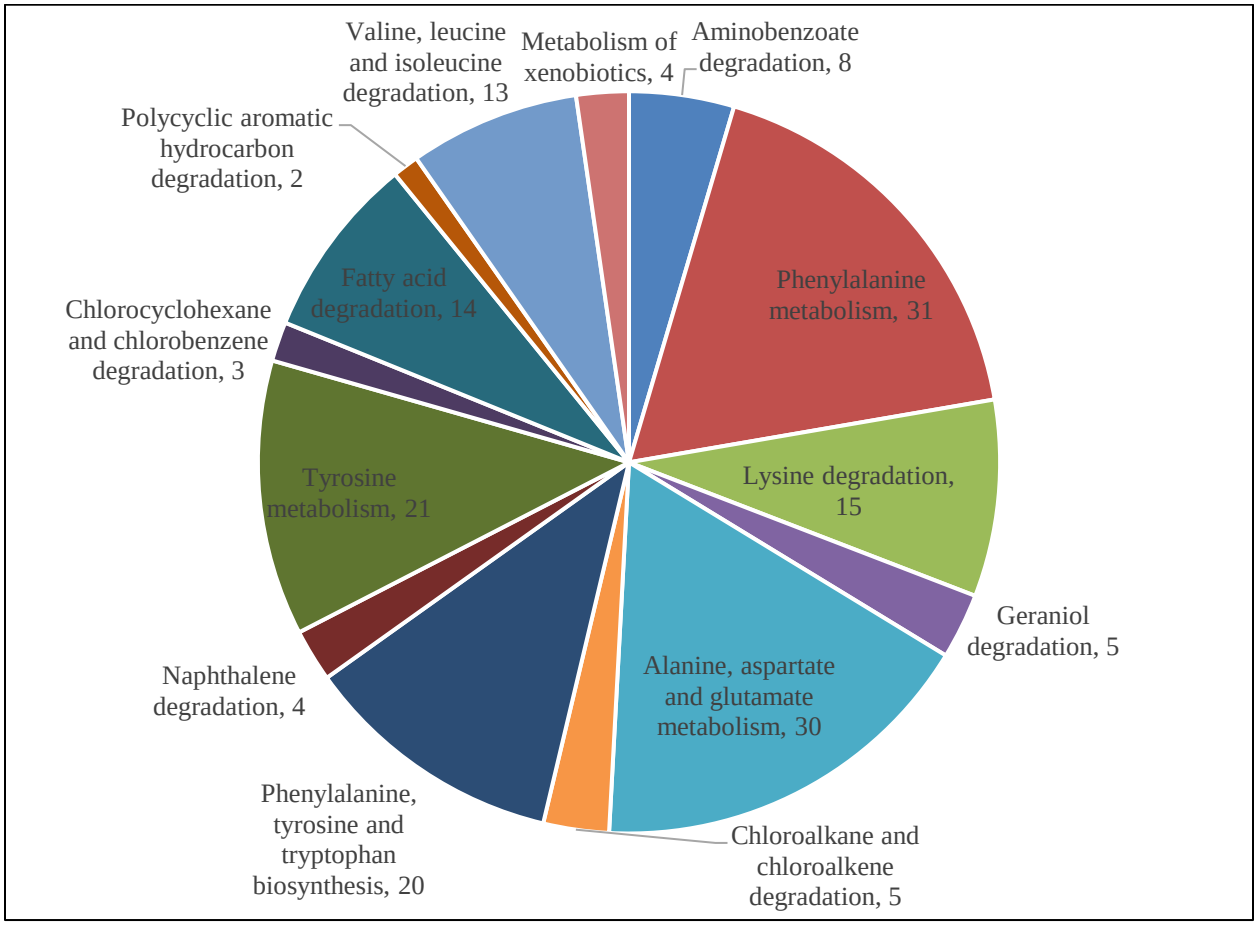

Figure 3. 5 Degradation metabolic pathways of the Whole genome of *KP_dye1*

Table 3. 1 Metabolic pathway annotation of the Whole genome of KP_dye1

KO & Metabolic pathway	Enrichment number
02010 ABC transporters	205
02020 Two-component system	105
00230 Purine metabolism	63
00620 Pyruvate metabolism	57
02024 Quorum sensing	54
03010 Ribosome	44
00010 Glycolysis / Gluconeogenesis	43
00240 Pyrimidine metabolism	43
00270 Cysteine and methionine metabolism	43
03070 Bacterial secretion system	43
00190 Oxidative phosphorylation	41
00520 Amino sugar and nucleotide sugar metabolism	40
02060 Phosphotransferase system (PTS)	40
00260 Glycine, serine and threonine metabolism	38
02026 Biofilm formation - Escherichia coli	38
00051 Fructose and mannose metabolism	35
00860 Porphyrin and chlorophyll metabolism	35
00640 Propanoate metabolism	34
00500 Starch and sucrose metabolism	33
01503 Cationic antimicrobial peptide (CAMP) resistance	33
00650 Butanoate metabolism	31
00920 Sulfur metabolism	31
00360 Phenylalanine metabolism	31
00720 Carbon fixation pathways in prokaryotes	30
00250 Alanine, aspartate and glutamate metabolism	30
00362 Benzoate degradation	30
00630 Glyoxylate and dicarboxylate metabolism	28
00540 Lipopolysaccharide biosynthesis	28
05111 Biofilm formation - Vibrio cholerae	28
00030 Pentose phosphate pathway	27
00040 Pentose and glucuronate interconversions	27
00020 Citrate cycle (TCA cycle)	26
00680 Methane metabolism	26
03440 Homologous recombination	26
00052 Galactose metabolism	25
00564 Glycerophospholipid metabolism	24
00330 Arginine and proline metabolism	24
00790 Folate biosynthesis	24
00760 Nicotinate and nicotinamide metabolism	23
00970 Aminoacyl-tRNA biosynthesis	23

00130 Ubiquinone and other terpenoid-quinone biosynthesis	22
00350 Tyrosine metabolism	21
00480 Glutathione metabolism	21
03430 Mismatch repair	21
00561 Glycerolipid metabolism	20
00400 Phenylalanine, tyrosine and tryptophan biosynthesis	20
00550 Peptidoglycan biosynthesis	20
01501 beta-Lactam resistance	20
00770 Pantothenate and CoA biosynthesis	18
00910 Nitrogen metabolism	17
00220 Arginine biosynthesis	17
03060 Protein export	17
04122 Sulfur relay system	17
03018 RNA degradation	17
03030 DNA replication	16
00310 Lysine degradation	15
00053 Ascorbate and aldarate metabolism	14
00710 Carbon fixation in photosynthetic organisms	14
00061 Fatty acid biosynthesis	14
00071 Fatty acid degradation	14
00300 Lysine biosynthesis	14
00450 Selenocompound metabolism	14
00740 Riboflavin metabolism	14
02025 Biofilm formation - Pseudomonas aeruginosa	14
00280 Valine, leucine and isoleucine degradation	13
00290 Valine, leucine and isoleucine biosynthesis	13
00340 Histidine metabolism	13
00780 Biotin metabolism	13
01053 Biosynthesis of siderophore group nonribosomal peptides	13
03410 Base excision repair	13
00410 beta-Alanine metabolism	12
00541 O-Antigen nucleotide sugar biosynthesis	12
00900 Terpenoid backbone biosynthesis	12
00983 Drug metabolism - other enzymes	12
00670 One carbon pool by folate	11
04112 Cell cycle - Caulobacter	11
00660 C5-Branched dibasic acid metabolism	10
00562 Inositol phosphate metabolism	10
00380 Tryptophan metabolism	10
00730 Thiamine metabolism	10
00622 Xylene degradation	10

00440 Phosphonate and phosphinate metabolism	9
00750 Vitamin B6 metabolism	9
00195 Photosynthesis	8
00261 Monobactam biosynthesis	8
00627 Aminobenzoate degradation	8
00364 Fluorobenzoate degradation	7
03420 Nucleotide excision repair	7
05230 Central carbon metabolism in cancer	7
00430 Taurine and hypotaurine metabolism	6
00460 Cyanoamino acid metabolism	6
00470 D-Amino acid metabolism	6
00960 Tropane, piperidine and pyridine alkaloid biosynthesis	6
00521 Streptomycin biosynthesis	6
04922 Glucagon signaling pathway	6
04212 Longevity regulating pathway - worm	6
04626 Plant-pathogen interaction	6
05133 Pertussis	6
00281 Geraniol degradation	5
00625 Chloroalkane and chloroalkene degradation	5
00623 Toluene degradation	5
04066 HIF-1 signaling pathway	5
04146 Peroxisome	5
04217 Necroptosis	5
05208 Chemical carcinogenesis - reactive oxygen species	5
05418 Fluid shear stress and atherosclerosis	5
01502 Vancomycin resistance	5
00903 Limonene and pinene degradation	4
00401 Novobiocin biosynthesis	4
00621 Dioxin degradation	4
00626 Naphthalene degradation	4
00980 Metabolism of xenobiotics by cytochrome P450	4
00982 Drug metabolism - cytochrome P450	4
02030 Bacterial chemotaxis	4
04213 Longevity regulating pathway - multiple species	4
05200 Pathways in cancer	4
05134 Legionellosis	4
05415 Diabetic cardiomyopathy	4
00600 Sphingolipid metabolism	3
00785 Lipoic acid metabolism	3
00830 Retinol metabolism	3
00940 Phenylpropanoid biosynthesis	3
00950 Isoquinoline alkaloid biosynthesis	3
00333 Prodigiosin biosynthesis	3

00361 Chlorocyclohexane and chlorobenzene degradation	3
00791 Atrazine degradation	3
00930 Caprolactam degradation	3
04016 MAPK signaling pathway - plant	3
04070 Phosphatidylinositol signaling system	3
02040 Flagellar assembly	3
03320 PPAR signaling pathway	3
05120 Epithelial cell signaling in Helicobacter pylori infection	3
05132 Salmonella infection	3
05152 Tuberculosis	3
05014 Amyotrophic lateral sclerosis	3
05016 Huntington disease	3
05022 Pathways of neurodegeneration - multiple diseases	3
05417 Lipid and atherosclerosis	3
01523 Antifolate resistance	3
00590 Arachidonic acid metabolism	2
00592 alpha-Linolenic acid metabolism	2
01040 Biosynthesis of unsaturated fatty acids	2
00603 Glycosphingolipid biosynthesis - globo and isoglobo series	2
00523 Polyketide sugar unit biosynthesis	2
00966 Glucosinolate biosynthesis	2
00332 Carbapenem biosynthesis	2
00525 Acarbose and validamycin biosynthesis	2
00633 Nitrotoluene degradation	2
00643 Styrene degradation	2
00624 Polycyclic aromatic hydrocarbon degradation	2
03020 RNA polymerase	2
03008 Ribosome biogenesis in eukaryotes	2
04068 FoxO signaling pathway	2
04152 AMPK signaling pathway	2
04216 Ferroptosis	2
04621 NOD-like receptor signaling pathway	2
04910 Insulin signaling pathway	2
04918 Thyroid hormone synthesis	2
04964 Proximal tubule bicarbonate reclamation	2
04724 Glutamatergic synapse	2
04727 GABAergic synapse	2
04211 Longevity regulating pathway	2
04714 Thermogenesis	2
05206 MicroRNAs in cancer	2
05207 Chemical carcinogenesis - receptor activation	2

05225 Hepatocellular carcinoma	2
05340 Primary immunodeficiency	2
05012 Parkinson disease	2
04931 Insulin resistance	2
01524 Platinum drug resistance	2
00565 Ether lipid metabolism	1
00591 Linoleic acid metabolism	1
00531 Glycosaminoglycan degradation	1
00542 O-Antigen repeat unit biosynthesis	1
00511 Other glycan degradation	1
00572 Arabinogalactan biosynthesis - Mycobacterium	1
00981 Insect hormone biosynthesis	1
00908 Zeatin biosynthesis	1
01051 Biosynthesis of ansamycins	1
01055 Biosynthesis of vancomycin group antibiotics	1
00965 Betalain biosynthesis	1
00524 Neomycin, kanamycin, and gentamicin biosynthesis	1
00405 Phenazine biosynthesis	1
00998 Biosynthesis of various secondary metabolites - part 2	1
00642 Ethylbenzene degradation	1
04141 Protein processing in endoplasmic reticulum	1
04013 MAPK signaling pathway - fly	1
04011 MAPK signaling pathway - yeast	1
04072 Phospholipase D signaling pathway	1
04151 PI3K-Akt signaling pathway	1
04214 Apoptosis - fly	1
04622 RIG-I-like receptor signaling pathway	1
04612 Antigen processing and presentation	1
04659 Th17 cell differentiation	1
04657 IL-17 signaling pathway	1
04920 Adipocytokine signaling pathway	1
04915 Estrogen signaling pathway	1
04914 Progesterone-mediated oocyte maturation	1
04917 Prolactin signaling pathway	1
04919 Thyroid hormone signaling pathway	1
04970 Salivary secretion	1
04972 Pancreatic secretion	1
04973 Carbohydrate digestion and absorption	1
04975 Fat digestion and absorption	1
04978 Mineral absorption	1
04361 Axon regeneration	1
05205 Proteoglycans in cancer	1

05204 Chemical carcinogenesis - DNA adducts	1
05203 Viral carcinogenesis	1
05231 Choline metabolism in cancer	1
05211 Renal cell carcinoma	1
05219 Bladder cancer	1
05215 Prostate cancer	1
05165 Human papillomavirus infection	1
05130 Pathogenic Escherichia coli infection	1
05131 Shigellosis	1
05146 Amoebiasis	1
05142 Chagas disease	1
05143 African trypanosomiasis	1
05010 Alzheimer disease	1
05020 Prion disease	1
04930 Type II diabetes mellitus	1
04940 Type I diabetes mellitus	1
04934 Cushing syndrome	1

3.3 Decolorization assay

All decolorization experiments were performed in triplicates with an abiotic and biotic medium as the control. All the results stated are the mean of the three values. In a 250 mL Erlenmeyer conical flask, 150 mL of sterile M9 minimal media spiked with salts and dye was inoculated with 45 mg (dry weight) of live cells to maintain the food to biomass ratio as 1:3 (w/w). Decolorization assays performed with and without M9 media spiked with dye and salts represented as “co-metabolism (COM)” and “standalone pathway (STA)” respectively. The conical flasks were covered with 0.22 µm sterile filters and incubated in a temperature-controlled incubator shaker (Sartorius, Japan) at 37 °C and away from direct light as shown in *Figure 3.3*. The experiment was carried out in both shaking and static conditions with the orbital shaking speed adjusted to 120 rpm and 0 rpm referred to as aerobic [7], [23], [141] and microaerobic [19] respectively henceforth. Microaerobic condition refers to no aeration and no agitation. 5 mL aliquots of the culture media were sampled at periodic time intervals till the dye is completely disappeared or equilibrium is achieved in the concentration of the dye.

Figure 3. 6 Decolorization assay performed in conical flasks incubated in a temperature-controlled incubator

3.4 Biosorption – desorption assay

Klebsiella pneumoniae strain dye1 was cultured in M9 minimal media and harvested after 24h. The harvested pellets were inactivated by autoclaving and washed with DI water twice to remove any enzyme co-factors that are postulated to be released upon cell lysis [171]. The pellets were then reconstituted with DI water and stored at room temperature till further use.

To determine the biosorptive capacity of the biomass, a biosorption and desorption assay was carried out by incubating the dyes with the autoclaved cells with the experimental conditions as mentioned in *Section 3.3.* 5 mL aliquots of the culture media were sampled at periodic time intervals till the dye could no longer be removed or equilibrium is achieved in the concentration of the dye, which is 6 hours. The pellets were separated from the supernatant upon sampling and the supernatant is analyzed for the residual dye concentration.

The pellets were reconstituted to the same volume with 100 % methanol, vortexed at full speed for 5 min and centrifuged at 7000 rcf. The supernatant was analyzed for the desorbed dye from the cells.

3.5 Phytotoxicity assay

A standard seed germination bioassay was performed to investigate the toxicity of the treated effluent using *Vigna radiata* seeds (mung beans) [172]. The experiments were conducted in sterile disposable petri plate with a layer of filter paper (Whatman no. 1) on the top of a cotton bed layer. Each plate contained 5 mL of the treated effluent or control and 5 seeds which were washed once before use. The plates were covered with lid and incubated in the dark at 28 °C for 48 h to let the seeds germinate. Germination rate and sprout length were recorded at specific time intervals and used as the toxicity indicators [173].

3.6 Analytical techniques

3.6.1 UV-VIS spectrophotometer analysis

The supernatant obtained by centrifugation at 7000 rcf for 5 min at 25 °C was used to detect absorbance at their respective peaks (indicated in *Table 3.2*) for each dye on a UV Visible Spectrophotometer (UV-VIS 1200, Shimadzu, Singapore) to quantify the decolorization. Percentage of decolorization was determined using the formula mentioned in *Equation 1*. The density of the cell pellet obtained after centrifugation was monitored at 600 nm (denoted as OD_{600}).

$$\boldsymbol{EFFICIENCY}(\%) = \left(\mathbf{1} - \frac{\boldsymbol{F}}{\boldsymbol{I}}\right) * \mathbf{100} \qquad (1)$$

Where, I = Concentration of the sample at the 0^{th} hour

F = Concentration of the sample at the n^{th} hour

Table 3. 2 Peak wavelength and molecular weight of the dyes under the current investigation (* represent the peak considered for the calibration of the instrument)

Dye	λ_{max} (nm)	Molecular weight (g/mol)	TOC (ppm)	TN (ppm)
AB113	568 *	681.65	34.13	1.611
DR81	538 * & 398	675.6	47.44	2.663
RO16	492.5 * & 387	617.54	33.42	1.457

Table 3. 3 Conductivity and Total Dissolved Salts (TDS) content of the samples

Sample ID	Conductivity (us/cm)	TDS (ppm)
AB113 STA	6600	3270
AB113 COM	16730	8370
DR81 STA	6800	3410
DR81 COM	16170	8120
RO16 STA	6770	3420
RO16 COM	16870	8490
Abiotic control with salts	16690	8360
Abiotic control	10990	5450

3.6.2 Organic load measurement

Total organic carbon (TOC) and Total Nitrogen (TN) contents were measured on TOC and TN analyzer (TOC-L and TNM-L, Shimadzu, Japan) equipped an autosampler (ASI-L, Shimadzu, Japan) by adopting the standard procedures [174]. The control and treated samples were diluted 30 times before injection to ensure the concentration fell in the calibration concentration range. The TOC and TN values for 100 ppm of dyes are as measured in *Table 3.2.*

3.6.3 EC and TDS measurement

The EC and TDS of the samples were measured on benchtop pH meter (Seven go duo, Mettler Toledo, Singapore.) and are as given in *Table 3.3.*

3.6.4 FTIR spectroscopy

One mL of the supernatant was frozen at –80 °C and freeze-dried overnight to obtain the sample residue analyzed on ATR setup of FTIR (FT-IR Spectrum 2000, PerkinElmer, Singapore). The mid IR region of 400 – 4000 cm^{-1} was the scanning range. Spectra was first calibrated for background signal scanning with a control sample i.e., air before the experimental sample was scanned. Transmittance of the samples was recorded and correlated with the standard table for infrared spectroscopy to determine the changes in the functional groups compared to the dye standard sample.

3.6.5 LC-QTOF-MS/MS analysis

The polymeric strong cation strata-XC-33 µm solid-phase extraction (SPE) cartridge was purchased from Phenomenex, Singapore. Standard sample preparation procedure was slightly modified: The cartridge was activated with 1 mL of MeOH and washed with 1 mL of acidified water. One mL of acidified sample with pH < 2 was loaded onto the cartridge which was washed with 0.5 mL of 0.1 N HCl in water twice. The sample was eluted twice with 0.5 mL of 5 % NH_4OH in MeOH. All the samples obtained were diluted 10 times before injecting into LC-MS.

The untargeted chromatographic analysis was performed on HPLC (HPLC 1290 Infinity II, Agilent Technologies, Singapore) in positive mode, interfaced with an Agilent 6460 electrospray triple quadrupole mass spectrometer (ESI-MS/MS; Agilent Technologies, Singapore) in MS^2 scan mode. Separation of the analytes was obtained with a Luna Omega Polar C18 column (100x2.1 mm, 1.6 µm particle size, Phenomenex, Singapore). 10 mM ammonium formate in water (A) (adjusted to pH 3.2 with formic acid) and 100 % acetonitrile (B) consisted of the mobile phases. The gradient elution program for chromatographic separation is as follows: 0 % B for 0 to 5 min, 25 % B at 10 min (50 % B at 15 min, 100 % B for 20 to 25 min, 50 % B at 26 min and returned to 0 % B at 30 min; with a flow rate set at 0.3 mL/min. The column temperature, gas temperature and sheath gas heater were set at 40 °C, 300 °C and 300 °C respectively. Sample injection volume was 5 µL. Gas and sheath gas flow rate were 10 L/min and 11 L/min, respectively. Nebulizer pressure was 25 psi. Capillary accelerator voltage, Capillary voltage and electron multiplier voltage were 7

V, 5000 V and 400 V, respectively. 2 to 1000 was the scanning range for mass to charge ration (m/z).

The data acquisition protocol was same for both control and treated samples. The precursor ions of unknown metabolites from treated samples were scanned for their product ions (PIs) and are confirmed upon comparing their spectrum with spectral databases and literature.

3.7 Determination of dry biomass weight

The bacterial cells were harvested and diluted to achieve different optical densities. These cells were then filtered through What-man No. 1 filter paper that were dried at 100 °C to a constant weight. The biomass retained on the filter paper was dried at 100 °C overnight to achieve a constant weight [175]. The difference in the weight was determined to find the biomass weight at the respective OD_{600}. A standard curve was plotted based on the OD_{600} and its respective biomass weight which is depicted in *Figure 3.7*. This plot is used for the conversion of OD_{600} to biomass concentration throughout this study

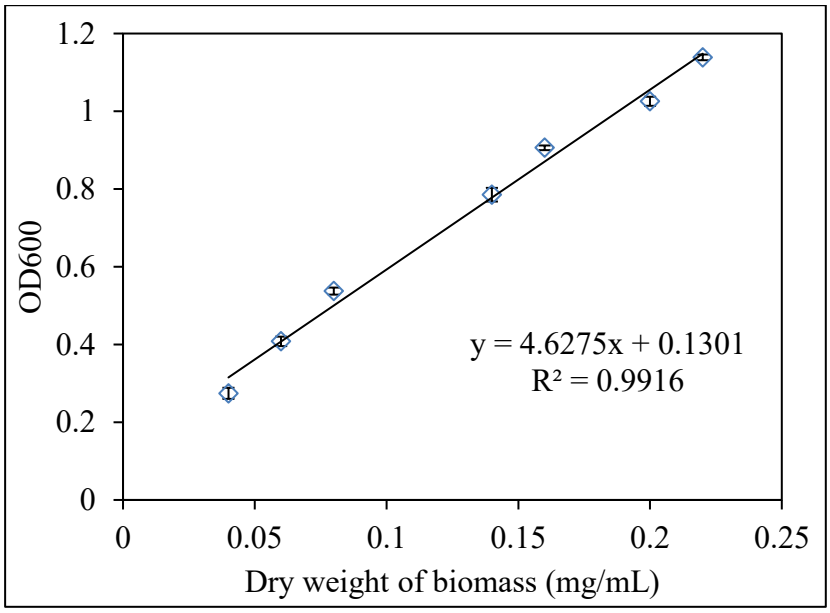

Figure 3. 7 OD_{600} vs. weight of biomass

Chapter 4 DECOLORIZATION AND DEGRADATION OF AZO DYES

4.1 Introduction

Dyes are one of the most apparent environmental pollution indicators due to their color and have high oxygen demand due to their organic strength [118]. It has been established that large amounts of dyes that are applied to fabrics end up being wasted, and the figures are speculated somewhere between 10 % to 50 % [10], [176]. Besides causing aesthetic issues to the water bodies, they are highly toxic, mutagenic, carcinogenic, and teratogenic [176], [177], and pose serious health problems in humans when they come in contact [16].

More than half of all the dyes listed in the Color Index (CI) are azo dyes holding approximately 70 % of the world's dye market [8], [31], [32]. Azo dyes are integral components of textile industries due to their ease in preparation, low cost, chemical stability, and application versatility [8], [31], [32], [51]. Anionic dyes are sulfonated azo dyes that are relatively smaller in size, with greater water solubility, and are more recalcitrant than the carboxylated ones [1], [18], [34], [36], [141], hence they are not easily converted to CO_2 by physical and chemical treatment methods [178]. In addition to that, the conventional WWTPs are deemed ineffective as most dyes are resistant to aerobic degradation [10]. Nevertheless, from the sustainability and effective utilization of resources viewpoints, microbial degradation is the most promising and economical treatment method for removing dyes from TWW [4], [16]. Besides that, the possibility to reclaim and reuse the decolorized water would contribute to over-all waste reduction [10].

Hence, many researchers investigated bacterial degradation under oxygen deficit conditions [56] which in turn resulted in the release of AAs that are mutagenic and carcinogenic, requiring downstream aerobic treatment for their detoxification [24], [140], [148]. Nevertheless, bacteria are easy to cultivate and rapid in their catalytic action [179] thereby exhibiting superior decolorization and mineralization [54], [140]. A facultative anaerobe that is less pathogenic and equally competent as *Pseudomonas* would serve the purpose [5], [17], [38], [126], [127], [144]–[146].

Decolorization efficacy of *Klebsiella pneumoniae* strain dye1, under shaking and static conditions, under stress conditions such as chlorides and sulfates that contribute to the osmotic pressure [140],

[180] and chemically combined oxygen [181] respectively, as observed in typical textile wastewater was investigated. Shaking condition was found to be conducive for AB113 while static incubation for RO16 and DR81 from the preliminary studies with both AS and the isolate. Further decolorization studies for each dye was conducted based on the most conducive incubation conditions. Based on the results obtained, a possible dye degradation pathway for each dye was also proposed.

4.2 Preliminary decolorization study

Activated sludge (AS) as a source biomass selected from Ulu Pandan wastewater treatment plant and Jurong water reclamation plant. The AS collected from Industrial and domestic treatment train from Jurong was designated as IJRP and DJRP. While the third one is designated as DUP. Decolorization assay performed in oxygen surplus conditions, with an initial dye concentration of 100 mg/L, using three sludges and 4 different azo dyes. AY17 was found to be least decolorized (refer to *Figure 4.1*) which was unexpected given that it is a mono azo dye. But the presence of pyrazole group which is more recalcitrant to biodegradation than benzene and naphthalene groups explains the decolorization performance of the sludge biomass [182].

IJRP is found to show better decolorization for all the 4 model dyes and the dye removal was found to be in the order AB113 followed by DR81, RO16 and AY17. Based on these preliminary results, AS from industrial stream of Jurong water reclamation plant was chosen for the further studies and AY17 was used as model dye for the isolation of the suitable microbe.

When similar studies were conducted to evaluate the performance of the *Klebsiella pneumoniae* strain dye1and find the suitable culture conditions for individual dyes, the dye elimination order followed the trend: AB113 > DR81 > RO16 (*Figures 4.2 and 4.3*).

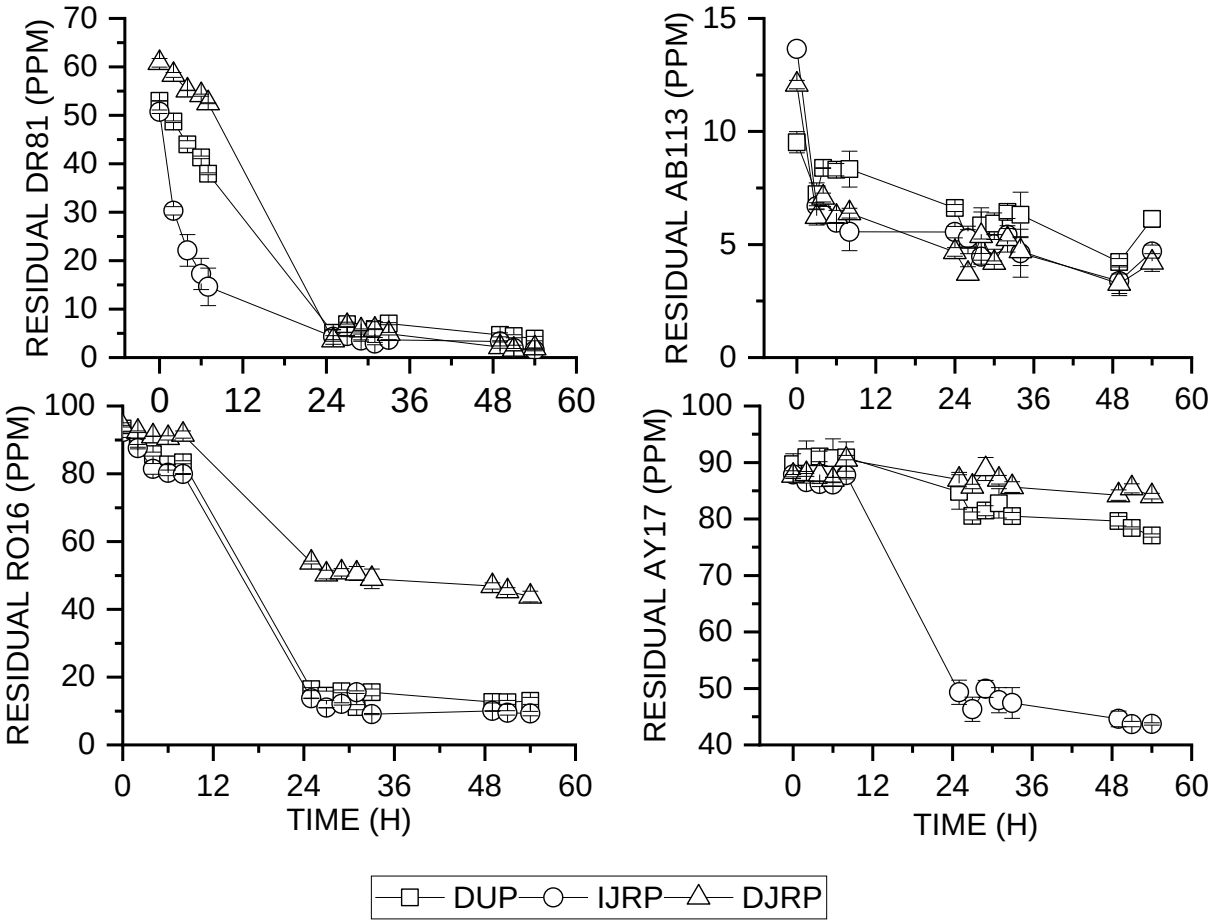

Figure 4. 1 Decolorization performance of various biomasses

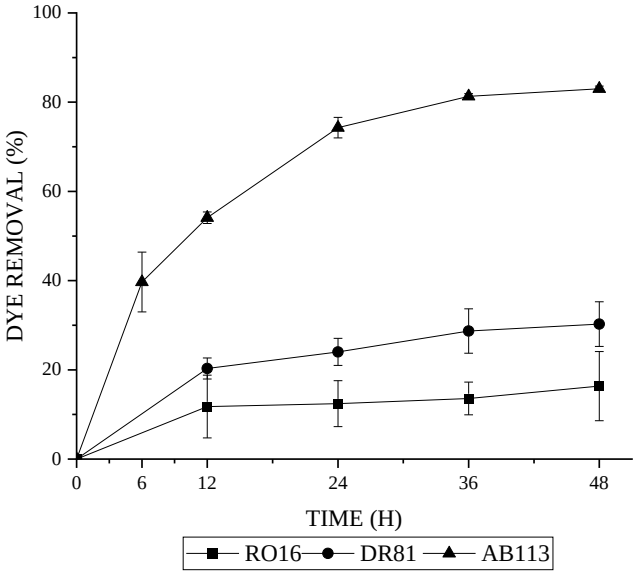

Figure 4. 2 Decolorization kinetics of all the dyes by *K. pneumoniae* in shaking conditions

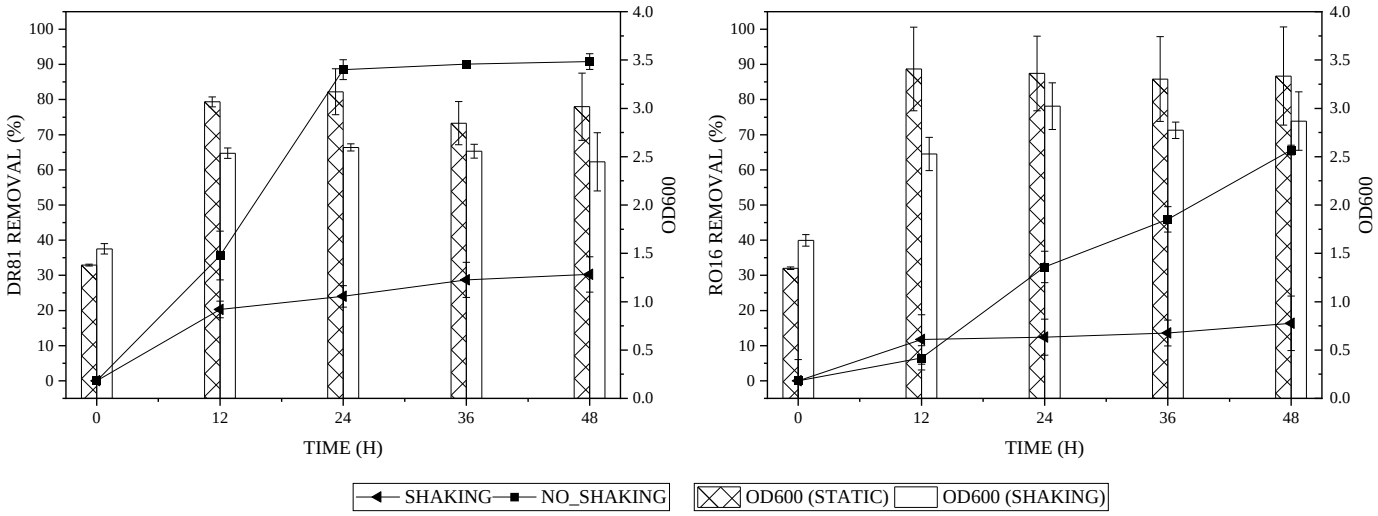

Figure 4. 3 Effect of shaking and static conditions on the dye removal and growth of *Klebsiella*

4.3 Decolorization of Acid blue 113 in shaking conditions

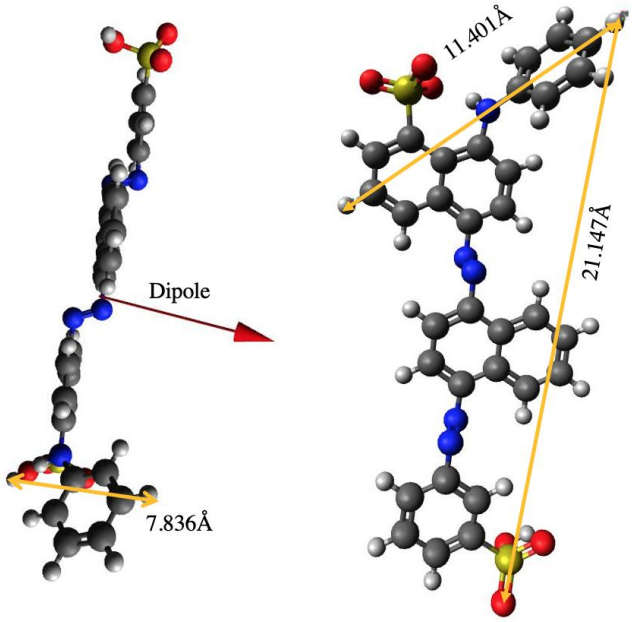

Figure 4. 4 3D structure and the dimensions of AB113

The reduction of chromophore bonds is the critical step in decolorizing azo dyes by bacteria, monitored using UV-Visible spectrophotometer [183]. The intensity of absorbance peaks decreased over time without peak shifts and visible new peaks that completely disappeared after 12 h. The dye's intrinsic properties, such as the functional group proximal to the azo bond and its structural orientation, oxidation potential and toxicity, and aromaticity [19], [38] could be why the 3 h latent period was observed before decolorization (refer to *Figure 4.6*). *K. pneumoniae* was able to decolorize AB113 by 40 %, 55 %, and 75 % within 6 h, 12 h, and 24 h, respectively. The decolorized samples were of the same color sterile media, i.e., beige (refer to *Figure 4.5*).

Despite the presence of sulfates and chlorides that reportedly retard the decolorization rate [129], the performance of *K. pneumoniae* is superior to similar other studies conducted on AB113 with different bacteria [130], [174], [184] (shown in *Table 4.1*). The decolorization at high saline conditions and pollutant degrading capability denotes the bacteria's ability to withstand the osmotic and ionic pressure, proving its ability to become a potential practical application in textile effluent treatment [140], [180].

Due to their complex nature, sulfonated azo dyes cannot penetrate the cell membrane, hence recalcitrant to degradation [129]. Nevertheless, *K. pneumoniae* reportedly degraded sulfonated azo dyes efficiently in the presence of supplementary organic carbon and nitrogen sources that promotes the growth of biomass [54], [182] and generates electron donors such as NADH for azo bond reduction [54]. During this study, a latent period of 3 h was observed, suggesting that adsorption was not involved. About 40 % of the dye was removed during the biomass's growth phase when active catalytic resources are abundant [179], [185]. These observations imply biodegradation as the predominant mechanism. However, lack of substrate availability, the toxicity of the metabolites towards the biomass, or their inhibitory effect on the enzymes involved in the decolorization could be the reason for the reduced dye removal efficacy in the stationery and death phases [31], [54], [177].

The TOC and TN were found to decrease in the same pattern as the decolorization rate. However, decolorization was faster than TOC reduction [186]. Since 100 mg/L of AB113 accounted for only ~ 1 % and 0.6 % of the total TOC and TN in the culture liquid, respectively, the reduction in their values could be only because of the consumption of external carbon and nitrogen sources by

biomass for its survival. At the same time, decolorization is a result of co-metabolism. The stable TN values after 36 h possibly indicate the accumulation of nitrogen-based compounds due to their recalcitrance and resistance or the biomass's death phase [187].

Figure 4. 5 Decolorized AB113 samples (0 h, 12 h, 24 h, 36 h, 48 h, 60 h (from left to right))

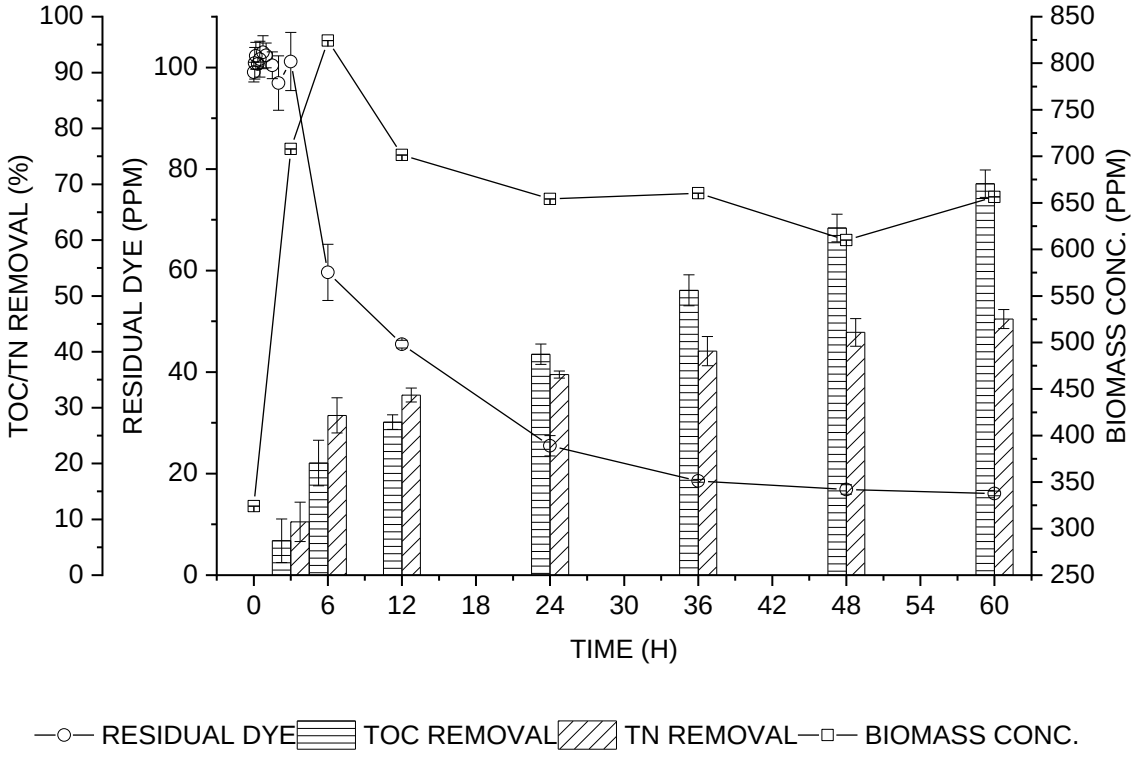

Figure 4. 6 TOC, TN removal and growth of biomass and residual AB113 concentration

Table 4. 1 AB113 decolorization performance of *K. pneumoniae* as compared with other bacteria

Name of the bacteria	η (%) at 24 h	Salt concentration (mg/L)	Initial dye concentration (mg/L)	Reference
Shigella Boydii	25	Not applicable (NA)	100	[174]
Staphylococcus Lentus	40	NA	100	[130]
Bacterial consortium	60	NA	200	[184]
K. Pneumoniae	**75**	**1700 Cl^- & 560 SO_4^{-2}**	**100**	**This study**

4.3.1 Degradation pathway of AB113

Through untargeted MS^2 scan on LC-QTOF, nine unknown metabolites appeared as shown in the *Figure 4.7.* Out of nine metabolites, only four were found to be the degraded by-products from the dye and the remaining were either present in the biotic or abiotic control as given in the *Table 4.3*. Therefore, only four newly appeared metabolites and the dye AB113 were subsequently scanned for their product ions (PIs) at 10, 20, and 40 eV individually via PI scan. The PIs in the chromatograms were matched by various web-based databases such as Mass bank of North America (MoNA), Human Metabolome Database (HMDB), METLIN (refer to *Figure 4.8*). *Table 4.2* has information regarding retention time, molecular weight, collision energy, and the intermediates identified. Despite the efforts, the identity of a metabolite (m/z 498.1122) could not be still established. Hence the pathway delineated in *Figure 4.10* excludes the same. The same protocol was adapted to track the fate of the degraded by-products from DR81 and RO16.

Asymmetric and symmetric azo bond cleavage results in AAs formation with different fragment masses followed by desulphonation, deamination, hydroxylation, and oxidation [130], [187]. Parent dye (m/z 638.1134) is detected with a predominant peak at a retention time (RT) of 16.535 min. Based on the degraded mass fragments, the pathway is illustrated as follows: The first step involved the symmetric cleavage of one of the azo bonds that resulted in 4- [(2-Amino naphthalen-1-yl) diazenyl] benzenesulfonate (m/z 328.0502) [188] which appeared only in 6 h and 12 h sample. It resembled the structure of Acid Orange 7 [37], [189] and the azo bridge was confirmed to be

further broken down by the detection of 1,4 Diamino naphthalene (m/z 159.0921). The ring-opening reactions resulted in long-chain aliphatic compound N,N'-Diacetyl 1,6-diamino hexane (m/z 202.106) [130]. Sekar et al. [130] and Zille et al. [190] have previously reported high molecular weight unknown compounds formed due to esterification of the dye by-products and the biochemical reactions between themselves or with the unreacted dye to give rise to long-chain fatty acids or alcohols. Similarly, in the present study, metabolite unknown_498 was detected but could not be identified.

The confirmation and verification of unknown metabolites is done with the help of standards based on RT during chromatographic separation and the corresponding MS^2 spectra [191]. Though testing with standard chemicals is laborious and cost-intensive, in most cases, the standard chemicals may be unavailable to acquire for further analytical confirmation. Most often these intermediates are the banned SAAs and AAs which are precursors in dye manufacturing [191], [192]. Though spectral libraries keep expanding and evolving, spectral matching depends entirely on the configuration of the machine used and the data acquisition settings [192]. Untargeted metabolomics analysis through mass-based search results in more than 100 putative identification because of isomers, which makes it impossible for further manual verification [192]. Therefore, the identification of unknown metabolites is till date, a bottleneck in metabolomics studies [192]. Further computational or analytical analysis is required to annotate the MS^2 spectra for the validation of the same. Consequently, to understand the nature of the unknown metabolites detected in this study, IR spectrometry is used as the supportive data [54], [192].

Compared with the FT-IR spectra of dye standard (data shown in *Figure 4.9*), 24 h treated sample had a broad peak in the region 2600 – 3703 cm^{-1}, indicating the presence of phenolic hydroxyl and carboxyl groups because of degradation [93], [131]. Peaks at 1552.7 cm^{-1} and 1344.38 cm^{-1} in the dye associated with the azo bond [193] and C-N stretch [145] respectively wholly disappeared in the 24 h treated sample. The former indicates the reduction of the chromophore and formation of amines. The appearance of new peaks in treated samples at 918.12 cm^{-1}, 1278.1 cm^{-1}, 1649 $cm^{-1,}$ and 3242. 34 cm^{-1} representing C-O stretch, asymmetric C-O-C stretch [131], aryl carboxylic acid or quinone [193] and N-H stretch in amides [145] respectively, pointed towards the formation of metabolites. Also, 461 cm^{-1} in dye spectrum has shifted to 503.42 cm^{-1} in the treated sample. Peaks in this region represent the ring in and out of plane bending. The peak at 621.8 cm^{-1} represents the

C-H of substituted aromatics [54], [131]. 1057 cm^{-1} pointed the asymmetric C-N stretch along with -SO_2 symmetric stretch [131], [145].

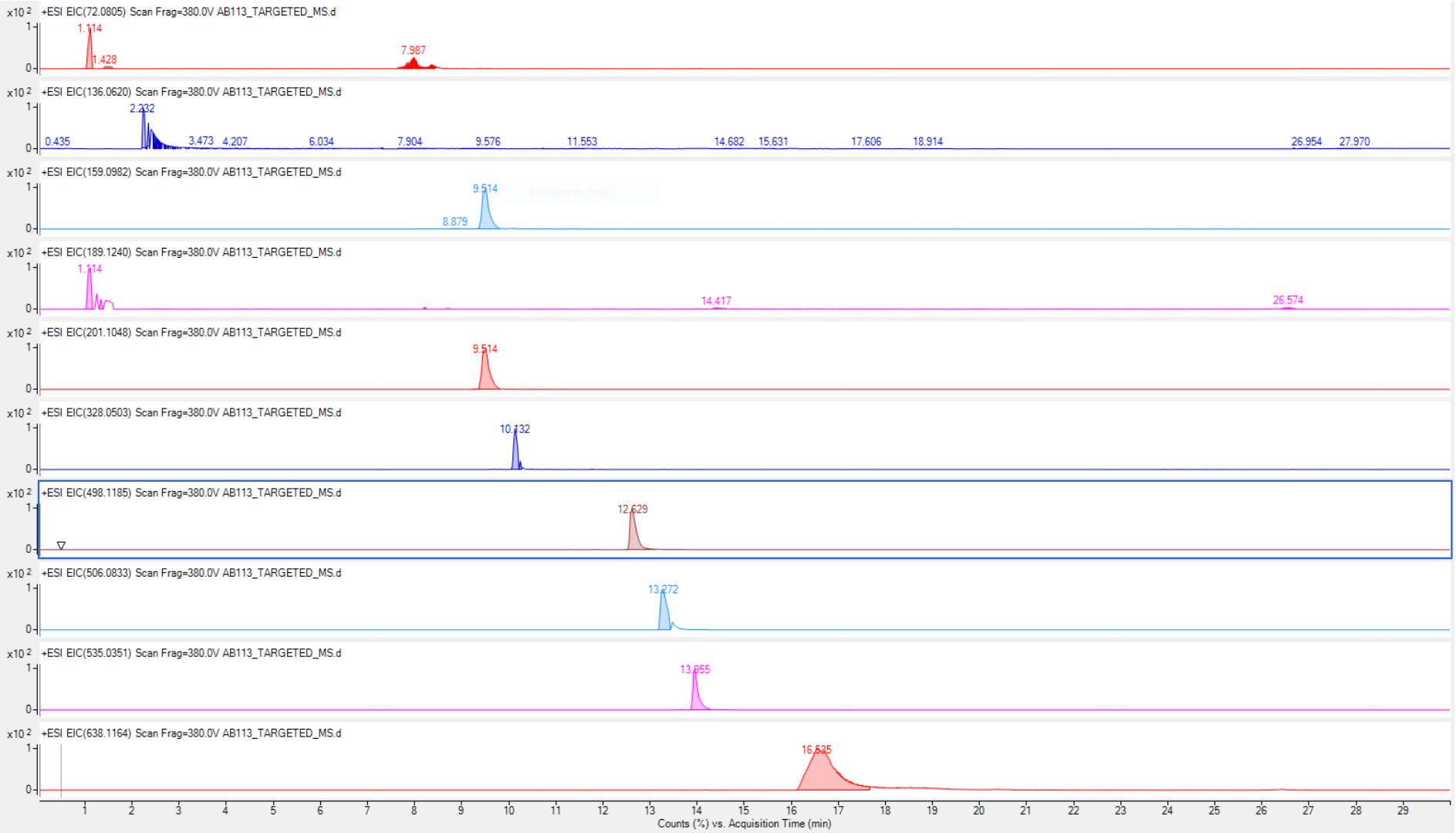

Figure 4. 7 LC-MS chromatograms of AB113 and its degradation by-products

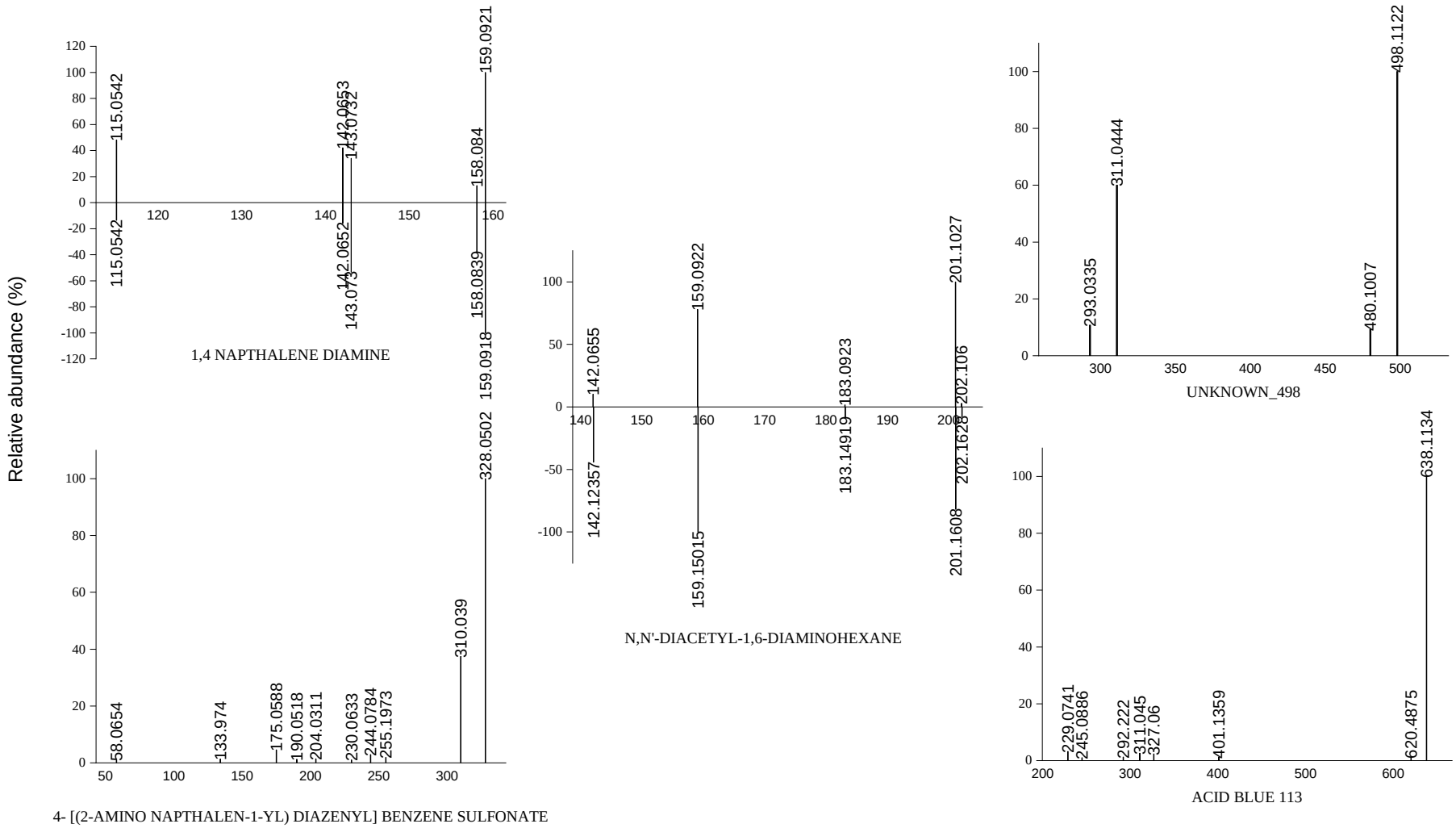

Figure 4. 8 MS^2 spectra for metabolites identified post degradation of AB113

Table 4. 2 The retention time, precursor ions, and the degradation intermediates of AB113

m/z	RT (min)	CE (V)	Metabolite identified
159.0922	9.514	20	Naphthalene-1,4-diamine
201.1027	9.514	10	N, N'-Diacetyl-1,6-diamino hexane
328.0534	10.132	20	4- [(2-Amino napthalen-1-yl) diazenyl] benzene sulfonate
498.1122	12.629	10	Unknown_498
638.1134	16.535	20	Acid blue 113

Table 4. 3 Metabolites identified in AB113 degraded samples and controls

Precursor ion m/z	Retention Time (min)	Treated sample	Biotic control	Abiotic control
72.0805	1.114			
136.062	2.232			
159.0982	9.514			
189.124	1.114			
201.1048	9.514			
328.0503	10.132			
498.1185	12.629			
506.0833	13.272			
535.0351	13.955			
638.1164	16.535			

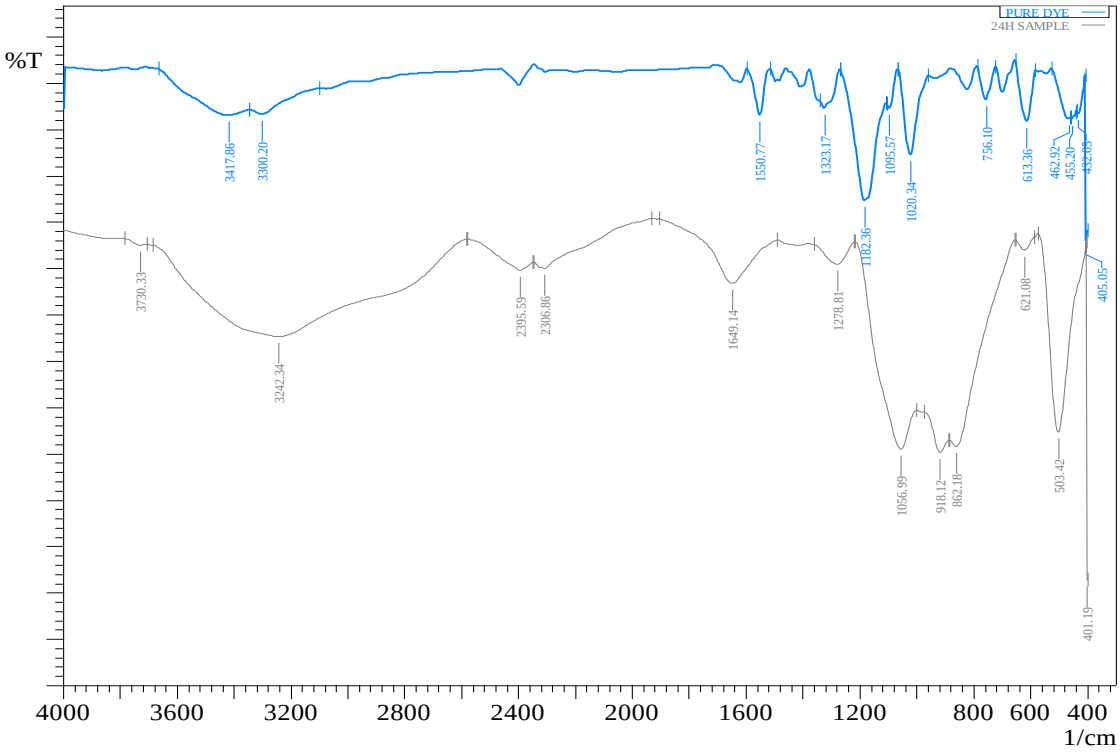

Figure 4. 9 FTIR spectrum of control dye and 24 h treated sample

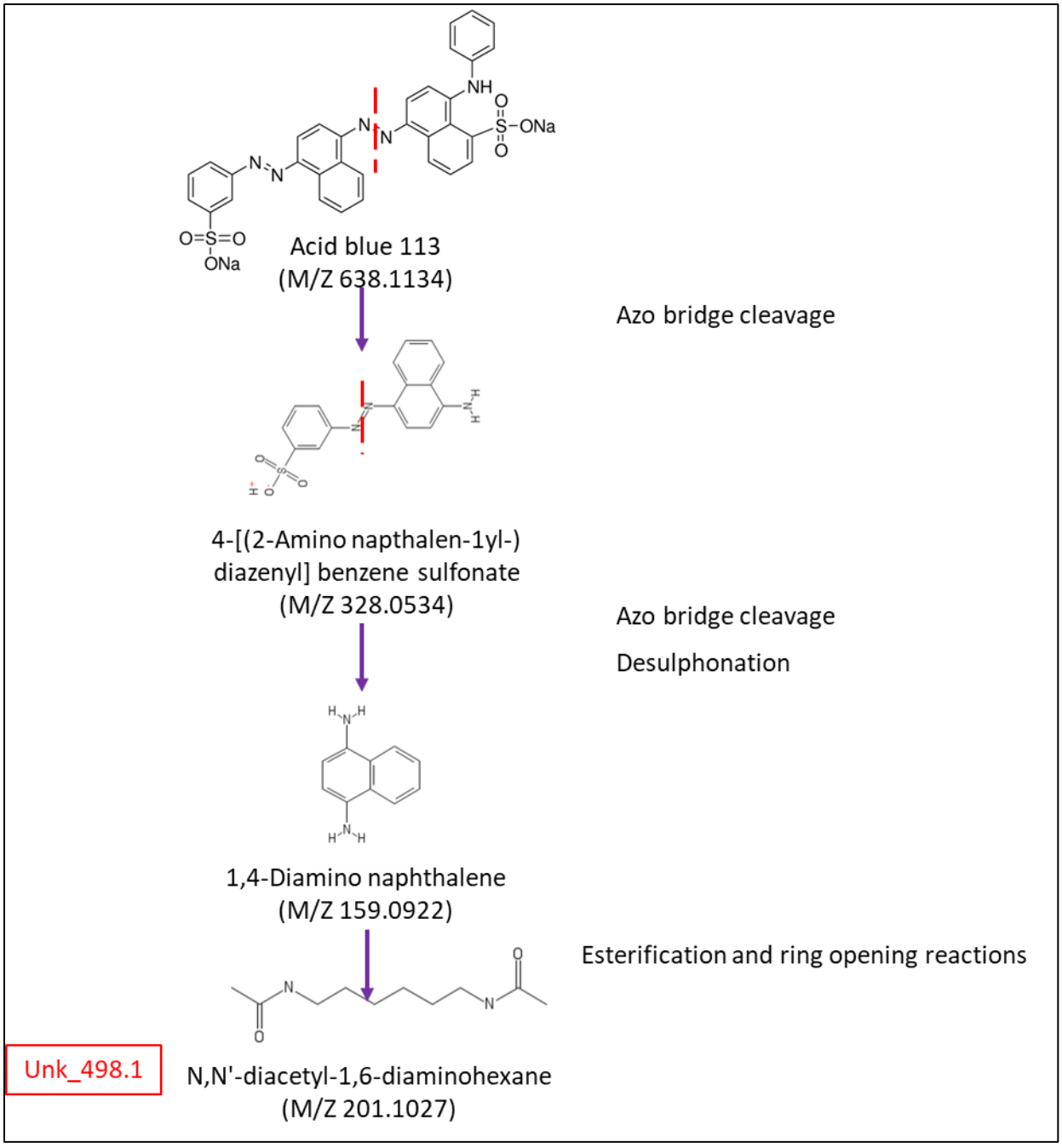

Figure 4. 10 Plausible degradation pathway of AB113

4.4 Decolorization of Direct Red 81 and Reactive Orange 16 in static conditions

Klebsiella is a facultative anaerobe, that can thrive via both aerobic and anaerobic respiration [194]. The biomass proliferated more in shaking cultures (refer to *Figure 4.3*) than the static cultures, demonstrating its favorability for aerobic conditions [194]. Although notable decolorization did not occur indicating the anaerobic culturing nature of this strain [138]. Even at 48 h, only 16.3 % and 30.2 % of dye removal was noted in shaking cultures while 65.6 % and 90.8 % of decolourisation was observed in stationary cultures for RO16 and DR81, respectively. Similar observations were made by various researchers upon testing various direct and reactive colourants with *Pseudomonas* [17] and bacterial consortium [7], [195]. The resistance of azo dyes to bacterial attack in aerobic conditions either due to the inhibition of azo reductases or the competitive oxidation of reduced redox mediator could be the reason for the poor decolorizing ability in aerobic experiments [195].

The decolorization is found to be effective in microaerobic conditions [196]. Static incubation promoted the depletion of oxygen, enabling *Klebsiella* to reduce azo dyes rapidly and achieving supreme dye removal efficacy [195], [197].

Dyes are large polar molecules that cannot diffuse through the microbial cell walls. Therefore, decolorization involves extracellular or membrane-bound activity [187], [198]. Bacteriological dye removal involves either a) biosorption onto the cell surface and/or b) stress-induced enzyme catalysis [129], [179], [199]. Cell membranes are comprised of active proteins, lipids and polysaccharides that possess amino, hydroxyl, carboxyl, and phosphate groups [61], [199] and azo dyes interact with the microbial cell walls via physical or chemical binding that involve active, metabolism dependent and passive dye transport mechanisms [61], [114].

From the biosorption and desorption assay, about 20 ppm of DR81 and 5 ppm of RO16 was found to be bound to the dead biomass. From the *Figure 4.14*, it can be interpreted that the reaction was almost instantaneous, and the dead biomass saturated in under an hour. The dye – cell interactions are greatly influenced by the chemistry of the dyes [61], which in turn drive the decolorization rates [7], [182]. From the chemical structures of the dyes as given in *Figure 4.11*, both DR81 and RO16 possess hydroxyl and sulfonate functional groups. But, RO16 has a sulfoxy ethyl sulfonate

group unlike only sulfonate groups in DR81. It is reported that sulfonate groups [200] greatly hamper the decolorization kinetics as compared to the hydroxyl groups [7]. Besides that, sulfur containing functional groups makes the dye molecules bulky and heavy [199]. This supports the better chemical affinity of DR81 to the biomass as compared to RO16 [108].

A substantial amount of dye decolorization was detected only after 6 h and 9 h of incubation for DR81 and RO16, respectively, while the cells were in log-phase with a predominant cell growth [133], [187]. Preferential utilization of glucose over dye as a carbon source [182] or saturation of the active cell sites with the dye [108] could be the reason for the staggered decolorization profile in the early log phase of the bacterial growth. The co-metabolic and standalone pathway studies (refer to *Figure 4.15*) indeed confirmed that the decolorization doesn't take place in the absence of an external carbon source i.e., glucose in this study.

Both DR81 and RO16 have electrophilic hydroxyl and sulfonate groups in the azo chromophore proximity, which inhibit the reduction of the conjugated azo bond as reported by [126]. The type of azo bond cleavage occurring – symmetric or asymmetric, is defined by the chemical structure of the dye [187]. The current study completely negotiates with the observations made by [143], [201] which reported that the complex and high molecular weight dyes require longer time for their abatement. In the present study, single azo dye (RO16) took 36 h longer to decolorize as compared to the double azo dye (DR81). Besides this, the latter has a straight-chain structure in contrast to the branched-chain structure of the former.[202]. Therefore, decolorization profiles cannot be explained solely based on the count of azo bonds and sulfonated groups present in the dye [182], [200].

The biomass doubled within 12 h and 24 h of incubation for DR81 and RO16 respectively (refer to *Figures 4.16 and 4.17*). Since the significant color removal was observed during the bacterial log-phase, decolorization could be because of both biosorption due to the multiplication of the cells which increase the availability of the sorption sites for dyes [199] and a biochemical reaction due to heightened metabolic activity [106], [174], [185].

The major absorbance peaks in the UV-Vis region decrease in proportion to each other in case of biosorption [203] while they completely disappear in case of degradation [158]. Inspection of the

cell pellets which did not retain their original color support biosorption. On the other hand, after 24 h and 60 h of incubation, peaks are completely disappeared for both DR81 and RO16 respectively (as shown in *Figure 4.12*) indicating that biodegradation has occurred. Detection of unknown by-products confirmed the same.

It was well documented that azo dye degradation is often a co-metabolic pathway and the addition of external organic carbon and nitrogen sources boost the decolorization [123], [204]. The carbon and nitrogen supplements: a) donate redox mediators such as NADH or $FADH_2$ that shuttle to the chromophore groups in the dye and b) multiply the actively respiring cells that rapidly remove the oxygen in the culture medium, triggering the production of enzymes that enable the transfer of redox mediators [54], [130], [133], [182]. Like the other studies, co-metabolism was proved to be the dye degradation mechanism in the present study (refer to *Figure 4.15).* The dye was actively removed only in the presence of M9 minimal media with glucose as carbon source and NH_4Cl as the nitrogen source. On the other hand, the microbe didn't survive in the media that didn't contain any simple carbon and nitrogen sources besides the dye.

Investigations using *Enterococcus* [131], *Nocardiopsis* [54], *Providencia* and *Pseudomonas* [7] as the degradants for DR81 and RO16 were reported in *Table 4.4*. All the studies are performed under identical experimental conditions as employed in the present study such as microaerobic conditions and 100 ppm of initial dye concentration [57], [132], [144], [148].

The inferior decolourisation performance of *Klebsiella* as compared to *Enterococcus* [131] that has shown a 100 % DR81 removal efficiency is due to the presence of chlorides and sulfates which hamper the bacterial metabolic activity [129], [203]. Likewise, RO16 was also not as effectively removed by *Klebsiella* as compared to the other strains. Yet, even in the presence of salts, *Klebsiella* outperformed *Providencia* and *Pseudomonas* [7] in the removal of DR81 by displaying a removal efficacy that is more than double.

Despite their structural complexity and xenobiotic nature, the sulfonated azo dyes in this study are susceptible to biodegradation emphasizing the bioremediation potential of *Klebsiella* [129]. Presence of salts only hampered but did not completely inhibit the bacterial degradation [129].

The degradation of azo dyes require more time than that is required for decolorization [202]. Hence, TOC/TN of the samples were monitored to find the degree of mineralization [202]. Though dye degradation occurred faster than TOC/TN removal [186], the mineralization was observed to be only ~ 50 % for both DR81 and RO16 [197]. The TOC-TN profiles (*Figures 4.16 and 4.17*) indicate that the nutrients are not completely depleted. However, the degradation metabolites which are not further converted into simple aliphatic compounds could have accumulated and inhibited the cell metabolic activity [123], [186]. The decolorized samples collected at preset time intervals were shown in *Figure 4.13*.

Table 4. 4 DR81 and RO16 decolorization performance of *K. pneumoniae* as compared with other bacteria

Microbe	**Dye**	**% at 24 h**	**Salt concentration (mg/L)**	**Reference**
Providencia rettgeri strain HSL1	DR81	~ 40	-NA	[7]
Pseudomonas sp. SUK1	DR81	~ 40	-NA	[7]
Enterococcus faecalis YZ 66	DR81	100	-NA	[131]
Microbial consortium NBNJ6	DR81	~ 50	-NA	[178]
***K. pneumoniae* strain Dye1**	**DR81**	**88.5**	**560 SO_4^{2-} and 1700 Cl^-**	**This study**
Pseudomonas sp. SUK1	RO16	~ 99	-NA	[7]
Providencia rettgeri strain HSL1	RO16	~ 99	-NA	[7]
Nocardiopsis alba	RO16	~ 95	-NA	[54]
***K. pneumoniae* strain Dye1**	**RO16**	**27.3**	**560 SO_4^{2-} and 1700 Cl^-**	**This study**

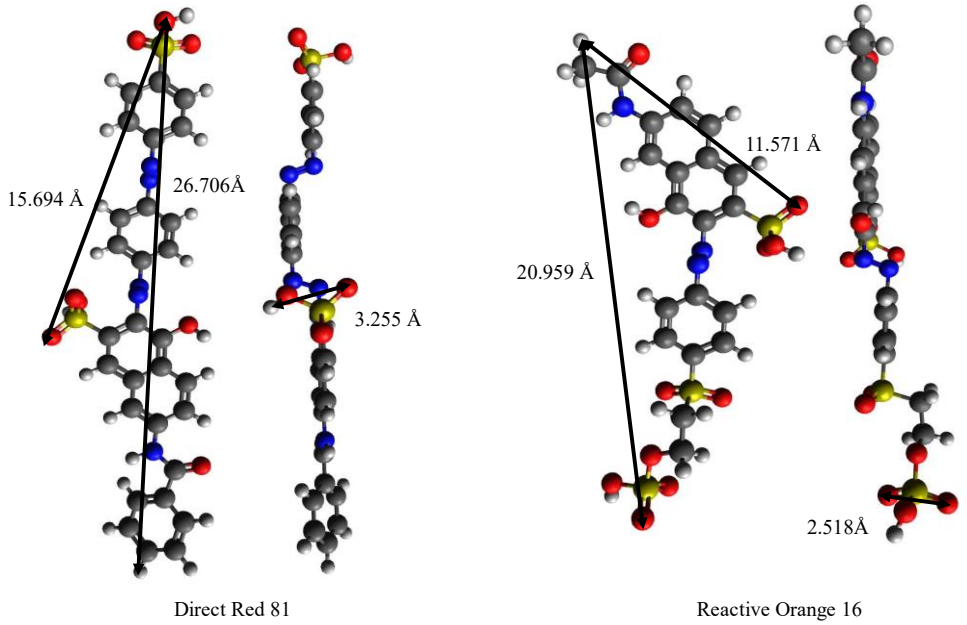

Figure 4. 11 3D Structure and the dimensions of DR81 and RO16

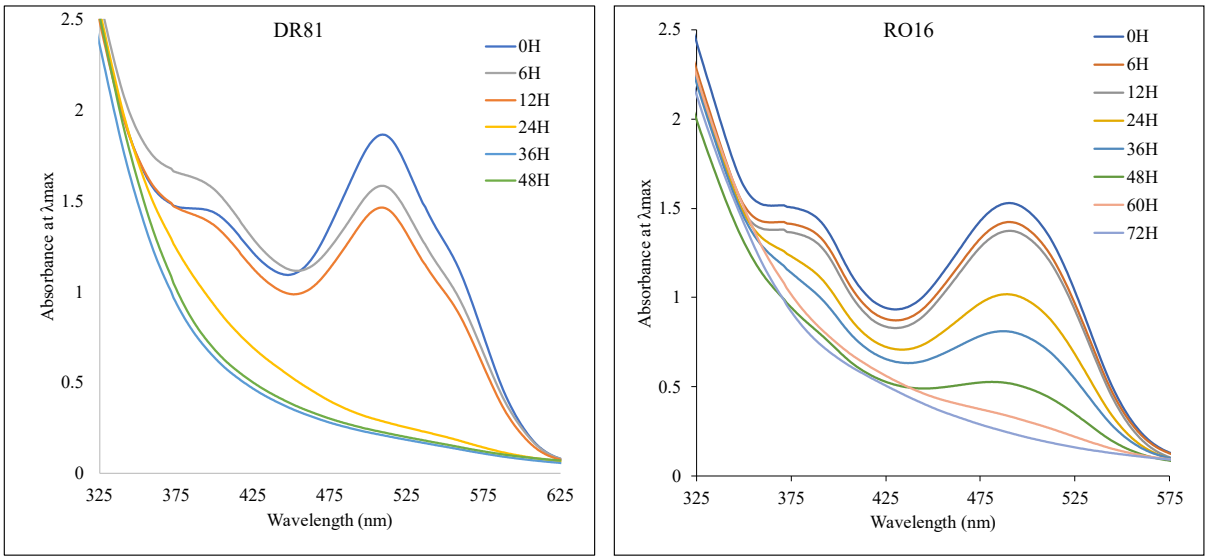

Figure 4. 12 UV-VIS spectral absorbance as a function of time

Figure 4. 13 Stepwise decolorization of samples in their respective sampling order (left – DR81 and right – RO16)

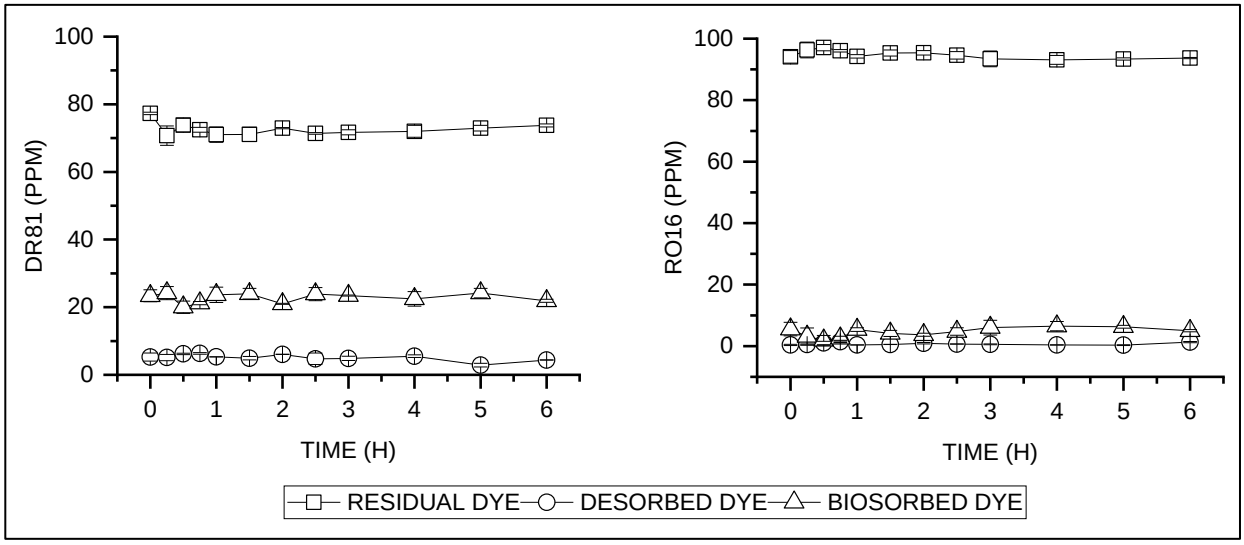

Figure 4. 14 Biosorption-desorption kinetics

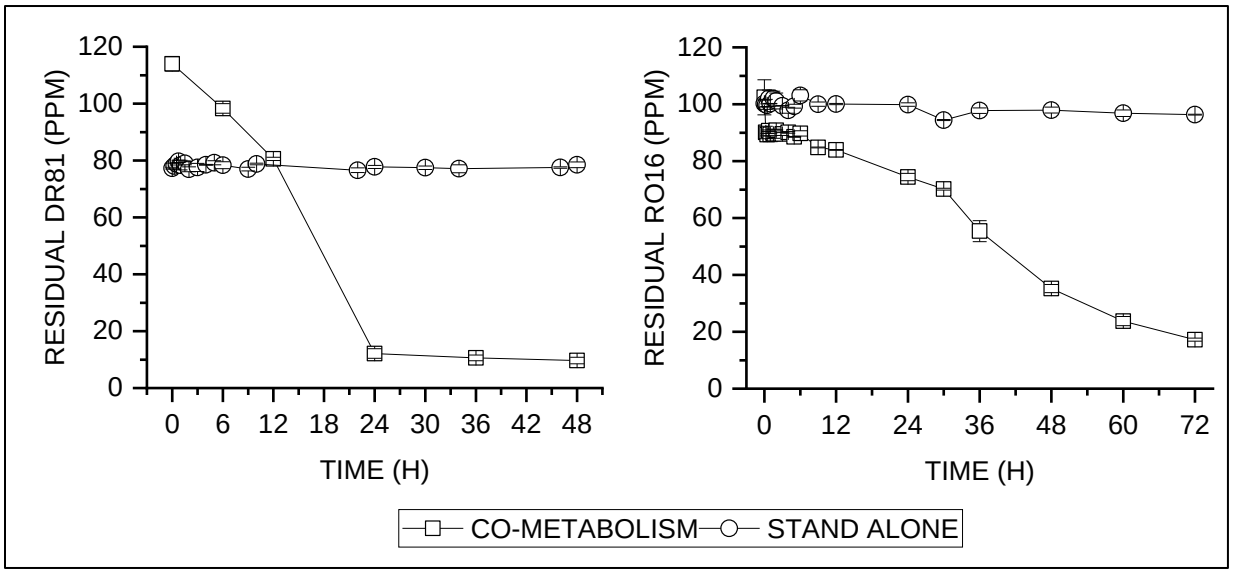

Figure 4. 15 Removal of DR81 and RO16 via co-metabolic and standalone pathways

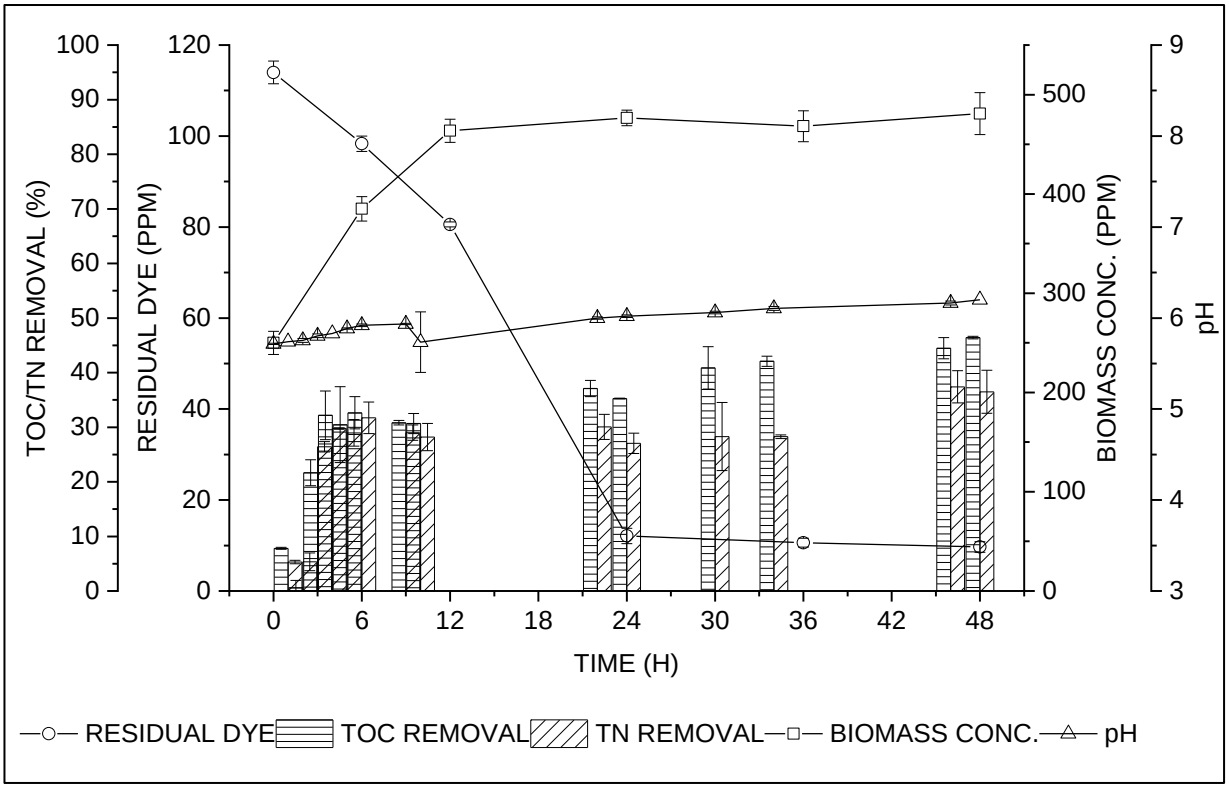

Figure 4. 16 TOC, TN removal, growth of biomass, pH and residual DR81 concentration

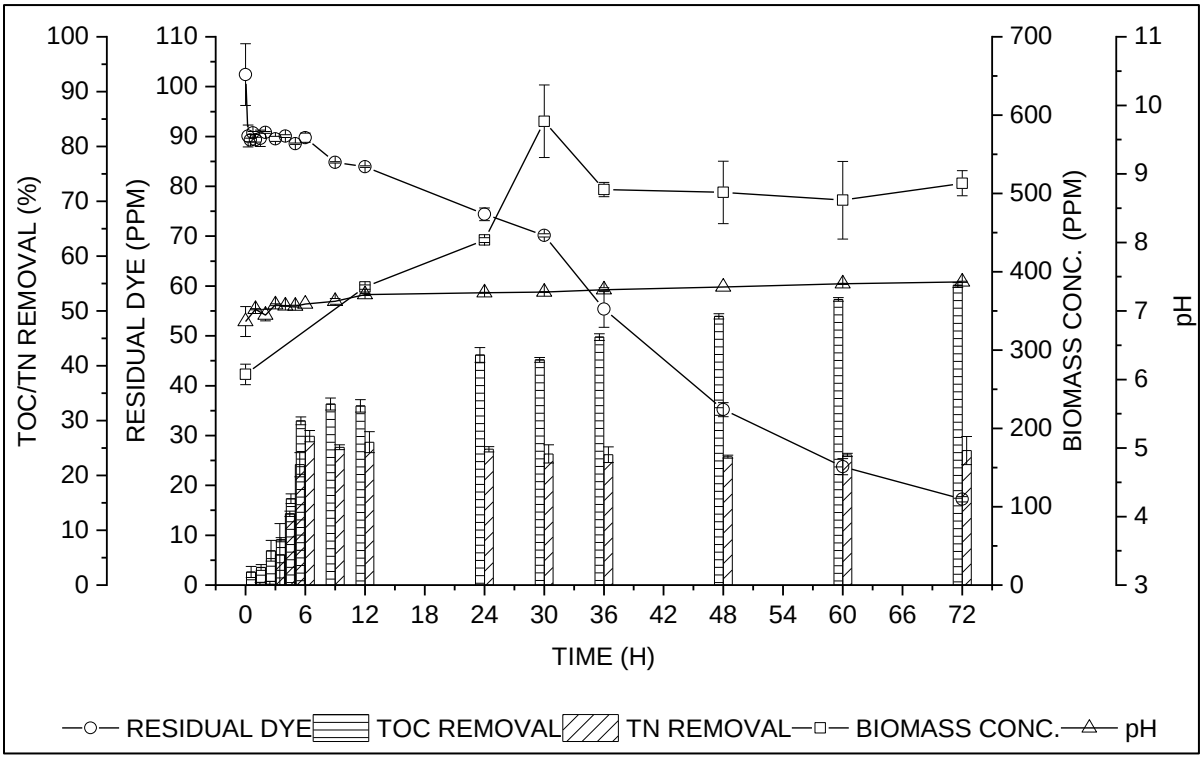

Figure 4. 17 TOC, TN removal, growth of biomass, pH and residual RO16 concentration

4.4.1 Degradation pathway of DR81

The SPE treated samples are subjected to LC-MS to find the intermediates formed during the degradation. The untargeted analysis followed by PI scan was performed as per the protocol mentioned in *Section 4.3.1*. Ten unknown metabolites appeared as shown in the *Figure 4.18.* Out of the ten metabolites, only six were found to be the degraded by-products from the dye and the remaining were either present in the biotic or abiotic control as given in the *Table 4.6*. *Table 4.5* has information regarding retention time, molecular weight, collision energy, and the intermediates identified. The PIs of the metabolites is as shown in *Figure 4.19.*

Azo dyes can be cleaved symmetrically, resulting in the formation of AAs or asymmetrically releasing of azo linkages as molecular nitrogen [129]. Likewise, DR81 also followed the same degradation pattern in the current study. The degradation pathway of DR81 is delineated in *Figure 4.22*.

Upon the symmetric cleavage of -N=N- bond the direct dye (m/z 632.0908) was broken down into two fragments to generate SAAs and AAs containing mono and di-substituted benzene and naphthalene rings [202]. The fragments were identified as: A) 4-((4-aminophenyl) diazenyl) benzene sulfonic acid (m/z 278.0596), B) 7- [(2-amino-4-methyl benzoyl) amino]-4-hydroxy-naphthalene-2-sulfonic acid (m/z 373.0503). Fragment A was structurally same as a simpler azo dye named Food yellow 6 which upon the azo bond disintegration and desulphonation, is converted to 4-aminobiphenyl (m/z 170.0843). This is further transformed to 3,3'-dimethoxy benzidine (m/z 245.0979). Besides this, asymmetric azo bridge cleavage was also observed in DR81 that resulted in the Fragment C: 3-diazenyl-7-benzamido-4-hydroxynaphthalene-2-sulfonic acid (m/z 372.0653) which further transformed to naphthalene-4-hydroxy-7-benzoyl amino-2-sulfonic acid (m/z 344.1394).

Lyophilized samples, along with the control are measured for their transmittance on FTIR. An obvious modification in the spectrum of the degraded sample was noted, confirming the breakdown of the dye molecules by *K. pneumoniae*. Broadening of the absorption spectra indicate the microbial destruction of the conjugated dye structure [130]. Comparing the FTIR spectra of the pure dye and the degraded sample (*Figures 4.20 and 4.21*), the absorption intensities in the

region 3100-3500 cm^{-1} were broadened. This represents the increase of hydroxyl and amine functional groups in the degraded products [93], [130]. A new peak appeared at 2974.23 cm^{-1} which denotes the asymmetric OH stretch [205]. A peak at 1656.48 cm^{-1} due to the presence of N=N symmetric stretch has completely disappeared in the treated sample supporting that the dye has cleaved into aromatic amines completely [131]. NH bending in acetanilide is represented by a new peak appeared in the treated sample at 1599 cm^{-1} [131]. Intense peaks at 619.15 cm^{-1} in the treated sample represent the C-H of substituted aromatics [54], [131]. Appearance of new peaks at 1452.4 cm^{-1} and 1263.37 cm^{-1} represent aromatic ring vibrations [206] and -C-O stretching vibrations [131].

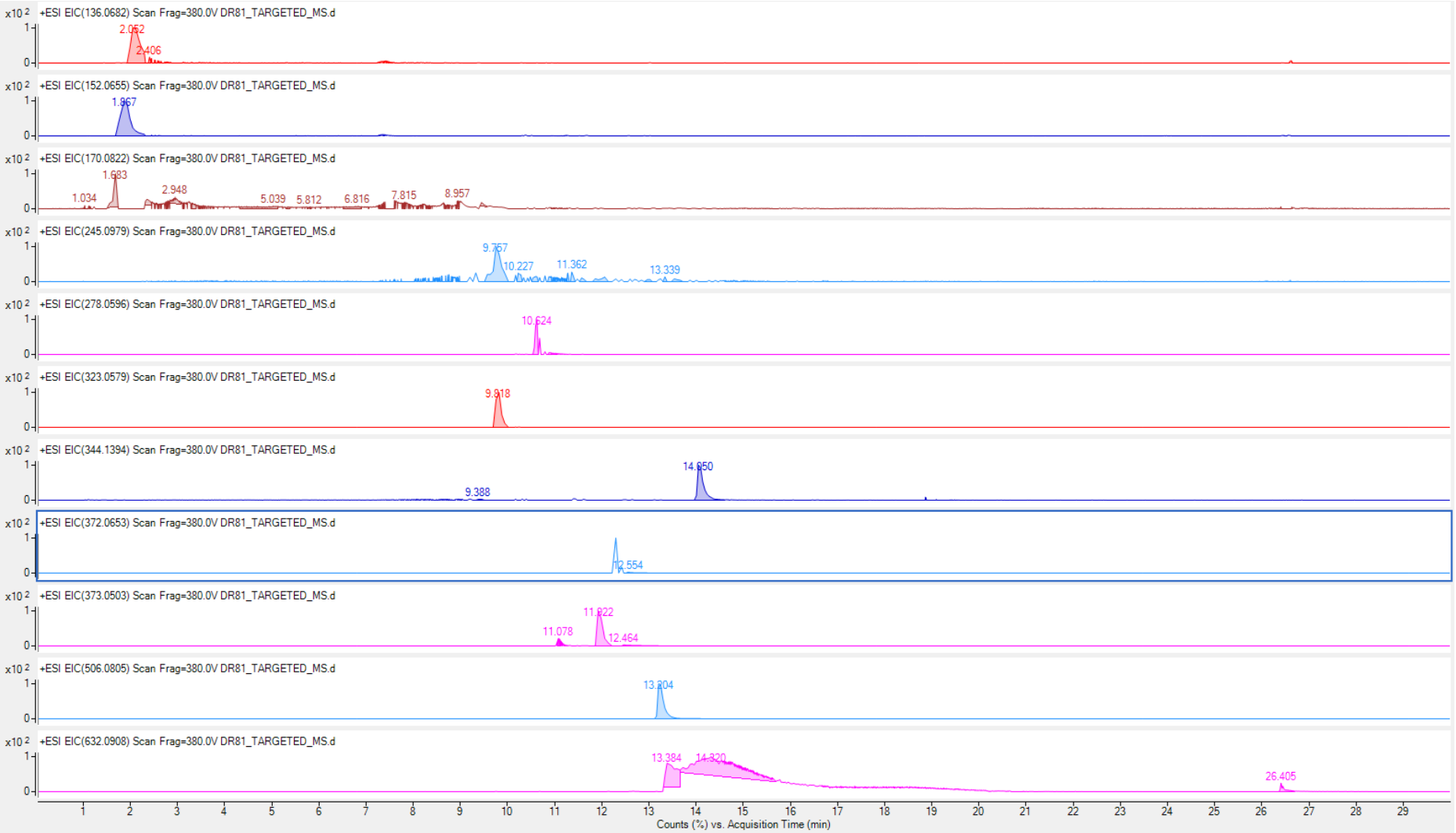

Figure 4. 18 LC-MS chromatograms of DR81 and its degradation by-products

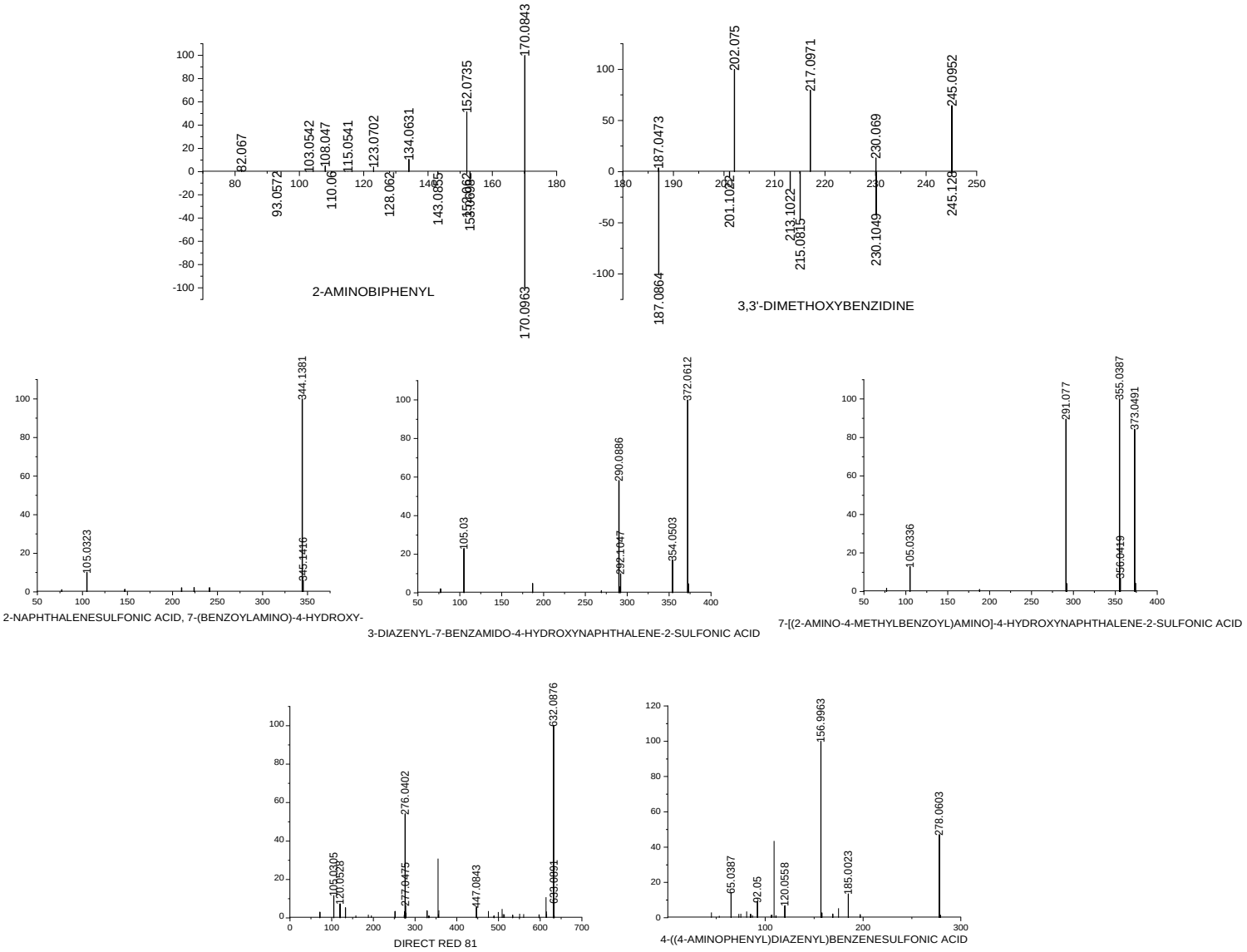

Figure 4. 19 MS^2 spectra for metabolites identified post degradation of DR81

Table 4. 5 Retention time, m/z and the by-products identified upon DR81 degradation

m/z	RT (min)	CE (V)	Metabolite identified
170.0843	1.683	10	4-aminobiphenyl
245.0979	9.757	20	3,3'-dimethoxybenzidine
278.0596	10.624	20	4-((4-aminophenyl) diazenyl) benzenesulfonic acid
344.1394	14.05	20	2-naphthalenesulfonic acid, 7-(benzoyl amino)-4-hydroxy-
372.0653	12.296	20	3-diazenyl-7-benzamido-4-hydroxynaphthalene-2-sulfonic acid
373.0503	11.922	10	7-[(2-amino-4-methylbenzoyl) amino]-4-hydroxynaphthalene-2-sulfonic acid
632.0908	13.384	20	Direct Red 81

Table 4. 6 Metabolites identified in DR81 degraded samples and controls

Precursor ion m/z	**Retention Time (min)**	**Treated sample**	**Biotic control**	**Abiotic control**
136.0682	2.052			
152.0655	1.867			
170.0822	1.683			
245.0979	9.757			
278.0596	10.624			
323.0579	9.818			
344.1394	14.05			
372.0653	12.296			
373.0503	11.922			
506.0805	13.204			
632.0908	13.384			

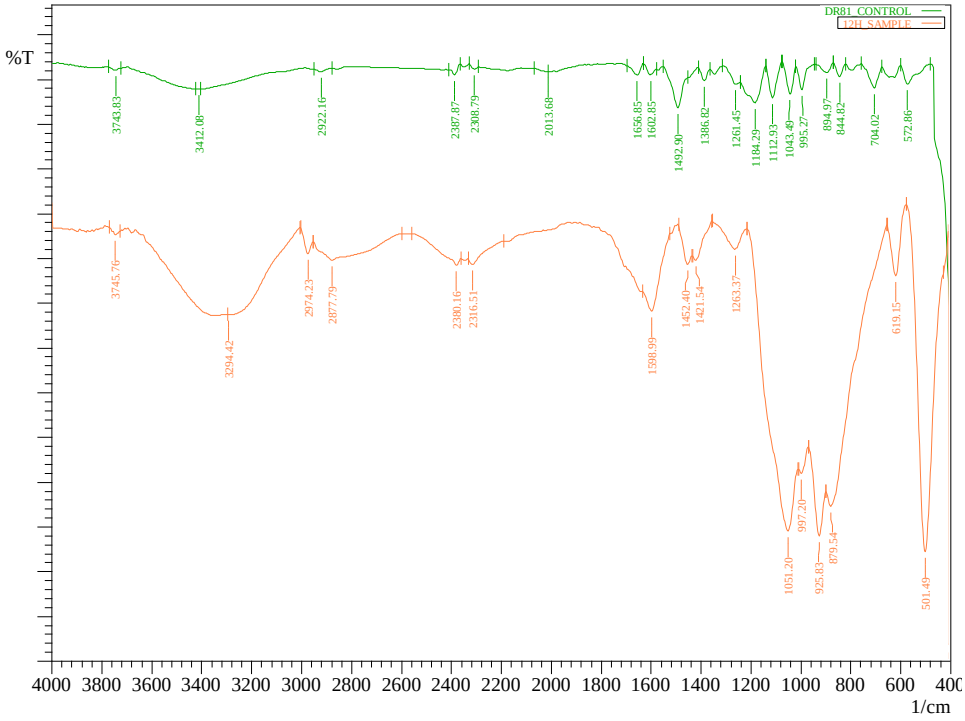

Figure 4. 20 FTIR spectra for DR81 control and 12 h sample

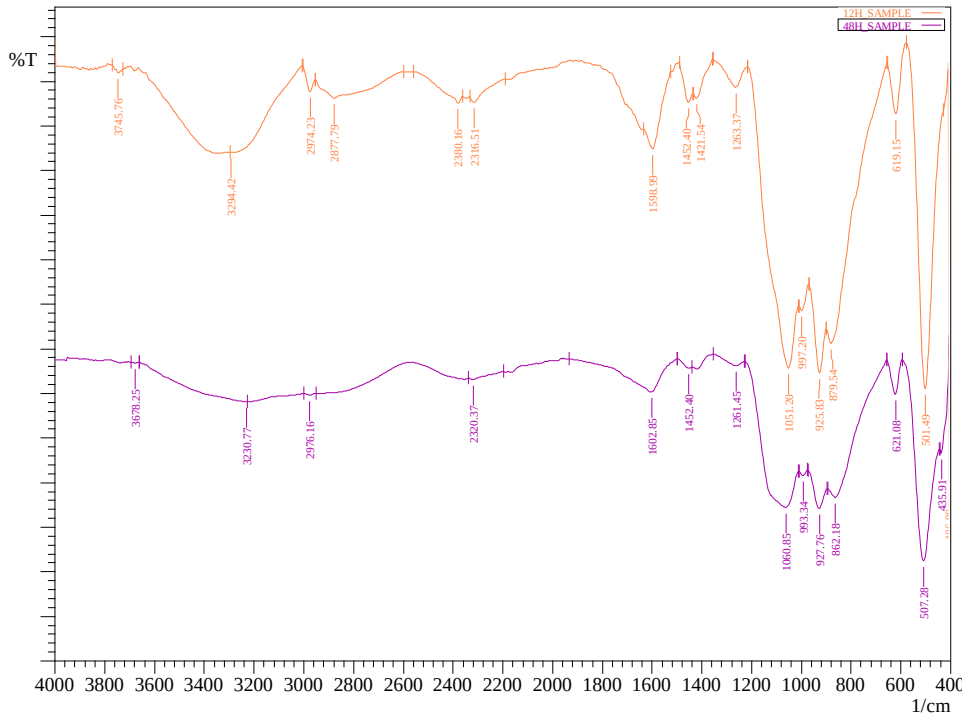

Figure 4. 21 FTIR spectra for DR81 12 h and 48 h sample

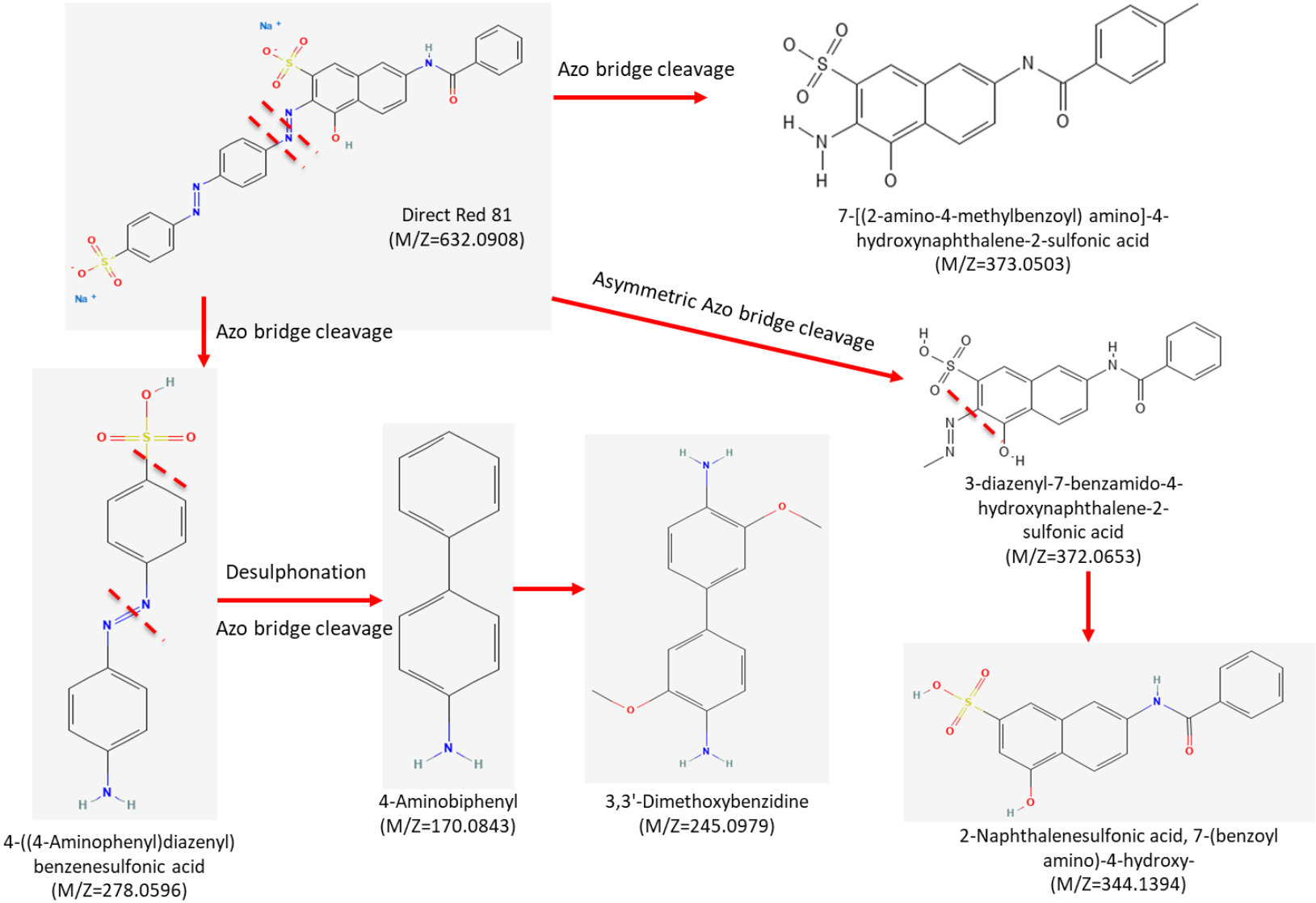

Figure 4. 22 Plausible degradation pathway of DR81

4.4.2. Degradation pathway of RO16

Following the protocol mentioned in *Section 4.3.1* in the identification of unknown metabolites post degradation of RO16, untargeted analysis was performed on LC-QTOF.

Eight unknown metabolites appeared as shown in *Figure 4.23.* Out of the eight metabolites, only four were found to be the degraded by-products from the dye and the remaining were either present in the biotic or abiotic control as given in the *Table 4.8*. *Table 4.7* has information regarding retention time, molecular weight, collision energy, and the intermediates identified. RO16 was detected in its vinyl form with m/z 476.0567. The dye was broken down to two different fragments. 1-amino-4-vinylsulfonyl benzene (m/z 184.0433) and 4-methylsulfonyl phenyl diazene (m/z 185.0963) due to symmetric and asymmetric cleavage of azo bond respectively. The latter was transformed to 4-methylsulfonyl aniline (m/z 157.1687) which further resulted in 4,4'-(Ethane-1,2-diyldisulfonyl) dianiline (m/z 341.062). The degradation pathway is shown in *Figure 4.27*.

Significant differences in the FTIR absorption spectra (*Figures 4.25 and 4.26*) supports the degradation of RO16. The peaks in the range 3207 cm^{-1} to 3232 cm^{-1} represent NH stretching in the treated samples [205]. Peaks at 2889.4 cm^{-1} and 2931.8 cm^{-1} in the treated samples are due to the stretching of alkanes [207]. The peak at 619.15 cm^{-1} has shifted to 621.08 cm^{-1} in the 12 h treated sample, which belongs to the CH bending in the hydrocarbon chromophore [54]. Peak at 2314.58 cm^{-1} represents the CN stretch [54]. Control dye has a peak at 3387.09 cm^{-1} due to the presence of 2^{c} amine and OH stretching [54], [193]. This peak broadened from 3100 cm^{-1} to 3500 cm^{-1} supporting the increase of hydroxyl and amine functional groups in the degraded products [93], [130]. 1049.28 cm^{-1} in the control shifted to 1053.13 cm^{-1} in the 12 h treated sample. This represents the presence of hydroxyl groups in both control and degraded sample [93]. The peaks at 1498.69 cm^{-1} and 1456.26 cm^{-1} in control and degraded samples (12 h, 48 h and 72h) denote the aromatic ring vibrations [206], suggesting the accumulation of aromatic compounds over time.

Peak at 1132.21 cm^{-1} in the control sample, which is due to the C-N stretch with symmetric SO_2 stretch, disappeared in the degraded samples [131]. A peak at 1660.71 cm^{-1} representing the symmetric stretch of azo bond has completely disappeared in all the treated samples supporting

that azo bond was reduced and cleaved into aromatic amines completely [131], [205]. Appearance of a new peak at 1641.42 cm^{-1} in the 48 h sample represents the carboxylic group [202].

Though the parent compound has broken-down into relatively smaller molecules, low-molecular-weight molecules that result from benzene ring cleavage were not detected. It could be due to the partial accumulation of degradation products of higher molar masses [179], [185], [187]. This explains the incomplete mineralization [208]. The determination of the intermediates' structures made it possible to propose a putative biodegradation pathway for DR81 and RO16 by *K. pneumoniae* [12].

It was reported that laccases catalyze coupling and polymerization reactions between undegraded dyes and their intermediates ignored in many studies dealing with the fate of dyes with azo bridges [185]. A comparatively large molecule with m/z 506.0805 was detected at the end of the incubation for both the direct and reactive dyes in this study. Similar high molecular weight compounds were also reported at the end of the degradation by Zille et al. [190]. All the by-products detected in the current study may not be wholly innocuous and might need further oxidative treatment. However, decolorization without completer mineralization is sufficient for reuse of the treated water in the textile processing industry as long as the metabolites generated are environmentally benign [203].

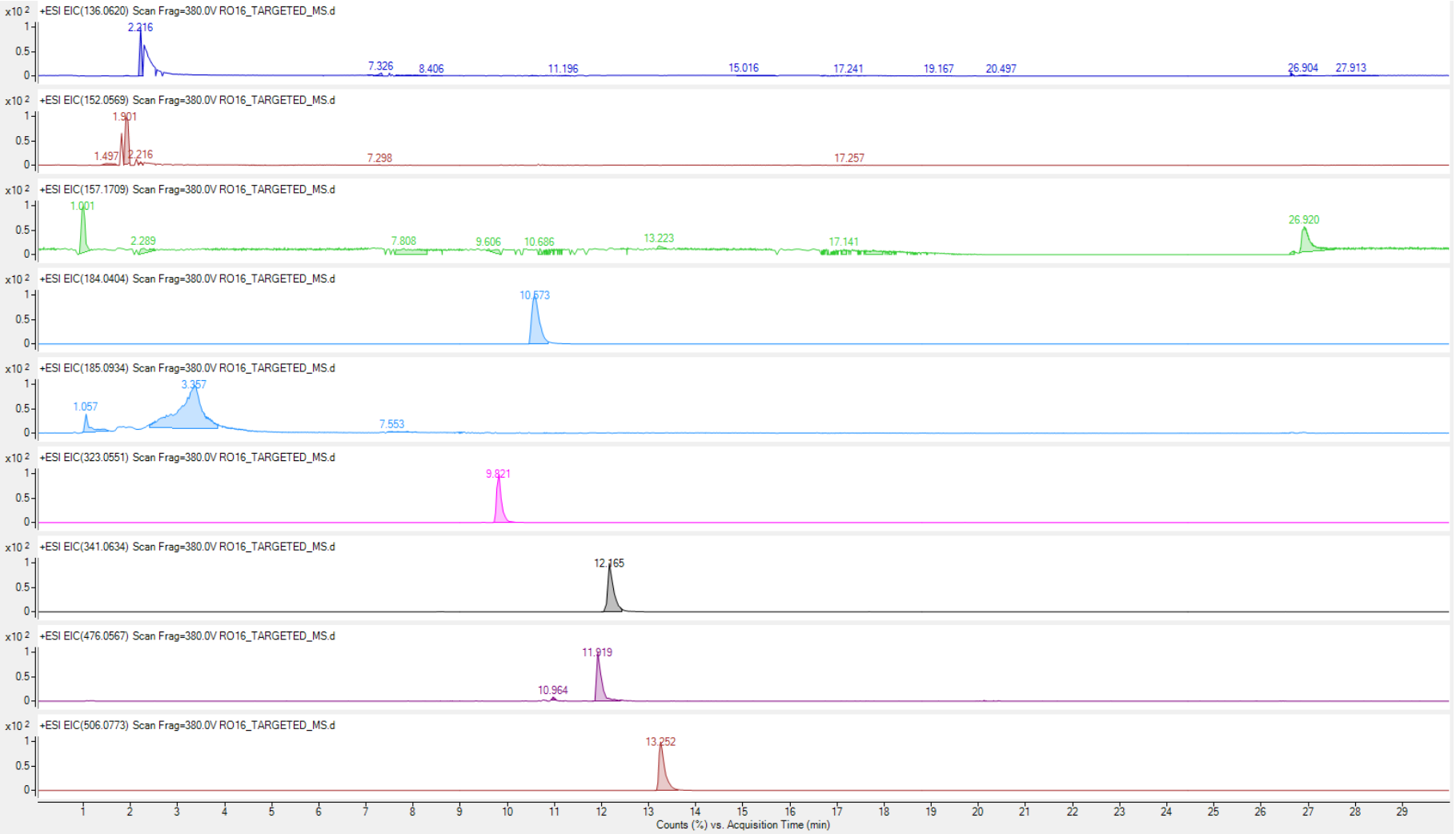

Figure 4. 23 LC-MS chromatograms of RO16 and its degradation by-products

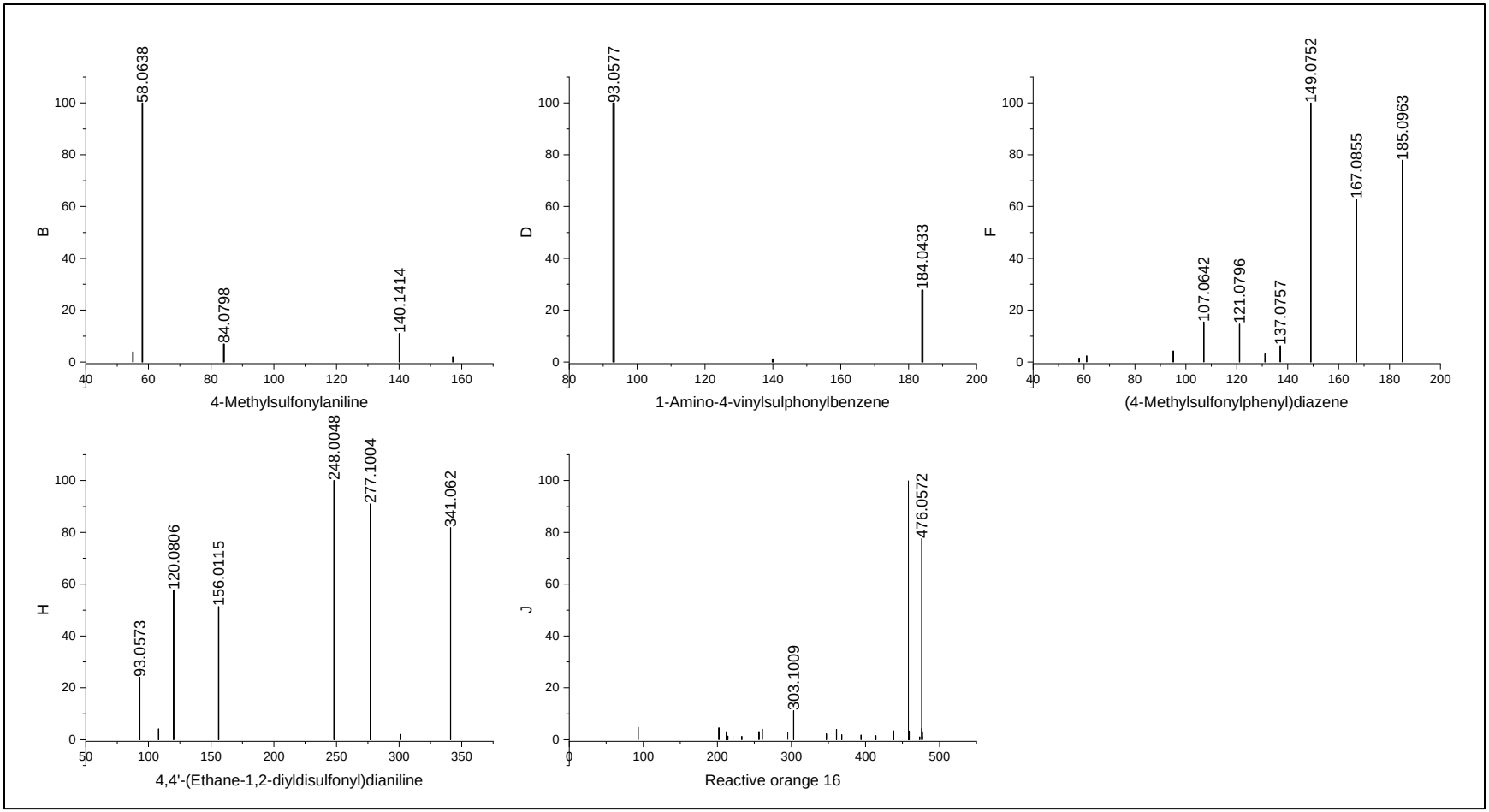

Figure 4. 24 MS^2 spectra for new compounds detected (RO16)

Table 4. 7 RT, m/z, CE of the identified by-products detected after RO16 degradation

m/z	RT (min)	CE (V)	Metabolite identified
157.1687	1.001	20	4-Methylsulfonylaniline
184.0433	10.573	10	1-Amino-4-vinylsulphonylbenzene
185.0963	3.357	10	(4-Methylsulfonylphenyl) diazene
341.062	12.165	10	4,4'-(Ethane-1,2-diyldisulfonyl) di aniline
476.0567	11.919	10	Reactive Orange 16 (Vinyl form)

Table 4. 8 Metabolites identified in RO16 degraded samples and controls

Precursor m/z	RT	Treated sample	Biotic control	Abiotic control
136.062	2.126			
152.0569	1.901			
157.1709	1.001			
184.0404	10.573			
185.0934	3.357			
323.0551	9.821			
341.0634	12.165			
476.0567	11.919			
506.0773	13.252			

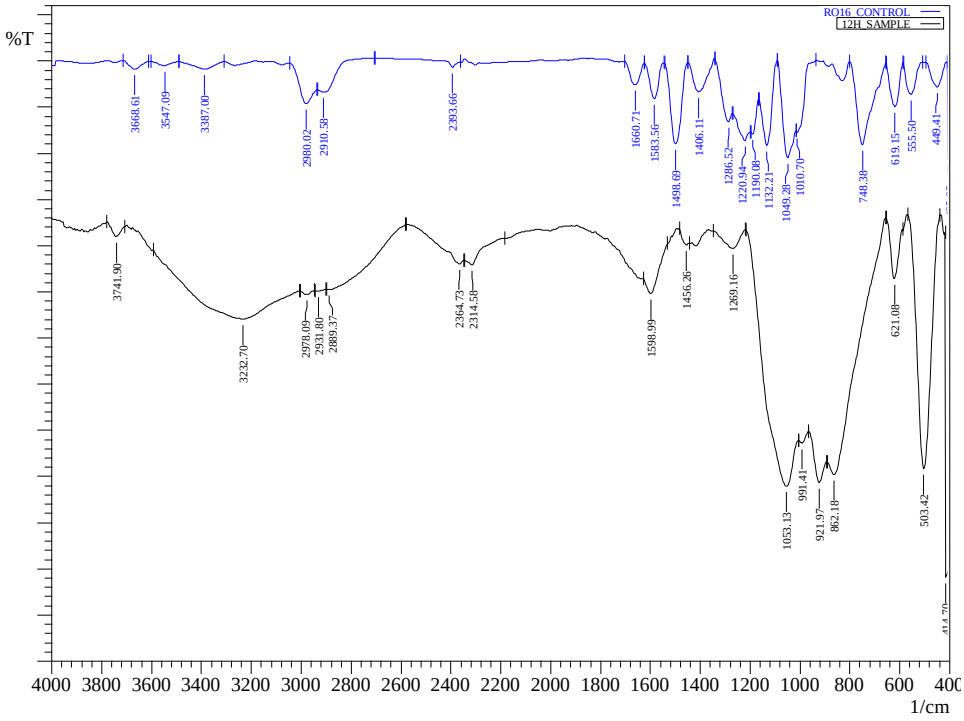

Figure 4. 25 FTIR spectra for RO16 and 12 h sample

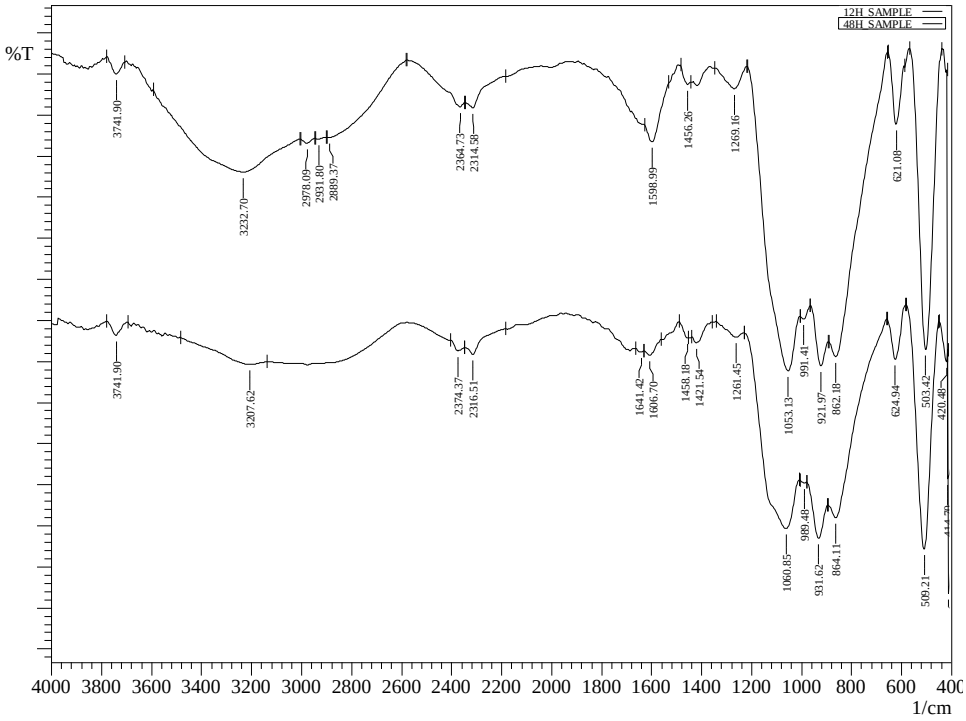

Figure 4. 26 FTIR spectra for RO16 12 h and 48 h sample

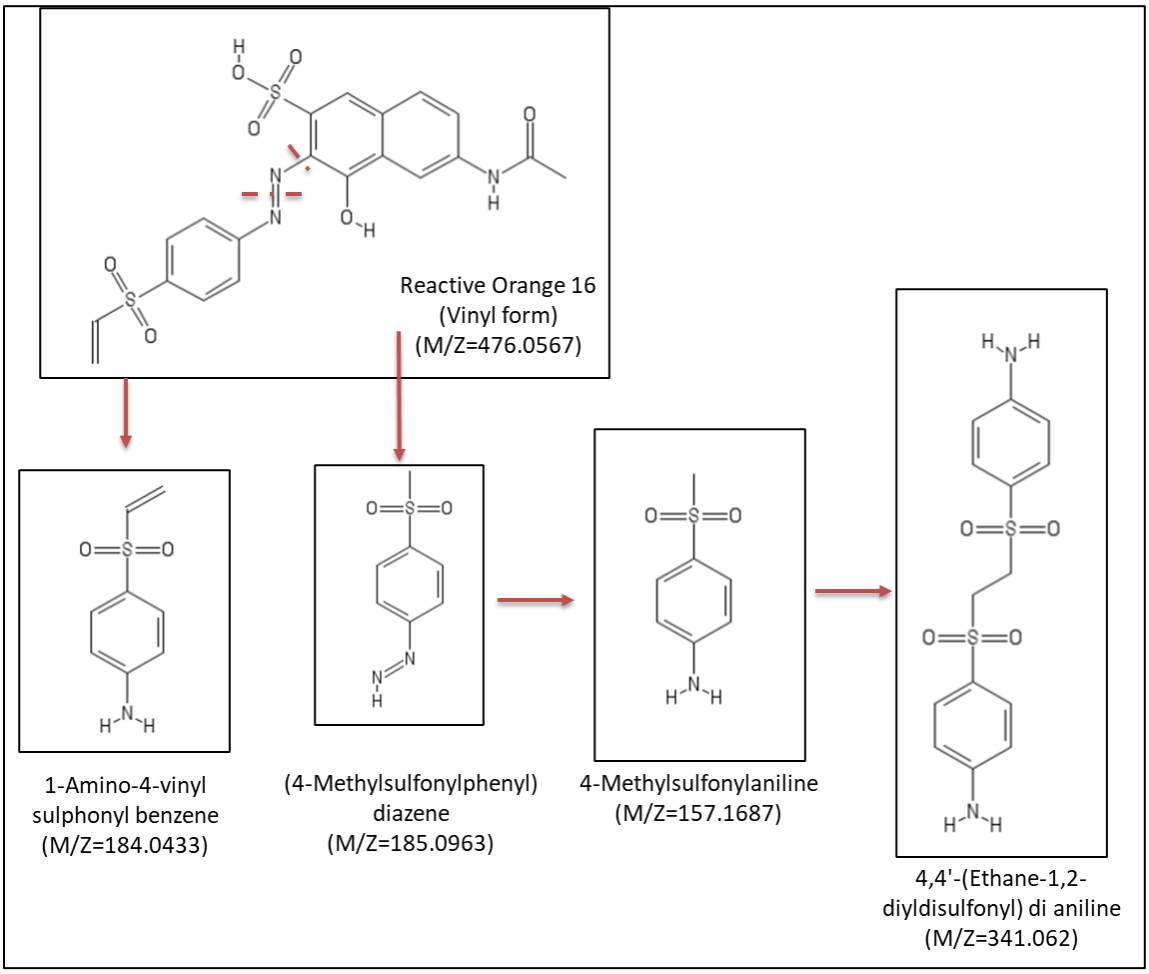

Figure 4. 27 Degradation pathway of RO16

4.5 Phytotoxicity assay

Phytotoxicity assay with *Vigna Radiata* seeds is a well-known, simple, and rapid test to assess the environmental toxicity of industrial wastewaters like TWW [172], [209]–[211]. The germination rate at 32 h was lesser in abiotic controls as compared to the treated samples as shown in *Figure 4.28*. DI water is the only sample to exhibit 100 % germination at 32 h whereas, the seeds in both DR81 treated sample and its respective control germinated 100 % at 48h. The biotic control, and treated sample and the controls of RO16 and AB113, have displayed a germination rate of 90 % at 48 h.

Though germination occurred in all the treated samples, biotic and abiotic controls, the root, shoot, and leaf development were observed only in seeds with DI water. The shoot length for all the treated samples and controls was under 5 cm while it is 4-fold higher for DI water as depicted in *Figure 4.29*. From the *Figure 4.30* it is evident that there is no sign of root and leaf growth other than shoot growth in all the treated samples and controls. Which means, the seeds remained undeveloped even after germination. High TDS and salinity retard the water uptake by the seeds that is necessary for the germination and therefore could be the reason for the inhibition [172]. At a TDS similar to that is observed in the present study (8120 – 8490 ppm), [172] reported inhibition in the growth of seeds.

However, the seeds in abiotic controls were damaged by the end of the experiment unlike the treated samples. At higher effluent concentration, the seeds could get low oxygen that restricts the energy supply thereby limiting the growth of the seedlings [209], [211]. Therefore, the treated samples are relatively safe to discharge upon dilution or desalination. Or for reuse within textile industries to achieve zero liquid discharge.

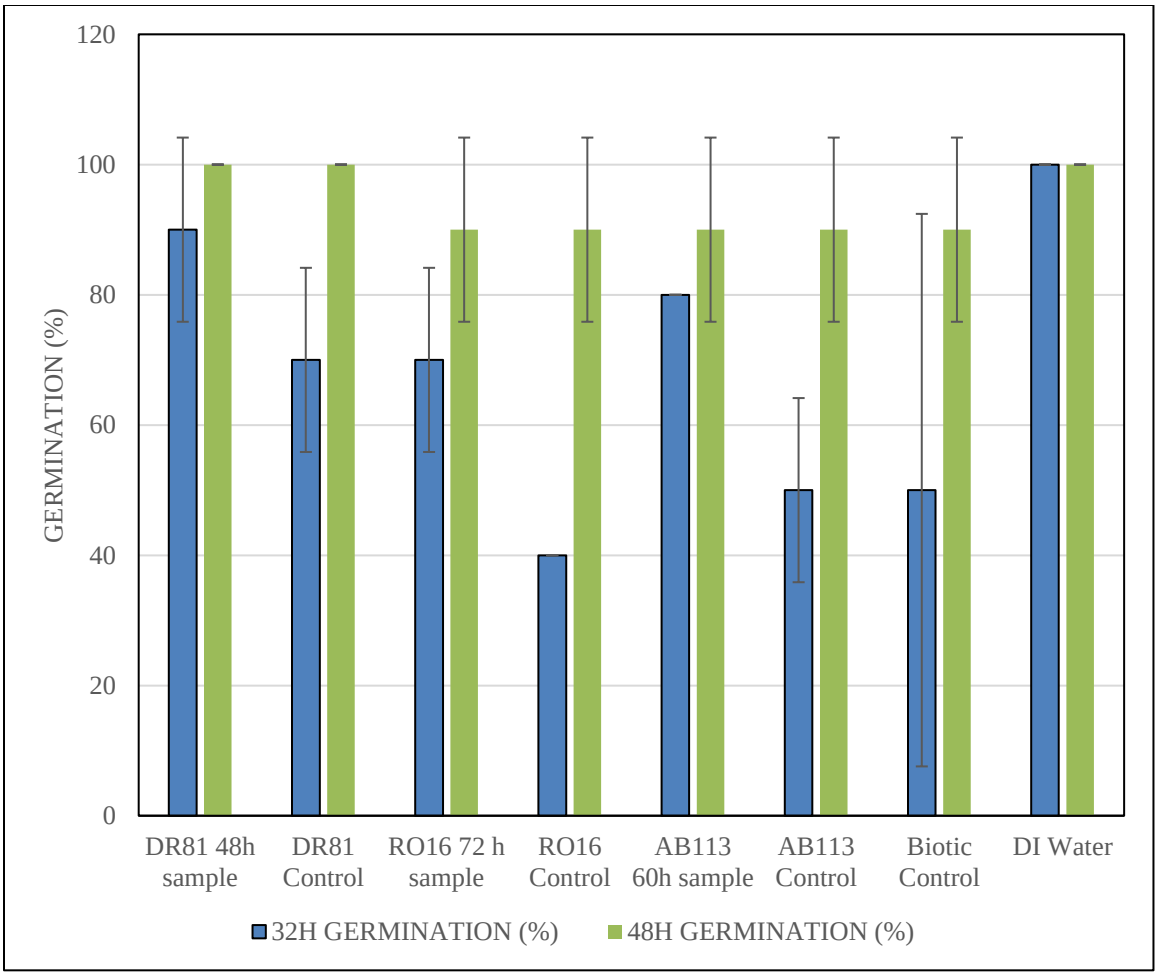

Figure 4. 28 Effect of the dye toxicity on the seed germination

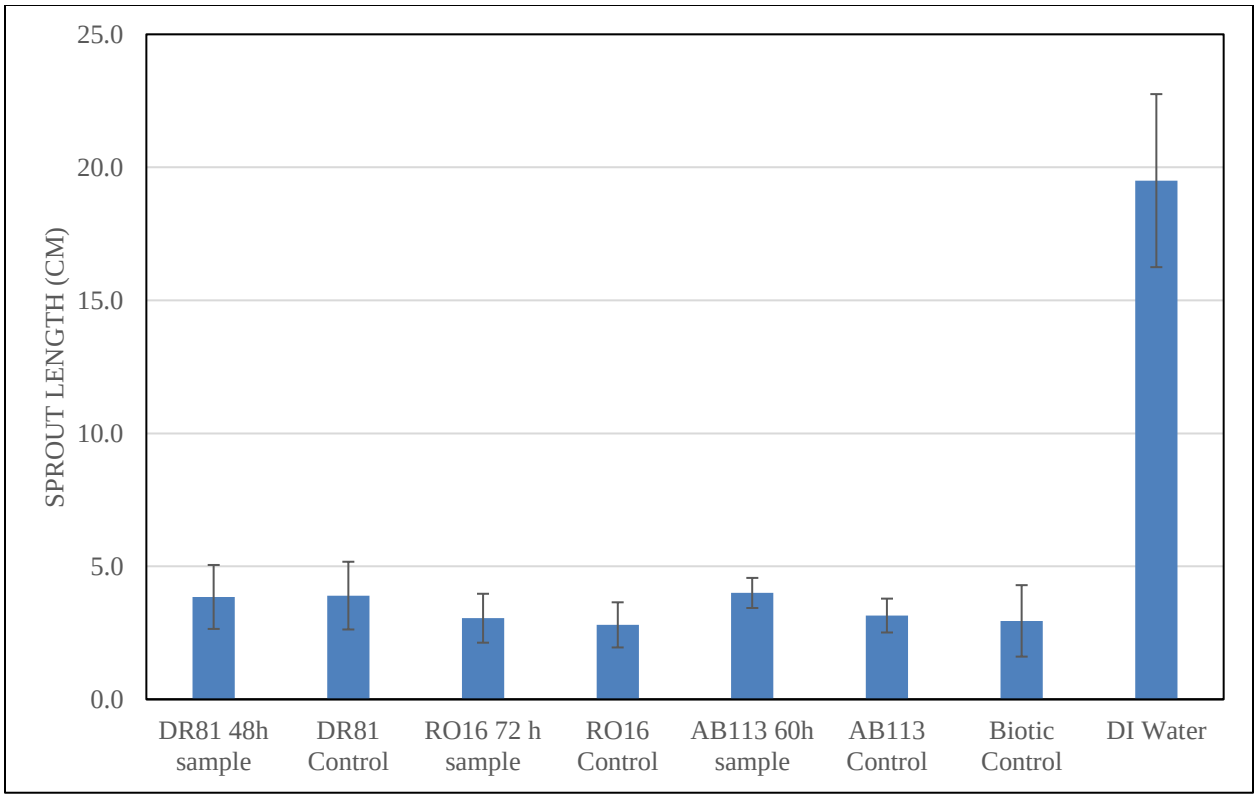

Figure 4. 29 Toxicity effect of the treated and untreated samples on the sprout length at 48 h

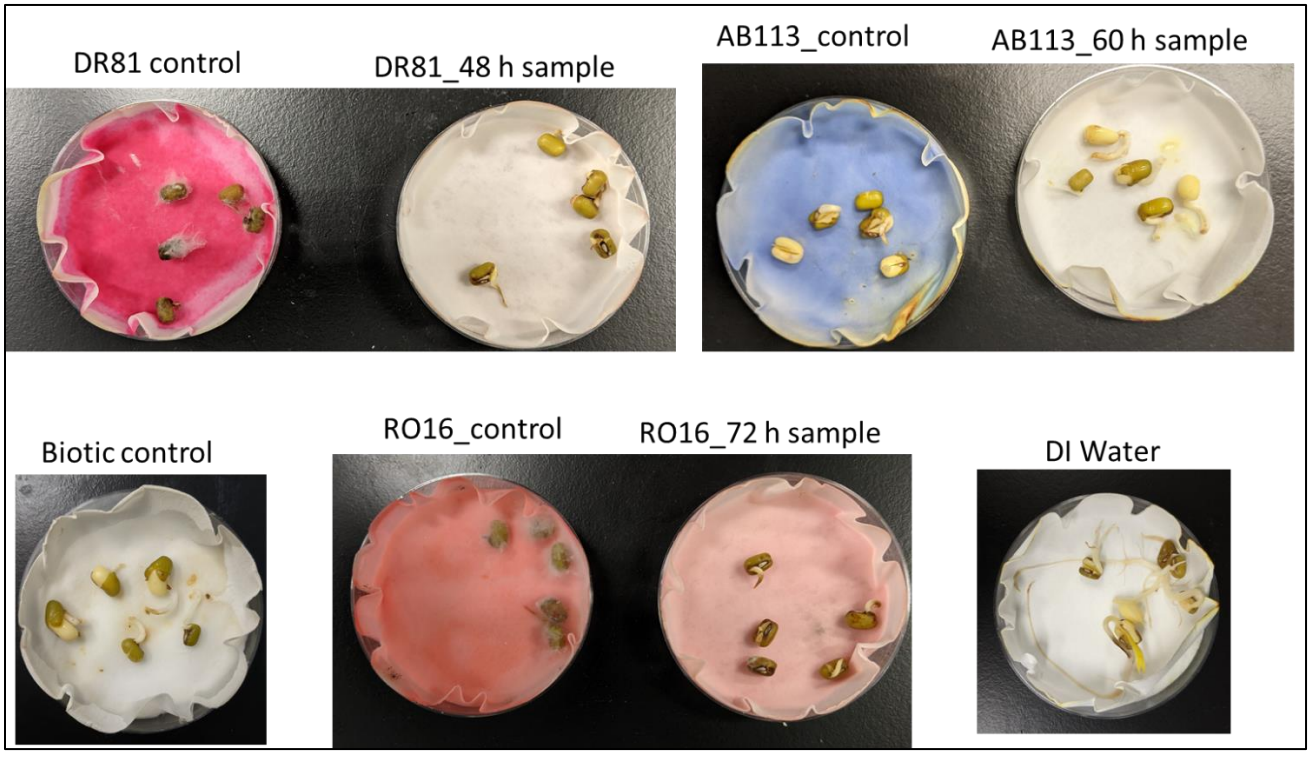

Figure 4. 30 Seedling growth at 48h in controls and treated samples

4.6 Conclusions

The dye decolorization performance of *Klebsiella* under salt stress conditions confirmed its halo tolerance and the ability to withstand the dye toxicity. In contrast to many previous reports, this study proved the possibility of aerobic dye decolorization. At 48 h, 82.9 % of AB113 removal was observed in aerobic conditions.

Though the sole aim of the present investigation is to aerobically degrade all the dyes considered for the study, static incubation conditions were found to be more conducive with a was substantial improvement in dye removal efficacy from 30.2 % to 91.5 % and 16.3 % to 65.6 % at 48 h for DR81 and RO16, respectively. Because *Klebsiella* is a facultative anaerobe, it functioned in both aerobic and microaerobic conditions. The presence of electrophilic sulfonate and hydroxyl functional groups in the azo bond proximity was reasoned to be responsible for the favoring of static conditions over shaking incubation for these two dyes unlike AB113 that had sulfonates at the periphery of the molecule.

Like most studies have reported, co-metabolism was found to be the dye degradation pathway. This study contradicted various previous reports that state the dye removal efficiency is dependent on the number of azo bonds and the molecular weight of the dye. DR81 and AB113 are diazo dyes and are heavier molecules in comparison to RO16, a mono azo dye. But the latter required 72 h to achieve about 80 % decolorization while the other two dyes require only 24 h. These findings emphasize the effect of steric hinderance due to functional groups in the azo bond proximity and their electron withdrawing nature on the dye removal efficiency, which were often not focused on in many previous studies. The FTIR data supports the formation of new by-products while LC-MS/MS confirms the same. A degradation pathway was delineated based on the by-products detected and identified for each dye.

Chapter 5 CONCLUSIONS AND RECOMMENDATIONS

5.1 Introduction

Textile dyes are persistent organic pollutants that can affect all segments of nature when discharged without proper treatment and management. Bioremediation of textile dyes was researched throughout the last decade and still is the most economical, efficient, and eco-friendly technique for removing and transforming dyes from TWW. Amongst all the bioremediation techniques, bacterial degradation was the most effective, eco-friendly, and economical for dye removal. This study's main objective is to aerobically decolorize and degrade a variety of structurally different and industrially important azo dyes in the presence of salts using *Klebsiella pneumoniae*. The degradation of complex organic pollutants is crucial to clean up the contaminated environment. To confirm degradation, the metabolites were tracked down to understand the mechanism involved and their degradation pathways. Phytotoxicity assay was performed on *Vigna Radiata* seeds to evaluate the toxicity of the treated dye effluent. All the three objectives of the current investigation are achieved, and this chapter sums up the research work outcomes of the same. Finally, it also recommends future works based on the limitations identified.

5.2 Study on isolation and identification of a halotolerant bacterium

In this study, three different biomasses sourced from three different local WWTPs were evaluated in aerobic conditions for their decolorization ability. From the preliminary dye decolorization kinetics, AB113 was the only dye to display up to 90 % of adsorption with all the three biomasses right at the 0^{th} hour. So, the most suitable biomass was chosen based on the dye removal efficiency of the other two dyes. IJRP was the only biomass to exhibit up to 90 % decolorization of DR81 and RO16 at the end of 54 h. The decolorization order is as follows: AB113 > DR81 > RO16. Hence it was expected to possess the right bacteria that can decolorize various dyes in aerobic conditions. Therefore, it was chosen for the isolation of decolorizing microbes upon shock loading with 1000 ppm of a pyridine based toxic sulfonated anionic azo dye as the sole carbon and nitrogen source under saline stress conditions. *K. pneumoniae* dye1 was the most active halotolerant strain

amongst the four strains isolated. Its facultative anaerobic nature is an added advantage because of its survivability in both oxygen limited and abundant conditions.

5.3 Study of dye decolorization kinetics under the influence of salts

In the previous study, *Klebsiella* was isolated. In this study, aerobic decolorization assay under the salt stress conditions was conducted with it for all the three dyes. About 80 % decolorization of AB113 was observed under 48 h while it was just under 30 % and 20 % for DR81 and RO16, respectively. To find the suitable incubation conditions for the dye decolorization, these two dyes were tested under static conditions and the efficiency improved by over two-fold. Despite the higher biomass growth in shaking incubation conditions, static microaerobic incubation conditions resulted in better dye removal efficiency than the shaking conditions for DR81 and RO16. Hence, decolorization assays were conducted in microaerobic conditions for these two dyes alone.

Based on the count of azo bonds and the molecular weight, the decolorization kinetics are supposed to be in the order: RO16 > DR81 > AB113. Contradicting many previous studies, the exact opposite was observed in this study i.e., *Klebsiella* decolorized diazo dyes faster than the mono azo dye. Structural differences and the position of the functional groups on the aromatic rings are found to be the primary driving factors in the decolorization kinetics. AB113 had no electron withdrawing functional group such as sulfonate and hydroxyl in the proximity of azo bond. Hence, despite having two azo bonds, it was the decolorized quicker than the other two dyes. This signifies the role of steric hinderance and the nature of the functional groups and the structural linearity of the dye besides the number of azo bonds or the molecular weight.

5.4 Study on dye transformation pathway

Firstly, this study investigates the applicability of *Klebsiella* for the aerobic degradation of AB113. The aerobic degradation of AB113 proceeds with a biotic redox reaction resulting in 4- [(2-Amino naphthalen-1-yl) diazenyl] benzenesulfonate due to symmetric azo bond cleavage. The dye was attacked only at one of the two conjugated azo bonds. Hence, the cleavage by-product had an azo bond, and the molecule resembled the structure of acid orange 7, which was further broken down into 1,4 Diamino naphthalene. 2 Amino benzene sulfonic acid was not detected. 1,4 Diamino

naphthalene underwent ring opening reactions to give a long chained aliphatic compound: N, N'-Diacetyl 1,6-diamino hexane. This work demonstrates the potential aerobic degradation of an industrially significant anionic azo dye, AB113. This study highlights the conversion of toxic AAs and SAAs to environmentally benign aliphatic compounds.

Secondly, the microaerobic degradation of DR81 also followed a similar degradation pattern as AB113. DR81 was attacked on one of the two azo bonds both symmetrically and asymmetrically unlike in the case of AB113 where the azo bond was attacked symmetrically. Symmetric azo bond reduction resulted in 4-((4-aminophenyl) diazenyl) benzene sulfonic acid which is a commonly known toxic azo dye - food yellow 6. It transformed into 4- Amino biphenyl. While the asymmetric azo bridge breakdown resulted in 3-diazenyl-7-benzamido-4-hydroxynaphthalene-2-sulfonic acid which further transformed to naphthalene-4-hydroxy-7-benzoyl amino-2-sulfonic acid.

Thirdly, the microaerobic degradation of RO16 also followed the same degradation pattern as DR81. RO16 was attacked both symmetrically and asymmetrically at the azo link which suggests that the azo bond reduction is unspecific. The dye was broken down to two different fragments. 1-amino-4-vinylsulfonyl benzene and 4-methylsulfonyl phenyl diazene due to symmetric and asymmetric cleavage of azo bond respectively. The latter was transformed to 4-methylsulfonyl aniline which further resulted in 4,4'-(Ethane-1,2-diyldisulfonyl) dianiline.

Anaerobic degradation can result in AAs and SAAs that can further impair the water quality due to their greater persistence and carcinogenicity compared to the parent dye. Therefore, the unknown degradation by-products were identified with a special focus on the AAs and SAAs. This study reports that the presence of sulfates and chlorides did not completely inhibit the degradation reaction. Therefore, a similar fate of the colorants can be expected in TWW typically spiked with salts like sulfates and chlorides.

Though all the dyes were broken-down into relatively smaller molecules, low-molecular-weight aliphatic molecules were not formed suggesting the partial accumulation of degradation by-products and incomplete mineralization. The TOC/TN removal efficacy supports the same. Moreover, unknown_498 was detected at the end of the incubation for AB113 in this study. Therefore, the treated effluents were tested for their toxicity on *Vigan Radiata* seeds. The

phytotoxicity assay suggested that the presence of salts could be also one of the reasons for the poor seed germination and seedling growth. Hence, the treated samples may not be completely innocuous and might need further desalination or dilution. These results carry environmental significance. Complete mineralization is not required for the reuse of the treated water in the textile processing industry if the metabolites generated are environmentally benign. Hence this data can be used in the design of the TWW treatment processes, to ensure that the treated effluent is safe to dispose or reuse within textile industries to achieve zero liquid discharge.

5.5 Scope for future studies

A few limitations have been identified in the present study, and corresponding recommendations are proposed:

1. The present study targeted the degradation of one dye at a time with *Klebsiella* to demonstrate and understand the fate of the dye and the by-products released. However, TWW often consists of a mixture of dyes. The isolate studied in this investigation can be tested with a mixture of all the three dyes used in this study. Further, its treatability of the real TWW can be investigated.
2. The utility of the microbe identified in this study can be evaluated for its practical applicability in industrial WWTPs upon coupling with suitable treatment techniques such as immobilization on biochar/granular activated carbon or in a membrane bioreactor. Efforts can be directed to commercialize the same, through pilot-scale study followed by full-scale studies with real TWW.
3. Bioprocesses using bacteria is an economic and environmentally benign solution to remove dyes from the textile effluent contaminated environments. The present study demonstrated the decolorizing ability of *Klebsiella* in saline stress conditions. Since mixed microbial populations are more effective and adaptable to diverse environment as witnessed in a real TWW, future studies could focus on the utilization of consortia comprising of bacteria that can decolorize all types of dyes in both aerobic conditions and under salt stress conditions.
4. Further, future studies can shed light on the reuse of the treated TWW within the textile industry to achieve “zero liquid discharge” as this would cutdown the consumption of huge quantities of clean water for dyeing purposes and avoid disposal problems altogether.

5. Research on the integration of “omics” data using computational biological tools with the dye metabolites data can provide a complete and detailed picture of the degradation pathways involved.
6. Gene expression and metabolic activity of the bacteria can be correlated to the metabolites released during dye degradation. Networks connecting these two datasets can provide valuable insights on the suitability of *Klebsiella* to other azo dyes.
7. Genetic modification of *Klebsiella* to overexpress the genes that produce the dye decolorizing enzymes can further finetune the TWW treatment system.

References

[1] A. M. Donia, A. A. Atia, W. A. Al-amrani, and A. M. El-Nahas, "Effect of structural properties of acid dyes on their adsorption behaviour from aqueous solutions by amine modified silica," *Journal of Hazardous Materials*, vol. 161, no. 2–3, pp. 1544–1550, 2009, doi: 10.1016/j.jhazmat.2008.05.042.

[2] R. V. Kandisa and N. Saibaba KV, "Dye Removal by Adsorption: A Review," *Journal of Bioremediation & Biodegradation*, vol. 07, no. 06, 2016, doi: 10.4172/2155-6199.1000371.

[3] T. Robinson, G. McMullan, R. Marchant, and P. Nigam, "Remediation of dyes in textile effluent: a critical review on current treatment technologies with a proposed alternative," *Bioresource technology*, vol. 77, no. 3, pp. 247–255, 2001, doi: https://doi.org/10.1016/S0960-8524(00)00080-8.

[4] R. Ganesh, G. D. Boardman, and D. Michelsen, "Fate of azo dyes in sludges," *Water Research*, vol. 28, no. 6, pp. 1367–1376, 1994, doi: https://doi.org/10.1016/0043-1354(94)90303-4.

[5] H. B. Mansour, R. Mosrati, D. Corroler, K. Ghedira, D. Barillier, and L. Chekir-Ghedira, "Mutagenicity and genotoxicity of acid yellow 17 and its biodegradation products," *Drug and Chemical Toxicology*, vol. 32, no. 3, pp. 222–229, 2009, doi: 10.1080/01480540902862269.

[6] P. Bansal, D. Singh, and D. Sud, "Photocatalytic degradation of azo dye in aqueous TiO2 suspension: Reaction pathway and identification of intermediates products by LC/MS," *Separation and Purification Technology*, vol. 72, no. 3, pp. 357–365, 2010, doi: 10.1016/j.seppur.2010.03.005.

[7] H. Lade, A. Kadam, D. Paul, and S. Govindwar, "Biodegradation and detoxification of textile azo dyes by bacterial consortium under sequential microaerophilic/aerobic processes," *EXCLI journal*, vol. 14, pp. 158–174, 2015, doi: http://dx.doi.org/10.17179/excli2014-642.

[8] K. Balapure, N. Bhatt, and D. Madamwar, "Mineralization of reactive azo dyes present in simulated textile wastewater using down flow microaerophilic fixed film bioreactor," *Bioresource Technology*, vol. 175, pp. 1–7, 2015, doi: 10.1016/j.biortech.2014.10.040.

[9] N. Azbar, T. Yonar, and K. Kestioglu, "Comparison of various advanced oxidation processes and chemical treatment methods for COD and color removal from a polyester and acetate fiber dyeing effluent," *Chemosphere*, vol. 55, no. 1, pp. 35–43, 2004, doi: 10.1016/j.chemosphere.2003.10.046.

[10] S. Papic, "Removal of some reactive dyes from synthetic wastewater by combined Al(III) coagulation/carbon adsorption process," *Dyes and Pigments*, vol. 62, no. 3, pp. 291–298, 2004, doi: 10.1016/S0143-7208(03)00148-7.

[11] J.-W. Lee, S.-P. Choi, R. Thiruvenkatachari, W.-G. Shim, and H. Moon, "Evaluation of the performance of adsorption and coagulation processes for the maximum removal of reactive dyes," *Dyes and Pigments*, vol. 69, no. 3, pp. 196–203, 2006, doi: 10.1016/j.dyepig.2005.03.008.

[12] M. Constapel, M. Schellenträger, J. M. Marzinkowski, and S. Gäb, "Degradation of reactive dyes in wastewater from the textile industry by ozone: Analysis of the products by accurate masses," *Water Research*, vol. 43, no. 3, pp. 733–743, 2009, doi: 10.1016/j.watres.2008.11.006.

[13] S. K. Sen, S. Raut, P. Bandyopadhyay, and S. Raut, "Fungal decolouration and degradation of azo dyes: A review," *Fungal Biology Reviews*, vol. 30, no. 3, pp. 112–133, 2016, doi: 10.1016/j.fbr.2016.06.003.

[14] E. Forgacs, T. Cserháti, and G. Oros, "Removal of synthetic dyes from wastewaters: a review," *Environment International*, vol. 30, no. 7, pp. 953–971, 2004, doi: 10.1016/j.envint.2004.02.001.

[15] J. Guo, J. Zhou, D. Wang, C. Tian, P. Wang, and M. S. Uddin, "A novel moderately halophilic bacterium for decolorizing azo dye under high salt condition," *Biodegradation*, vol. 19, no. 1, pp. 15–19, 2008, doi: 10.1007/s10532-007-9110-1.

[16] A. W. M. Ip, J. P. Barford, and G. McKay, “Reactive Black dye adsorption/desorption onto different adsorbents: Effect of salt, surface chemistry, pore size and surface area,” *Journal of Colloid and Interface Science*, vol. 337, no. 1, pp. 32–38, 2009, doi: 10.1016/j.jcis.2009.05.015.

[17] S. Hussain *et al.*, “Biodecolorization of reactive black-5 by a metal and salt tolerant bacterial strain Pseudomonas sp. RA20 isolated from Paharang drain effluents in Pakistan,” *Ecotoxicology and Environmental Safety*, vol. 98, pp. 331–338, 2013, doi: 10.1016/j.ecoenv.2013.09.018.

[18] A. S. Arun Prasad, V. S. V. Satyanarayana, and K. V. Bhaskara Rao, “Biotransformation of Direct Blue 1 by a moderately halophilic bacterium Marinobacter sp. strain HBRA and toxicity assessment of degraded metabolites,” *Journal of Hazardous Materials*, vol. 262, pp. 674–684, 2013, doi: 10.1016/j.jhazmat.2013.09.011.

[19] Y. Chen, L. Feng, H. Li, Y. Wang, G. Chen, and Q. Zhang, “Biodegradation and detoxification of Direct Black G textile dye by a newly isolated thermophilic microflora,” *Bioresource Technology*, vol. 250, pp. 650–657, 2018, doi: 10.1016/j.biortech.2017.11.092.

[20] J. Bacardit, J. Stötzner, E. Chamarro, and S. Esplugas, “Effect of Salinity on the Photo-Fenton Process,” *Ind. Eng. Chem. Res.*, vol. 46, no. 23, pp. 7615–7619, Nov. 2007, doi: 10.1021/ie070154o.

[21] M. E. Talukder, M. Kamruzzaman, M. Majumder, M. S. H. Rony, M. Hossain, and S. Das, “Effects of Salt Concentration on the Dyeing of Various Cotton Fabrics with Reactive Dyes,” *International Journal of Textile Science*, vol. 6, no. 1, pp. 7–14, 2017.

[22] M. A. Amoozegar, M. Hajighasemi, J. Hamedi, S. Asad, and A. Ventosa, “Azo dye decolorization by halophilic and halotolerant microorganisms,” *Annals of Microbiology*, vol. 61, no. 2, pp. 217–230, 2011, doi: 10.1007/s13213-010-0144-y.

[23] A. Khalid, M. Arshad, and D. E. Crowley, “Decolorization of azo dyes by Shewanella sp. under saline conditions,” *Applied Microbiology and Biotechnology*, vol. 79, no. 6, pp. 1053–1059, 2008, doi: 10.1007/s00253-008-1498-y.

[24] C. J. Ogugbue, T. Sawidis, and N. A. Oranusi, “Evaluation of colour removal in synthetic saline wastewater containing azo dyes using an immobilized halotolerant cell system,” *Ecological Engineering*, vol. 37, no. 12, pp. 2056–2060, 2011, doi: 10.1016/j.ecoleng.2011.09.003.

[25] H. Mirbolooki, R. Amirnezhad, and A. R. Pendashteh, “Treatment of high saline textile wastewater by activated sludge microorganisms,” *Journal of Applied Research and Technology*, vol. 15, no. 2, pp. 167–172, 2017, doi: 10.1016/j.jart.2017.01.012.

[26] A. R. Tehrani-Bagha, N. M. Mahmoodi, and F. M. Menger, “Degradation of a persistent organic dye from colored textile wastewater by ozonation,” *Desalination*, vol. 260, no. 1–3, pp. 34–38, 2010, doi: 10.1016/j.desal.2010.05.004.

[27] S. Sadri Moghaddam, M. R. Alavi Moghaddam, and M. Arami, “Coagulation/flocculation process for dye removal using sludge from water treatment plant: Optimization through response surface methodology,” *Journal of Hazardous Materials*, vol. 175, no. 1–3, pp. 651–657, 2010, doi: 10.1016/j.jhazmat.2009.10.058.

[28] S. Venkata Mohan, P. Sailaja, M. Srimurali, and J. Karthikeyan, “Color removal of monoazo acid dye from aqueous solution by adsorption and chemical coagulation,” *Environmental Engineering and Policy*, vol. 1, no. 3, pp. 149–154, 1998, doi: 10.1007/s100220050016.

[29] I. K. Konstantinou and T. A. Albanis, “TiO2-assisted photocatalytic degradation of azo dyes in aqueous solution: kinetic and mechanistic investigations,” *Applied Catalysis B: Environmental*, vol. 49, no. 1, pp. 1–14, 2004, doi: 10.1016/j.apcatb.2003.11.010.

[30] K. V. Kumar, V. Ramamurthi, and S. Sivanesan, “Modeling the mechanism involved during the sorption of methylene blue onto fly ash,” *Journal of Colloid and Interface Science*, vol. 284, no. 1, pp. 14–21, 2005, doi: 10.1016/j.jcis.2004.09.063.

[31] C. Fleischmann, M. Lievenbrück, and H. Ritter, “Polymers and Dyes: Developments and Applications,” *Polymers*, vol. 7, no. 4, pp. 717–746, 2015, doi: 10.3390/polym7040717.

[32] D. Rawat, V. Mishra, and R. S. Sharma, “Detoxification of azo dyes in the context of environmental processes,” *Chemosphere*, vol. 155, pp. 591–605, 2016, doi: 10.1016/j.chemosphere.2016.04.068.

[33] J. J. Porter, “The stability of acid, basic and direct dyes to light and water.” Textile research journal, 1973. [Online]. Available: https://doi.org/10.1177/004051757304301209

[34] D. Wesenberg, “White-rot fungi and their enzymes for the treatment of industrial dye effluents,” *Biotechnology Advances*, vol. 22, no. 1–2, pp. 161–187, 2003, doi: 10.1016/j.biotechadv.2003.08.011.

[35] A. A. Ahmad and B. H. Hameed, “Fixed-bed adsorption of reactive azo dye onto granular activated carbon prepared from waste,” *Journal of Hazardous Materials*, vol. 175, no. 1–3, pp. 298–303, 2010, doi: 10.1016/j.jhazmat.2009.10.003.

[36] S. Selvakumar, R. Manivasagan, and K. Chinnappan, “Biodegradation and decolourization of textile dye wastewater using Ganoderma lucidum,” *3 Biotech*, vol. 3, no. 1, pp. 71–79, 2013, doi: 10.1007/s13205-012-0073-5.

[37] G. Quan, W. Sun, J. Yan, and Y. Lan, “Nanoscale Zero-Valent Iron Supported on Biochar: Characterization and Reactivity for Degradation of Acid Orange 7 from Aqueous Solution,” *Water, Air, & Soil Pollution*, vol. 225, no. 11, 2014, doi: 10.1007/s11270-014-2195-3.

[38] S. Sandhya, S. Padmavathy, K. Swaminathan, Y. V. Subrahmanyam, and S. N. Kaul, “Microaerophilic–aerobic sequential batch reactor for treatment of azo dyes containing simulated wastewater,” *Process Biochemistry*, vol. 40, no. 2, pp. 885–890, 2005, doi: 10.1016/j.procbio.2004.02.015.

[39] Z. W. Wang, J. S. Liang, and Y. Liang, “Decolorization of Reactive Black 5 by a newly isolated bacterium Bacillus sp. YZU1,” *International Biodeterioration & Biodegradation*, vol. 76, pp. 41–48, 2013, doi: 10.1016/j.ibiod.2012.06.023.

[40] A. K. Verma, R. R. Dash, and P. Bhunia, “A review on chemical coagulation/flocculation technologies for removal of colour from textile wastewaters,” *Journal of Environmental Management*, vol. 93, no. 1, pp. 154–168, 2012, doi: 10.1016/j.jenvman.2011.09.012.

[41] M. Taskin and S. Erdal, “Reactive dye bioaccumulation by fungus Aspergillus niger isolated from the effluent of sugar fabric-contaminated soil,” *Toxicology and Industrial Health*, vol. 26, no. 4, pp. 239–247, 2010, doi: 10.1177/0748233710364967.

[42] M. K. Purkait, A. Maiti, S. DasGupta, and S. De, “Removal of congo red using activated carbon and its regeneration,” *Journal of Hazardous Materials*, vol. 145, no. 1–2, pp. 287–295, 2007, doi: 10.1016/j.jhazmat.2006.11.021.

[43] Y. Fu and T. Viraraghavan, “Column studies for biosorption of dyes from aqueous solutions on immobilised Aspergillus niger fungal biomass,” *Water Sa*, vol. 29, no. 4, pp. 465–472, 2003, doi: http://dx.doi.org/10.4314/wsa.v29i4.5054.

[44] C. D. Shah and D. K. Jain, “Dyeing of Modified Polypropylene—Cationic Dyes on Brominated Polypropylene,” *Textile Research Journal*, vol. 54, no. 11, pp. 742–748, 1984, doi: https://doi.org/10.1177/004051758405401107.

[45] Z. Wang, M. Xue, K. Huang, and Z. Liu, “Textile dyeing wastewater treatment,” in *Advances in treating textile effluent*, vol. 5, InTech, 2011, pp. 91–117. [Online]. Available: http://www.intechopen.com/books/advances-in-treating-textile-effluent/textile-dyeing-wastewater- treatment

[46] Ö. Gerçel, H. F. Gerçel, A. S. Koparal, and Ü. B. Öğütveren, “Removal of disperse dye from aqueous solution by novel adsorbent prepared from biomass plant material,” *Journal of Hazardous Materials*, vol. 160, no. 2–3, pp. 668–674, 2008, doi: 10.1016/j.jhazmat.2008.03.039.

[47] Y. Wang, B.-Y. Gao, Q.-Y. Yue, J.-C. Wei, W.-Z. Zhou, and R. Gu, "Color Removal from Textile Industry Wastewater Using Composite Flocculants," *Environmental Technology*, vol. 28, no. 6, pp. 629–637, 2007, doi: 10.1080/09593332808618824.

[48] Y. Al-Degs, M. A. M. Khraisheh, S. J. Allen, and M. N. Ahmad, "Effect of carbon surface chemistry on the removal of reactive dyes from textile effluent." Wat. Res., 2000. [Online]. Available: https://doi.org/10.1016/S0043-1354(99)00200-6

[49] M. Ajaz, S. Shakeel, and A. Rehman, "Microbial use for azo dye degradation—a strategy for dye bioremediation," *Int Microbiol*, vol. 23, no. 2, pp. 149–159, 2020, doi: 10.1007/s10123-019-00103-2.

[50] C. R. Holkar, H. Arora, D. Halder, and D. V. Pinjari, "Biodegradation of reactive blue 19 with simultaneous electricity generation by the newly isolated electrogenic Klebsiella sp. C NCIM 5546 bacterium in a microbial fuel cell," *International Biodeterioration & Biodegradation*, vol. 133, pp. 194–201, 2018, doi: 10.1016/j.ibiod.2018.07.011.

[51] I. Mielgo, M. T. Moreira, G. Feijoo, and J. M. Lema, "A packed-bed fungal bioreactor for the continuous decolourisation of azo-dyes (Orange II)," *Journal of biotechnology*, vol. 89, no. 2, pp. 99–106, 2001, doi: https://doi.org/10.1016/S0168-1656(01)00319-4.

[52] D. G. Lynch, "Estimating the properties of synthetic organic dyes," *Handbook of Property Estimation Methods for Chemicals: Environmental and Health Sciences. Lewis, Boca Raton, FL, USA*, pp. 447–463, 2000, doi: https://doi.org/10.1201/9781420026283.

[53] S. W. Won, S. B. Choi, B. W. Chung, D. Park, J. M. Park, and Y.-S. Yun, "Biosorptive Decolorization of Reactive Orange 16 Using the Waste Biomass of *Corynebacterium glutamicum*," *Industrial & Engineering Chemistry Research*, vol. 43, no. 24, pp. 7865–7869, 2004, doi: 10.1021/ie049559o.

[54] S. Shobana and B. E. Thangam, "Biodegradation and Decolorization of Reactive Orange 16 by Nocardiopsis alba Soil Isolate," *Journal of Bioremediation and Biodegradation*, vol. 03, no. 06, 2012, doi: 10.4172/2155-6199.1000155.

[55] D. Georgiou, J. Hatiras, and A. Aivasidis, "Microbial immobilization in a two-stage fixed-bed-reactor pilot plant for on-site anaerobic decolorization of textile wastewater," *Enzyme and Microbial Technology*, vol. 37, no. 6, pp. 597–605, 2005, doi: 10.1016/j.enzmictec.2005.03.019.

[56] A. Gomes, R. Brás, M. I. A. Ferra, M. T. P. Amorim, and R. S. Porter, "Biological treatment of effluent containing textile dyes," *Coloration Technology*, vol. 116, no. 12, pp. 393–397, 2000, doi: https://doi.org/10.1111/j.1478-4408.2000.tb00016.x.

[57] R. G. Saratale, G. D. Saratale, D. C. Kalyani, J. S. Chang, and S. P. Govindwar, "Enhanced decolorization and biodegradation of textile azo dye Scarlet R by using developed microbial consortium-GR," *Bioresource Technology*, vol. 100, no. 9, pp. 2493–2500, 2009, doi: 10.1016/j.biortech.2008.12.013.

[58] J.-W. Lee, S.-P. Choi, R. Thiruvenkatachari, W.-G. Shim, and H. Moon, "Submerged microfiltration membrane coupled with alum coagulation/powdered activated carbon adsorption for complete decolorization of reactive dyes," *Water Research*, vol. 40, no. 3, pp. 435–444, 2006, doi: 10.1016/j.watres.2005.11.034.

[59] M. S. Nawaz and M. Ahsan, "Comparison of physico-chemical, advanced oxidation and biological techniques for the textile wastewater treatment," *Alexandria Engineering Journal*, vol. 53, no. 3, pp. 717–722, 2014, doi: 10.1016/j.aej.2014.06.007.

[60] N. Ertugay and F. N. Acar, "Removal of COD and color from Direct Blue 71 azo dye wastewater by Fenton's oxidation: Kinetic study," *Arabian Journal of Chemistry*, vol. 10, pp. S1158–S1163, 2013, doi: 10.1016/j.arabjc.2013.02.009.

[61] G. Crini, "Non-conventional low-cost adsorbents for dye removal: A review," *Bioresource Technology*, vol. 97, no. 9, pp. 1061–1085, 2006, doi: 10.1016/j.biortech.2005.05.001.

[62] M. A. Ashraf *et al.*, "Removal of acid yellow-17 dye from aqueous solution using eco-friendly biosorbent," *Desalination and Water Treatment*, vol. 51, no. 22–24, pp. 4530–4545, 2013, doi: 10.1080/19443994.2012.747187.

[63] G. Moussavi and R. Khosravi, "Preparation and characterization of a biochar from pistachio hull biomass and its catalytic potential for ozonation of water recalcitrant contaminants," *Bioresource Technology*, vol. 119, pp. 66–71, 2012, doi: 10.1016/j.biortech.2012.05.101.

[64] S. Sadri Moghaddam, M. R. Alavi Moghaddam, and M. Arami, "Response surface optimization of acid red 119 dye from simulated wastewater using Al based waterworks sludge and polyaluminium chloride as coagulant," *Journal of Environmental Management*, vol. 92, no. 4, pp. 1284–1291, 2011, doi: 10.1016/j.jenvman.2010.12.015.

[65] C. Galindo, P. Jacques, and A. Kalt, "Photochemical and photocatalytic degradation of an indigoid dye: a case study of acid blue 74 (AB74)," *Journal of Photochemistry and Photobiology A: Chemistry*, vol. 141, no. 1, pp. 47–56, 2001, doi: https://doi.org/10.1016/S1010-6030(01)00435-X.

[66] G. Zayani, L. Bousselmi, F. Mhenni, and A. Ghrabi, "Solar photocatalytic degradation of commercial textile azo dyes: Performance of pilot plant scale thin film fixed-bed reactor," *Desalination*, vol. 246, no. 1–3, pp. 344–352, 2009, doi: 10.1016/j.desal.2008.03.059.

[67] I. Koyuncu, "Reactive dye removal in dye/salt mixtures by nanofiltration membranes containing vinylsulphone dyes: effects of feed concentration and cross flow velocity," *Desalination*, vol. 143, no. 3, pp. 243–253, 2002, doi: https://doi.org/10.1016/S0011-9164(02)00263-1.

[68] M. Liu *et al.*, "High efficient removal of dyes from aqueous solution through nanofiltration using diethanolamine-modified polyamide thin-film composite membrane," *Separation and Purification Technology*, vol. 173, pp. 135–143, 2017, doi: 10.1016/j.seppur.2016.09.023.

[69] J. Hao and Q. Zhao, "The development of membrane technology for wastewater treatment in the textile industry in China," *Desalination*, vol. 98, no. 1–3, pp. 353–360, 1994, doi: https://doi.org/10.1016/0011-9164(94)00161-8.

[70] S. A. Ahmed and Y. C. Rotliwala, "Adsorption of reactive dyes on pyrolytic bio-char derived activated carbon," *International journal of advanced research in engineering, science and management*, vol. 3, no. 4, 2014.

[71] W. Ghani, A. Mohd, D. K. Mahmoud, N. Z. Rebitanim, L. Sanyang, and R. B. Zainudin, "Adsorption of methylene blue on sawdust-derived biochar and its adsorption isotherms," *J. Purity Util. Reac. Environ*, vol. 2, no. 2, pp. 34–50, 2013.

[72] P. K. Malik, "Dye removal from wastewater using activated carbon developed from sawdust: adsorption equilibrium and kinetics," *Journal of Hazardous Materials*, vol. 113, no. 1–3, pp. 81–88, 2004, doi: 10.1016/j.jhazmat.2004.05.022.

[73] M. A. Hassaan, A. El Nemr, and F. F. Madkour, "Testing the advanced oxidation processes on the degradation of Direct Blue 86 dye in wastewater," *The Egyptian Journal of Aquatic Research*, vol. 43, no. 1, pp. 11–19, 2016, doi: 10.1016/j.ejar.2016.09.006.

[74] M. Neamtu, A. Yediler, I. Siminiceanu, and A. Kettrup, "Oxidation of commercial reactive azo dye aqueous solutions by the photo-Fenton and Fenton-like processes," *Journal of Photochemistry and Photobiology A: Chemistry*, vol. 161, no. 1, pp. 87–93, 2003, doi: 10.1016/S1010-6030(03)00270-3.

[75] A. Pandey, P. Singh, and L. Iyengar, "Bacterial decolorization and degradation of azo dyes," *International Biodeterioration & Biodegradation*, vol. 59, no. 2, pp. 73–84, 2007, doi: 10.1016/j.ibiod.2006.08.006.

[76] S. Papic *et al.*, "Advanced oxidation process in azo dye waste water treatment." Water environment research, 2006. [Online]. Available: https://www.jstor.org/stable/25053549

[77] S. Chakraborty, M. K. Purkait, S. DasGupta, S. De, and J. K. Basu, “Nanofiltration of textile plant effluent for color removal and reduction in COD,” *Separation and purification Technology*, vol. 31, no. 2, pp. 141–151, 2003, doi: https://doi.org/10.1016/S1383-5866(02)00177-6.

[78] A. Akbari, S. Desclaux, J. C. Remigy, and P. Aptel, “Treatment of textile dye effluents using a new photografted nanofiltration membrane,” *Desalination*, vol. 149, no. 1–3, pp. 101–107, 2002, doi: https://doi.org/10.1016/S0011-9164(02)00739-7.

[79] S. D. Ashrafi, H. Kamani, and A. H. Mahvi, “The optimization study of direct red 81 and methylene blue adsorption on NaOH-modified rice husk,” *Desalination and Water Treatment*, vol. 57, no. 2, pp. 738–746, 2016, doi: 10.1080/19443994.2014.979329.

[80] V. K. Gupta, A. Mittal, and V. Gajbe, “Adsorption and desorption studies of a water soluble dye, Quinoline Yellow, using waste materials,” *Journal of Colloid and Interface Science*, vol. 284, no. 1, pp. 89–98, 2005, doi: 10.1016/j.jcis.2004.09.055.

[81] K. Santhy and P. Selvapathy, “Removal of reactive dyes from wastewater by adsorption on coir pith activated carbon,” *Bioresource Technology*, vol. 97, no. 11, pp. 1329–1336, 2006, doi: 10.1016/j.biortech.2005.05.016.

[82] M. Özacar and İ. A. Şengil, “Application of kinetic models to the sorption of disperse dyes onto alunite,” *Colloids and Surfaces A: Physicochemical and Engineering Aspects*, vol. 242, no. 1–3, pp. 105–113, 2004, doi: 10.1016/j.colsurfa.2004.03.029.

[83] T.-H. Kim, C. Park, J. Yang, and S. Kim, “Comparison of disperse and reactive dye removals by chemical coagulation and Fenton oxidation,” *Journal of Hazardous Materials*, vol. 112, no. 1–2, pp. 95–103, 2004, doi: 10.1016/j.jhazmat.2004.04.008.

[84] S. Zodi, B. Merzouk, O. Potier, F. Lapicque, and J.-P. Leclerc, “Direct red 81 dye removal by a continuous flow electrocoagulation/flotation reactor,” *Separation and Purification Technology*, vol. 108, pp. 215–222, 2013, doi: 10.1016/j.seppur.2013.01.052.

[85] J. Jia, J. Yang, J. Liao, W. Wang, and Z. Wang, “Treatment of dyeing wastewater with ACF electrodes,” *Water Resources*, vol. 33, no. 3, pp. 881–884, 1999, doi: https://doi.org/10.1016/S0043-1354(98)00277-2.

[86] W. Lemlikchi, S. Khaldi, M. O. Mecherri, H. Lounici, and N. Drouiche, “Degradation of Disperse Red 167 Azo Dye by Bipolar Electrocoagulation,” *Separation Science and Technology*, vol. 47, no. 11, pp. 1682–1688, 2012, doi: 10.1080/01496395.2011.647374.

[87] H. Lan, A. Wang, R. Liu, H. Liu, and J. Qu, “Heterogeneous photo-Fenton degradation of acid red B over Fe2O3 supported on activated carbon fiber,” *Journal of Hazardous Materials*, vol. 285, pp. 167–172, 2015, doi: 10.1016/j.jhazmat.2014.10.057.

[88] V. K. Gupta, R. Jain, A. Nayak, S. Agarwal, and M. Shrivastava, “Removal of the hazardous dye—Tartrazine by photodegradation on titanium dioxide surface,” *Materials Science and Engineering: C*, vol. 31, no. 5, pp. 1062–1067, 2011, doi: 10.1016/j.msec.2011.03.006.

[89] S. Chakrabarti and B. Dutta, “Photocatalytic degradation of model textile dyes in wastewater using ZnO as semiconductor catalyst,” *Journal of Hazardous Materials*, vol. 112, no. 3, pp. 269–278, 2004, doi: 10.1016/j.jhazmat.2004.05.013.

[90] Y. Anjaneyulu, N. Sreedhara Chary, and D. Samuel Suman Raj, “Decolourization of industrial effluents – available methods and emerging technologies – A review,” *Reviews in Environmental Science and Bio/Technology*, vol. 4, no. 4, pp. 245–273, 2005, doi: 10.1007/s11157-005-1246-z.

[91] R. Ullah and J. Dutta, “Photocatalytic degradation of organic dyes with manganese-doped ZnO nanoparticles,” *Journal of Hazardous Materials*, vol. 156, no. 1–3, pp. 194–200, 2008, doi: 10.1016/j.jhazmat.2007.12.033.

[92] H. S. Rai, M. S. Bhattacharyya, J. Singh, T. K. Bansal, P. Vats, and U. C. Banerjee, “Removal of dyes from the effluent of Textile and Dyestuff Manufacturing Industry: A review of emerging

techniques with reference to biological treatment," *Critical Reviews in Environmental Science and Technology*, vol. 35, no. 3, pp. 219–238, 2005, doi: 10.1080/10643380590917932.

[93] J. Gao, Q. Zhang, K. Su, R. Chen, and Y. Peng, "Biosorption of Acid Yellow 17 from aqueous solution by non-living aerobic granular sludge," *Journal of Hazardous Materials*, vol. 174, no. 1–3, pp. 215–225, 2010, doi: 10.1016/j.jhazmat.2009.09.039.

[94] M. Shirzad-Siboni, S. J. Jafari, O. Giahi, I. Kim, S.-M. Lee, and J.-K. Yang, "Removal of acid blue 113 and reactive black 5 dye from aqueous solutions by activated red mud," *Journal of Industrial and Engineering Chemistry*, vol. 20, no. 4, pp. 1432–1437, 2014, doi: 10.1016/j.jiec.2013.07.028.

[95] S. Santos, V. Vilar, and R. Boaventura, "Waste metal hydroxide sludge as adsorbent for a reactive dye," *Journal of Hazardous Materials*, vol. 153, no. 3, pp. 999–1008, 2008, doi: 10.1016/j.jhazmat.2007.09.050.

[96] L. Yang, Z. Wang, and J. Zhang, "Zeolite imidazolate framework hybrid nanofiltration (NF) membranes with enhanced permselectivity for dye removal," *Journal of Membrane Science*, vol. 532, pp. 76–86, 2017, doi: 10.1016/j.memsci.2017.03.014.

[97] S. Nadupalli, N. Koorbanally, and S. B. Jonnalagadda, "Chlorine Dioxide-Facilitated Oxidation of the Azo Dye Amaranth," *The Journal of Physical Chemistry A*, vol. 115, no. 42, pp. 11682–11688, 2011, doi: 10.1021/jp206175s.

[98] J. Wu, M. A. Eiteman, and S. E. Law, "Evaluation of membrane filtration and ozonation processes for treatment of reactive-dye wastewater," *Journal of Environmental Engineering*, vol. 124, no. 3, pp. 272–277, 1998, doi: https://doi.org/10.1061/(ASCE)0733-9372(1998)124:3(272).

[99] F. Han, V. S. R. Kambala, M. Srinivasan, D. Rajarathnam, and R. Naidu, "Tailored titanium dioxide photocatalysts for the degradation of organic dyes in wastewater treatment: A review," *Applied Catalysis A: General*, vol. 359, no. 1–2, pp. 25–40, 2009, doi: 10.1016/j.apcata.2009.02.043.

[100] H. H. Omar, "Algal decolorization and degradation of mono azo and diazo dyes." Pakisthan Journal of Biological sciences, 2008. [Online]. Available: 10.3923/pjbs.2008.1310.1316

[101] X. Meng, G. Liu, J. Zhou, and Q. S. Fu, "Effects of redox mediators on azo dye decolorization by Shewanella algae under saline conditions," *Bioresource Technology*, vol. 151, pp. 63–68, 2014, doi: 10.1016/j.biortech.2013.09.131.

[102] L. Jinqi and L. Houtian, "Degradation of azo dyes by algae," *Environmental pollution*, vol. 75, no. 3, pp. 273–278, 1992, doi: 10.1016/0269-7491(92)90127-v.

[103] M. M. El-Sheekh, M. M. Gharieb, and G. W. Abou-El-Souod, "Biodegradation of dyes by some green algae and cyanobacteria," *International Biodeterioration & Biodegradation*, vol. 63, no. 6, pp. 699–704, 2009, doi: 10.1016/j.ibiod.2009.04.010.

[104] S. J. Kim, K. Ishikawa, M. Hirai, and M. Shoda, "Characteristics of a newly isolated fungus, Geotrichum candidum Dec 1, which decolorizes various dyes," *Journal of Fermentation and Bioengineering*, vol. 79, no. 6, pp. 601–607, 1995, doi: https://doi.org/10.1016/0922-338X(95)94755-G.

[105] A. Paszczynski, M. B. Pasti-Grigsby, S. Goszczynski, R. L. Crawford, and D. L. Crawford, "Mineralization of sulfonated azo dyes and sulfanilic acid by Phanerochaete chrysosporium and Streptomyces chromofuscus.," *Applied and environmental microbiology*, vol. 58, no. 11, pp. 3598–3604, 1992, doi: 0099-2240/92/113598-07$02.00/0.

[106] B.-Y. Chen, "Understanding decolorization characteristics of reactive azo dyes by Pseudomonas luteola: toxicity and kinetics," *Process Biochemistry*, vol. 38, no. 3, pp. 437–446, 2002, doi: https://doi.org/10.1016/S0032-9592(02)00151-6.

[107] K. Selvam, K. Swaminathan, and K.-S. Chae, "Decolourization of azo dyes and a dye industry effluent by a white rot fungus Thelephora sp.," *Bioresource Technology*, vol. 88, no. 2, pp. 115–119, 2003, doi: 10.1016/s0960-8524(02)00280-8.

[108] Z. Aksu and S. Tezer, “Equilibrium and kinetic modelling of biosorption of Remazol Black B by Rhizopus arrhizus in a batch system: effect of temperature,” *Process Biochemistry*, vol. 36, no. 5, pp. 431–439, 2000, doi: https://doi.org/10.1016/S0032-9592(00)00233-8.

[109] J. Joshi and O. Sahu, “Adsorption of Heavy Metals by Biomass.” Journal of Applied & Environmental Microbiology, 2014. [Online]. Available: 10.12691/jaem-2-1-5

[110] W. Xu *et al.*, “Removal of Chromium (VI) from Aqueous Solution Using Mycelial Pellets of Penicillium simplicissimum Impregnated with Powdered Biochar,” *Bioremediation Journal*, vol. 19, no. 4, pp. 259–268, 2015, doi: 10.1080/10889868.2015.1066302.

[111] K.-W. Jung, T.-U. Jeong, H.-J. Kang, and K.-H. Ahn, “Characteristics of biochar derived from marine macroalgae and fabrication of granular biochar by entrapment in calcium-alginate beads for phosphate removal from aqueous solution,” *Bioresource Technology*, vol. 211, pp. 108–116, 2016, doi: 10.1016/j.biortech.2016.03.066.

[112] K.-W. Jung, T.-U. Jeong, B. H. Choi, H.- Jeong Kang, and K.-H. Ahn, “Phosphate adsorption from aqueous solution by *Laminaria japonica* -derived biochar-calcium alginate beads in a fixed-bed column: Experiments and prediction of breakthrough curves,” *Environmental Progress & Sustainable Energy*, vol. 36, no. 5, pp. 1365–1373, 2017, doi: 10.1002/ep.12580.

[113] Z. Aksu, “Biosorption of reactive dyes by dried activated sludge: equilibrium and kinetic modelling,” *Biochemical Engineering Journal*, vol. 7, no. 1, pp. 79–84, 2001, doi: https://doi.org/10.1016/S1369-703X(00)00098-X.

[114] T. O’mahony, E. Guibal, and J. M. Tobin, “Reactive dye biosorption by Rhizopus arrhizus biomass,” *Enzyme and Microbial Technology*, vol. 31, no. 4, pp. 456–463, 2002, doi: https://doi.org/10.1016/S0141-0229(02)00110-2.

[115] M. Khalaf, “Biosorption of reactive dye from textile wastewater by non-viable biomass of Aspergillus niger and Spirogyra sp.,” *Bioresource Technology*, vol. 99, no. 14, pp. 6631–6634, 2008, doi: 10.1016/j.biortech.2007.12.010.

[116] O. Aksakal and H. Ucun, “Equilibrium, kinetic and thermodynamic studies of the biosorption of textile dye (Reactive Red 195) onto Pinus sylvestris L.,” *Journal of Hazardous Materials*, vol. 181, no. 1–3, pp. 666–672, 2010, doi: 10.1016/j.jhazmat.2010.05.064.

[117] Z. Zhang *et al.*, “A novel biosorbent for dye removal: Extracellular polymeric substance (EPS) of Proteus mirabilis TJ-1,” *Journal of Hazardous Materials*, vol. 163, no. 1, pp. 279–284, 2009, doi: 10.1016/j.jhazmat.2008.06.096.

[118] D. Wei *et al.*, “Role of extracellular polymeric substances in biosorption of dye wastewater using aerobic granular sludge,” *Bioresource Technology*, vol. 185, pp. 14–20, 2015, doi: 10.1016/j.biortech.2015.02.084.

[119] R. Li *et al.*, “Decolorization and biodegradation of the Congo red by Acinetobacter baumannii YNWH 226 and its polymer production’s flocculation and dewatering potential,” *Bioresource Technology*, vol. 194, pp. 233–239, Oct. 2015, doi: 10.1016/j.biortech.2015.06.139.

[120] J.-F. Gao, Q. Zhang, J.-H. Wang, X.-L. Wu, S.-Y. Wang, and Y.-Z. Peng, “Contributions of functional groups and extracellular polymeric substances on the biosorption of dyes by aerobic granules,” *Bioresource Technology*, vol. 102, no. 2, pp. 805–813, 2011, doi: 10.1016/j.biortech.2010.08.119.

[121] Y. Liu *et al.*, “Rapid and high-efficiency removal of methylene blue onto low-cost activated sludge: Role and significance of extracellular polymeric substances,” *Bioresource Technology Reports*, vol. 7, p. 100240, 2019, doi: 10.1016/j.biteb.2019.100240.

[122] N. A. Oranusi and C. J. Ogugbue, “Effect of pH and nutrient starvation on biodegradation of azo dyes by Pseudomonas sp,” *Journal of Applied Sciences and Environmental Management*, vol. 9, no. 1, pp. 39–43, 2005, doi: http://www.bioline.org.br/abstract?id=ja05007.

[123] K. H. Balapure, K. Jain, S. Chattaraj, N. S. Bhatt, and D. Madamwar, "Co-metabolic degradation of diazo dye—Reactive blue 160 by enriched mixed cultures BDN," *Journal of Hazardous Materials*, vol. 279, pp. 85–95, 2014, doi: 10.1016/j.jhazmat.2014.06.057.

[124] S. Ortiz-Monsalve, J. Dornelles, E. Poll, M. Ramirez-Castrillón, P. Valente, and M. Gutterres, "Biodecolourisation and biodegradation of leather dyes by a native isolate of Trametes villosa," *Process Safety and Environmental Protection*, vol. 109, pp. 437–451, 2017, doi: 10.1016/j.psep.2017.04.028.

[125] M. Işik and D. T. Sponza, "Effect of oxygen on decolorization of azo dyes by Escherichia coli and Pseudomonas sp. and fate of aromatic amines," *Process Biochemistry*, vol. 38, no. 8, pp. 1183–1192, 2003, doi: https://doi.org/10.1016/S0032-9592(02)00282-0.

[126] T. Zimmermann, H. G. Kulla, and T. Leisinger, "Properties of Purified Orange II Azoreductase, the Enzyme Initiating Azo Dye Degradation by Pseudomonas KF46," *European Journal of Biochemistry*, vol. 129, no. 1, pp. 197–203, 1982, doi: 10.1111/j.1432-1033.1982.tb07040.x.

[127] J.-S. Chang, C. Chou, Y.-C. Lin, P.-J. Lin, J.-Y. Ho, and T. L. Hu, "Kinetic characteristics of bacterial azo-dye decolorization by Pseudomonas luteola," *Water Research*, vol. 35, no. 12, pp. 2841–2850, 2001, doi: 10.1016/s0043-1354(00)00581-9.

[128] R. L. Singh, P. K. Singh, and R. P. Singh, "Enzymatic decolorization and degradation of azo dyes – A review," *International Biodeterioration & Biodegradation*, vol. 104, pp. 21–31, 2015, doi: 10.1016/j.ibiod.2015.04.027.

[129] A. A. Telke, D. C. Kalyani, V. V. Dawkar, and S. P. Govindwar, "Influence of organic and inorganic compounds on oxidoreductive decolorization of sulfonated azo dye C.I. Reactive Orange 16," *Journal of Hazardous Materials*, vol. 172, no. 1, pp. 298–309, 2009, doi: 10.1016/j.jhazmat.2009.07.008.

[130] S. Sekar, S. Mahadevan, B. K. Shanmugam, and A. B. Mandal, "Bioenergetics and pathway of acid blue 113 degradation by *Staphylococcus lentus*," *Biotechnology Progress*, vol. 28, no. 6, pp. 1400–1408, 2012, doi: 10.1002/btpr.1626.

[131] M. M. Sahasrabudhe, R. G. Saratale, G. D. Saratale, and G. R. Pathade, "Decolorization and detoxification of sulfonated toxic diazo dye C.I. Direct Red 81 by Enterococcus faecalis YZ 66," *Journal of Environmental Health Science and Engineering*, vol. 12, no. 151, 2014, doi: 10.1186/s40201-014-0151-1.

[132] R. S. Dhanve, U. U. Shedbalkar, and J. P. Jadhav, "Biodegradation of diazo reactive dye Navy blue HE2R (Reactive blue 172) by an isolated Exiguobacterium sp. RD3," *Biotechnology and Bioprocess Engineering*, vol. 13, no. 1, pp. 53–60, 2008, doi: 10.1007/s12257-007-0165-y.

[133] M. Z. Nawahwi, "Degradation of the Azo Dye Reactive Red 195 by Paenibacillus spp. R2," *Journal of Bioremediation and Biodegradation*, vol. 04, no. 01, 2013, doi: 10.4172/2155-6199.1000174.

[134] S. Agrawal, D. Tipre, B. Patel, and S. Dave, "Optimization of triazo Acid Black 210 dye degradation by Providencia sp. SRS82 and elucidation of degradation pathway," *Process Biochemistry*, vol. 49, no. 1, pp. 110–119, 2014, doi: 10.1016/j.procbio.2013.10.006.

[135] A. Naresh Kumar, C. Nagendranatha Reddy, and S. Venkata Mohan, "Biomineralization of azo dye bearing wastewater in periodic discontinuous batch reactor: Effect of microaerophilic conditions on treatment efficiency," *Bioresource Technology*, vol. 188, pp. 56–64, 2015, doi: 10.1016/j.biortech.2015.01.098.

[136] M. Karataş and S. Dursun, "Bio-decolourization of azo-dye under anaerobic batch conditions," *J. Int. Environmental Application & Science*, vol. 2, no. 1 & 2, pp. 20–25, 2007, doi: https://doi.org/10.1081/ESE-120028417.

[137] A. Spagni, S. Grilli, S. Casu, and D. Mattioli, "Treatment of a simulated textile wastewater containing the azo-dye reactive orange 16 in an anaerobic-biofilm anoxic–aerobic membrane

bioreactor," *International Biodeterioration & Biodegradation*, vol. 64, no. 7, pp. 676–681, 2010, doi: 10.1016/j.ibiod.2010.08.004.

[138] L. Yu, W.-W. Li, M. H.-W. Lam, H.-Q. Yu, and C. Wu, "Isolation and characterization of a Klebsiella oxytoca strain for simultaneous azo-dye anaerobic reduction and bio-hydrogen production," *Appl Microbiol Biotechnol*, vol. 95, no. 1, pp. 255–262, 2012, doi: 10.1007/s00253-011-3688-2.

[139] P. C. Vandevivere, R. Bianchi, and W. Verstraete, "Review: Treatment and reuse of wastewater from the textile wet-processing industry: Review of emerging technologies," *J. Chem. Technol. Biotechnol.*, vol. 72, pp. 289–302, 1998, doi: https://doi.org/10.1002/(SICI)1097-4660(199808)72:4<289::AID-JCTB905>3.0.CO;2-%23.

[140] R. C. Senan and T. E. Abraham, "Bioremediation of textile azo dyes by aerobic bacterial consortium aerobic degradation of selected azo dyes by bacterial consortium," *Biodegradation*, vol. 15, no. 4, pp. 275–280, 2004, doi: https://doi.org/10.1023/B:BIOD.0000043000.18427.0a.

[141] K. M. Kodam, I. Soojhawon, P. D. Lokhande, and K. R. Gawai, "Microbial decolorization of reactive azo dyes under aerobic conditions," *World Journal of Microbiology and Biotechnology*, vol. 21, no. 3, pp. 367–370, 2005, doi: 10.1007/s11274-004-5957-z.

[142] W. Przystas, E. Zablocka-Godlewska, and E. Grabinska-Sota, "Efficacy of fungal decolorization of a mixture of dyes belonging to different classes," *Brazilian Journal of Microbiology*, vol. 46, no. 2, pp. 415–424, 2015, doi: 10.1590/S1517-838246246220140167.

[143] E. Franciscon, M. J. Grossman, J. A. R. Paschoal, F. G. R. Reyes, and L. R. Durrant, "Decolorization and biodegradation of reactive sulfonated azo dyes by a newly isolated Brevibacterium sp. strain VN-15," *SpringerPlus*, vol. 1, no. 1, p. 37, 2012, doi: 10.1186/2193-1801-1-37.

[144] S. Kalme, S. Jadhav, M. Jadhav, and S. Govindwar, "Textile dye degrading laccase from Pseudomonas desmolyticum NCIM 2112," *Enzyme and Microbial Technology*, vol. 44, no. 2, pp. 65–71, 2009, doi: 10.1016/j.enzmictec.2008.10.005.

[145] S. D. Kalme, G. K. Parshetti, S. U. Jadhav, and S. P. Govindwar, "Biodegradation of benzidine based dye Direct Blue-6 by Pseudomonas desmolyticum NCIM 2112," *Bioresource Technology*, vol. 98, no. 7, pp. 1405–1410, 2007, doi: 10.1016/j.biortech.2006.05.023.

[146] E. Silveira, P. P. Marques, S. S. Silva, J. L. Lima-Filho, A. L. F. Porto, and E. B. Tambourgi, "Selection of Pseudomonas for industrial textile dyes decolourization," *International Biodeterioration & Biodegradation*, vol. 63, no. 2, pp. 230–235, 2009, doi: 10.1016/j.ibiod.2008.09.007.

[147] S. Galai, F. Limam, and M. N. Marzouki, "Decolorization of an industrial effluent by free and immobilized cells of Stenotrophomonas maltophilia AAP56. Implementation of efficient down flow column reactor," *World Journal of Microbiology and Biotechnology*, vol. 26, no. 8, pp. 1341–1347, 2010, doi: 10.1007/s11274-010-0306-x.

[148] R. G. Saratale, G. D. Saratale, J. S. Chang, and S. P. Govindwar, "Ecofriendly degradation of sulfonated diazo dye C.I. Reactive Green 19A using Micrococcus glutamicus NCIM-2168," *Bioresource Technology*, vol. 100, no. 17, pp. 3897–3905, 2009, doi: 10.1016/j.biortech.2009.03.051.

[149] A. Spagni, S. Casu, and S. Grilli, "Decolourisation of textile wastewater in a submerged anaerobic membrane bioreactor," *Bioresource Technology*, vol. 117, pp. 180–185, 2012, doi: 10.1016/j.biortech.2012.04.074.

[150] G. F. Chan, N. A. A. Rashid, L. S. Chua, N. Ab.llah, R. Nasiri, and M. R. M. Ikubar, "Communal microaerophilic–aerobic biodegradation of Amaranth by novel NAR-2 bacterial consortium," *Bioresource Technology*, vol. 105, pp. 48–59, 2012, doi: 10.1016/j.biortech.2011.11.094.

[151] Z. Dhaouefi *et al.*, "Assessing textile wastewater treatment in an anoxic-aerobic photobioreactor and the potential of the treated water for irrigation," *Algal Research*, vol. 29, pp. 170–178, 2018, doi: 10.1016/j.algal.2017.11.032.

[152] D. Georgiou and A. Aivasidis, “Decoloration of textile wastewater by means of a fluidized-bed loop reactor and immobilized anaerobic bacteria,” *Journal of Hazardous Materials*, vol. 135, no. 1–3, pp. 372–377, 2006, doi: 10.1016/j.jhazmat.2005.11.081.
[153] M. Karataþ, Þ. Dursun, and M. E. Argun, “The Decolorization of Azo Dye Reactive Black 5 in a Sequential Anaerobic-Aerobic System,” vol. 19, no. 74, pp. 15–23, 2010.
[154] M. Khehra, H. Saini, D. Sharma, B. Chadha, and S. Chimni, “Decolorization of various azo dyes by bacterial consortium,” *Dyes and Pigments*, vol. 67, no. 1, pp. 55–61, 2005, doi: 10.1016/j.dyepig.2004.10.008.
[155] J. P. Jadhav, S. S. Phugare, R. S. Dhanve, and S. B. Jadhav, “Rapid biodegradation and decolorization of Direct Orange 39 (Orange TGLL) by an isolated bacterium Pseudomonas aeruginosa strain BCH,” *Biodegradation*, vol. 21, no. 3, pp. 453–463, 2010, doi: 10.1007/s10532-009-9315-6.
[156] L. Yu *et al.*, “Microbial community structure associated with treatment of azo dye in a start-up anaerobic sequenced batch reactor,” *Journal of the Taiwan Institute of Chemical Engineers*, vol. 54, pp. 118–124, 2015, doi: 10.1016/j.jtice.2015.03.012.
[157] U. G. Ozkan-Yucel and C. F. Gokcay, “Effect of Anaerobic Azo Dye Reduction on Continuous Sludge Digestion: Effect of Anaerobic Azo Dye Reduction on Continuous Sludge Digestion,” *CLEAN - Soil, Air, Water*, vol. 42, no. 10, pp. 1457–1463, 2014, doi: 10.1002/clen.201300046.
[158] P. S. Patil, U. U. Shedbalkar, D. C. Kalyani, and J. P. Jadhav, “Biodegradation of Reactive Blue 59 by isolated bacterial consortium PMB11,” *Journal of Industrial Microbiology & Biotechnology*, vol. 35, no. 10, pp. 1181–1190, 2008, doi: 10.1007/s10295-008-0398-6.
[159] S. Asad, M. A. Amoozegar, A. A. Pourbabaee, M. N. Sarbolouki, and S. M. M. Dastgheib, “Decolorization of textile azo dyes by newly isolated halophilic and halotolerant bacteria,” *Bioresource Technology*, vol. 98, no. 11, pp. 2082–2088, 2007, doi: 10.1016/j.biortech.2006.08.020.
[160] J. Wang, J. Yan, and W. Xu, “Treatment of dyeing wastewater by MIC anaerobic reactor,” *Biochemical Engineering Journal*, vol. 101, pp. 179–184, 2015, doi: 10.1016/j.bej.2015.06.001.
[161] J. Rathod, S. Dhebar, and G. Archana, “Efficient approach to enhance whole cell azo dye decolorization by heterologous overexpression of Enterococcus sp. L2 azoreductase (azoA) and Mycobacterium vaccae formate dehydrogenase (fdh) in different bacterial systems,” *International Biodeterioration & Biodegradation*, vol. 124, pp. 91–100, 2017, doi: 10.1016/j.ibiod.2017.04.023.
[162] P. Saranraj, V. Sumathi, D. Reetha, and D. Stella, “Decolourization and Degradation of Dirct Azo Dyes and Biodegradation of Textile Dye Effluent by using Bacteria Isolated from Textile Dye Effluent,” *Journal of Ecobiotechnology*, vol. 2, no. 7, pp. 07–11, 2010.
[163] “Cold Spring Harbour Laboratory. M9 minimal medium (standard).,” *Cold Spring Harb Protoc*, 2010, doi: 10.1101/pdb.rec12295.
[164] G. Eremektar, H. Selcuk, and S. Meric, “Investigation of the relation between COD fractions and the toxicity in a textile finishing industry wastewater: Effect of preozonation,” *Desalination*, vol. 211, no. 1–3, pp. 314–320, 2007, doi: 10.1016/j.desal.2006.02.096.
[165] R. J. L. Paulton, “The bacterial growth curve, Journal of Biological Education,” vol. 25, no. 2, pp. 92–94, 1991, doi: 10.1080/00219266.1991.9655183.
[166] J. Monod, “THE GROWTH OF BACTERIAL CULTURES,” *Annual Review of Microbiology*, vol. 3, pp. 371–394, Oct. 1949, doi: https://doi.org/10.1146/annurev.mi.03.100149.002103.
[167] X. Huang, “CAP3: A DNA Sequence Assembly Program,” *Genome Research*, vol. 9, no. 9, pp. 868–877, 1999, doi: 10.1101/gr.9.9.868.

[168] W. Cheng *et al.*, "Isolation, identification, and whole genome sequence analysis of the alginate-degrading bacterium Cobetia sp. cqz5-12," *Scientific Reports*, vol. 10, no. 1, 2020, doi: 10.1038/s41598-020-67921-7.

[169] Sk. Md. A. Rahman, A. Kumar Saha, R. A. Ruhi, Md. F. Haque, and M. K. Mohanta, "Decolourization of Textile Azo Dye Direct Red 81 by Bacteria from Textile Industry Effluent," *International Journal of Current Microbiology and Applied Sciences*, vol. 8, no. 04, pp. 1742–1754, 2019, doi: 10.20546/ijcmas.2019.804.203.

[170] S. Kumar, G. Stecher, M. Li, C. Knyaz, and K. Tamura, "MEGA X: Molecular Evolutionary Genetics Analysis across Computing Platforms," *Molecular Biology and Evolution*, vol. 35, no. 6, pp. 1547–1549, 2018, doi: 10.1093/molbev/msy096.

[171] F. P. van der Zee, I. A. E. Bisschops, V. G. Blanchard, R. H. M. Bouwman, G. Lettinga, and J. A. Field, "The contribution of biotic and abiotic processes during azo dye reduction in anaerobic sludge," *Water Research*, vol. 37, no. 13, pp. 3098–3109, 2003, doi: 10.1016/S0043-1354(03)00166-0.

[172] V. Kumari *et al.*, "EFFECT OF TANNERY EFFLUENT TOXICITY ON SEED GERMINATION á-AMYLASE ACTIVITY AND EARLY SEEDLING GROWTH OF MUNG BEAN (VIGNA RADIATA) SEEDS," p. 7, 2014.

[173] M. A. Kumar *et al.*, "Mineralization of aromatic amines liberated during the degradation of a sulfonated textile colorant using Klebsiella pneumoniae strain AHM," *Process Biochemistry*, vol. 57, pp. 181–189, 2017, doi: 10.1016/j.procbio.2017.03.012.

[174] T. Senthilvelan, J. Kanagaraj, and R. C. Panda, "Enzyme-Mediated Bacterial Biodegradation of an Azo Dye (C.I. Acid Blue 113): Reuse of Treated Dye Wastewater in Post-Tanning Operations," *Applied Biochemistry and Biotechnology*, vol. 174, no. 6, pp. 2131–2152, 2014, doi: 10.1007/s12010-014-1158-x.

[175] A. Manubens, P. Canessa, C. Folch, M. Avila, L. Salas, and R. Vicuna, "Manganese affects the production of laccase in the basidiomycete Ceriporiopsis subvermispora," *FEMS Microbiol Lett*, vol. 275, no. 1, pp. 139–45, 2007, doi: 10.1111/j.1574-6968.2007.00874.x.

[176] V. Janaki, K. Vijayaraghavan, A. K. Ramasamy, K.-J. Lee, B.-T. Oh, and S. Kamala-Kannan, "Competitive adsorption of Reactive Orange 16 and Reactive Brilliant Blue R on polyaniline/bacterial extracellular polysaccharides composite—A novel eco-friendly polymer," *Journal of Hazardous Materials*, vol. 241–242, pp. 110–117, 2012, doi: 10.1016/j.jhazmat.2012.09.019.

[177] V. S. Munagapati, V. Yarramuthi, Y. Kim, K. M. Lee, and D.-S. Kim, "Removal of anionic dyes (Reactive Black 5 and Congo Red) from aqueous solutions using Banana Peel Powder as an adsorbent," *Ecotoxicology and Environmental Safety*, vol. 148, pp. 601–607, 2018, doi: 10.1016/j.ecoenv.2017.10.075.

[178] N. Junnarkar, D. S. Murty, N. S. Bhatt, and D. Madamwar, "Decolorization of diazo dye Direct Red 81 by a novel bacterial consortium," *World Journal of Microbiology and Biotechnology*, vol. 22, no. 2, pp. 163–168, 2006, doi: 10.1007/s11274-005-9014-3.

[179] T. Calvete, E. C. Lima, N. F. Cardoso, J. C. P. Vaghetti, S. L. P. Dias, and F. A. Pavan, "Application of carbon adsorbents prepared from Brazilian-pine fruit shell for the removal of reactive orange 16 from aqueous solution: Kinetic, equilibrium, and thermodynamic studies," *Journal of Environmental Management*, vol. 91, no. 8, pp. 1695–1706, 2010, doi: 10.1016/j.jenvman.2010.03.013.

[180] S. Biala, P. Chauhan, B. S. Chadha, B. Singh, and H. S. Saini, "Biotransformation of CI Acid Blue 113 and other dyes by Shewanella sp. P6," *Coloration Technology*, vol. 129, no. 5, pp. 330–337, 2013, doi: 10.1111/cote.12045.

[181] R. E. McKinney, “The Role of Chemically Combined Oxygen in Biological Systems,” *Journal of the Sanitary Engineering Division*, vol. 82, no. 4, pp. 1–9, 1956, doi: https://doi.org/10.1061/JSEDAI.0000030.

[182] S. Dixit and S. Garg, “Biodegradation of Environmentally Hazardous Azo Dyes and Aromatic Amines Using *Klebsiella pneumoniae*,” *Journal of Environmental Engineering*, vol. 144, no. 6, p. 04018035, 2018, doi: 10.1061/(ASCE)EE.1943-7870.0001353.

[183] M. Zhuang *et al.*, “Azo dye degrading bacteria tolerant to extreme conditions inhabit nearshore ecosystems: Optimization and degradation pathways,” *Journal of Environmental Management*, vol. 261, p. 110222, 2020, doi: 10.1016/j.jenvman.2020.110222.

[184] B. K. Shanmugam and S. Mahadevan, “Metabolism and biotransformation of azo dye by bacterial consortium studied in a bioreaction calorimeter,” *Bioresource Technology*, vol. 196, pp. 500–508, 2015, doi: 10.1016/j.biortech.2015.07.108.

[185] K. Svobodová, M. Senholdt, Č. Novotný, and A. Rehorek, “Mechanism of Reactive Orange 16 degradation with the white rot fungus Irpex lacteus,” *Process Biochemistry*, vol. 42, no. 9, pp. 1279–1284, 2007, doi: 10.1016/j.procbio.2007.06.002.

[186] C.-Y. Chen, “Photocatalytic Degradation of Azo Dye Reactive Orange 16 by TiO2,” *Water, Air, and Soil Pollution*, vol. 202, no. 1–4, pp. 335–342, 2009, doi: 10.1007/s11270-009-9980-4.

[187] P. Mani *et al.*, “Degradation of Azo Dye (Acid Orange 7) in a Microbial Fuel Cell: Comparison Between Anodic Microbial-Mediated Reduction and Cathodic Laccase-Mediated Oxidation,” *Frontiers in Energy Research*, vol. 7, 2019, doi: 10.3389/fenrg.2019.00101.

[188] T. Kim, M. Kim, Y. Lim, and Y. Son, “Degradation of the disazo acid dye by the sulfur-containing amino acids of wool fibers,” *Dyes and Pigments*, vol. 67, no. 2, pp. 127–132, 2005, doi: 10.1016/j.dyepig.2004.09.025.

[189] W.-E. Thung *et al.*, “A highly efficient single chambered up-flow membrane-less microbial fuel cell for treatment of azo dye Acid Orange 7-containing wastewater,” *Bioresource Technology*, vol. 197, pp. 284–288, 2015, doi: 10.1016/j.biortech.2015.08.078.

[190] A. Zille, B. Gornacka, A. Rehorek, and A. Cavaco-Paulo, “Degradation of Azo Dyes by Trametes villosa Laccase over Long Periods of Oxidative Conditions,” *Applied and Environmental Microbiology*, vol. 71, no. 11, pp. 6711–6718, 2005, doi: 10.1128/AEM.71.11.6711-6718.2005.

[191] P. Sutthivaiyakit *et al.*, “LC-MS/MS method for the confirmatory determination of aromatic amines and its application in textile analysis,” *Analytical and Bioanalytical Chemistry*, vol. 381, no. 1, pp. 268–276, 2005, doi: 10.1007/s00216-004-2852-2.

[192] J. F. Xiao, B. Zhou, and H. W. Ressom, “Metabolite identification and quantitation in LC-MS/MS-based metabolomics,” *Trends in Analytical Chemistry*, vol. 32, pp. 1–14, 2012, doi: 10.1016/j.trac.2011.08.009.

[193] N. Ayaz, R. Thankappan, S. V. Srinivasan, and A. TamilSelvi, “Studies on decolourisation of Acid Blue 113 using Staphylococcus Aureus and Escherichia Coli isolated from tannery wastewater,” *International Journal of Innovative Research in Science, Engineering and Technology*, vol. 04, no. 03, pp. 938–948, 2015, doi: 10.15680/IJIRSET.2015.0403021.

[194] L. D. Clements, B. S. Miller, and U. N. Streips, “Comparative Growth Analysis of the Facultative Anaerobes Bacillus subtilis, Bacillus licheniformis, and Escherichia coli,” *Systematic and Applied Microbiology*, vol. 25, no. 2, pp. 284–286, 2002, doi: 10.1078/0723-2020-00108.

[195] S. Moosvi, H. Keharia, and D. Madamwar, “Decolourization of textile dye Reactive Violet 5 by a newly isolated bacterial consortium RVM 11.1,” *World Journal of Microbiology and Biotechnology*, vol. 21, no. 5, pp. 667–672, 2005, doi: 10.1007/s11274-004-3612-3.

[196] Z. K. Bagewadi, A. G. Vernekar, A. Y. Patil, and V. M. Jain, “Biodegradation of industrially important textile dyes by actinomycetes isolated from activated sludge,” *Biotech. Bioinf. Bioeng.*, vol. 1, no. 3, pp. 351–360, 2011.

[197] E. Franciscon, A. Zille, F. Fantinatti-Garboggini, I. S. Silva, A. Cavaco-Paulo, and L. R. Durrant, "Microaerophilic–aerobic sequential decolourization/biodegradation of textile azo dyes by a facultative Klebsiella sp. strain VN-31," *Process Biochemistry*, vol. 44, no. 4, pp. 446–452, 2009, doi: 10.1016/j.procbio.2008.12.009.

[198] A. Brigé, B. Motte, J. Borloo, G. Buysschaert, B. Devreese, and J. J. Van Beeumen, "Bacterial decolorization of textile dyes is an extracellular process requiring a multicomponent electron transfer pathway: Bacterial dye reduction pathway," *Microbial Biotechnology*, vol. 1, no. 1, pp. 40–52, 2008, doi: 10.1111/j.1751-7915.2007.00005.x.

[199] P. K. Singh and R. L. Singh, "Bio-removal of Azo Dyes: A Review," *International Journal of Applied Sciences and Biotechnology*, vol. 5, no. 2, pp. 108–126, 2017, doi: 10.3126/ijasbt.v5i2.16881.

[200] R. Bras, A. Gomes, M. I. A. Ferra, H. M. Pinheiro, and I. C. Goncalves, "Monoazo and diazo dye decolourisation studies in a methanogenic UASB reactor," *Journal of Biotechnology*, p. 10, 2005, doi: https://doi.org/10.1016/j.jbiotec.2004.08.001.

[201] C. Pearce, "The removal of colour from textile wastewater using whole bacterial cells: a review," *Dyes and Pigments*, vol. 58, no. 3, pp. 179–196, 2003, doi: 10.1016/S0143-7208(03)00064-0.

[202] J. Zhao, J. Chen, and J. Gao, "Decolorization of Azo Dyes C.I.Acid Yellow 17 and C.I.Direct Red 31 by Dielectric-Barrier Discharge Air Plasma," *IEEE Transactions on Plasma Science*, vol. 38, no. 3, pp. 488–495, 2010, doi: 10.1109/TPS.2009.2039232.

[203] K. Meerbergen, K. A. Willems, R. Dewil, J. Van Impe, L. Appels, and B. Lievens, "Isolation and screening of bacterial isolates from wastewater treatment plants to decolorize azo dyes," *Journal of Bioscience and Bioengineering*, vol. 125, no. 4, pp. 448–456, 2018, doi: 10.1016/j.jbiosc.2017.11.008.

[204] Q. Zhang *et al.*, "Co-metabolic degradation of refractory dye: A metagenomic and metaproteomic study," *Environmental Pollution*, vol. 256, p. 113456, 2020, doi: 10.1016/j.envpol.2019.113456.

[205] P. A. Bedekar, R. G. Saratale, G. D. Saratale, and S. P. Govindwar, "Oxidative stress response in dye degrading bacterium Lysinibacillus sp. RGS exposed to Reactive Orange 16, degradation of RO16 and evaluation of toxicity," *Environmental Science and Pollution Research*, vol. 21, no. 18, pp. 11075–11085, 2014, doi: 10.1007/s11356-014-3041-2.

[206] G. K. Parshetti, A. A. Telke, D. C. Kalyani, and S. P. Govindwar, "Decolorization and detoxification of sulfonated azo dye methyl orange by Kocuria rosea MTCC 1532," *Journal of Hazardous Materials*, vol. 176, no. 1–3, pp. 503–509, 2010, doi: 10.1016/j.jhazmat.2009.11.058.

[207] M. Ajaz, A. Rehman, Z. Khan, M. A. Nisar, and S. Hussain, "Degradation of azo dyes by Alcaligenes aquatilis 3c and its potential use in the wastewater treatment," *AMB Express*, vol. 9, no. 1, 2019, doi: 10.1186/s13568-019-0788-3.

[208] J. N. Neetha, K. Sandesh, K. Girish Kumar, B. Chidananda, and P. Ujwal, "Optimization of Direct Blue-14 dye degradation by Bacillus fermus (Kx898362) an alkaliphilic plant endophyte and assessment of degraded metabolite toxicity," *Journal of Hazardous Materials*, vol. 364, pp. 742–751, 2019, doi: 10.1016/j.jhazmat.2018.10.074.

[209] A. Kannan and R. K. Upreti, "Influence of distillery effluent on germination and growth of mung bean (Vigna radiata) seeds," *Journal of Hazardous Materials*, vol. 153, no. 1–2, pp. 609–615, May 2008, doi: 10.1016/j.jhazmat.2007.09.004.

[210] K. Nath, D. Singh, S. Shyam, and Y. K. Sharma, "Effect of chromium and tannery effluent toxicity on metabolism and growth in cowpea (Vigna sinensis L. Saviex Hassk) seedling," p. 5.

[211] A. Zereen, A. Wahid, Z.-U.-D. Khan, and A. A. Sardar, "Effect of tannery wastewater on the growth and yield of sunflower (Helianthus Annuus L.)." Bangladesh J. Bot., 2013.